AD-A069 840 EG AND G INC SALEM MASS ELECTRONIC COMPONENTS DIV F/G 9/5
REPETITIVE SERIES INTERRUPTER II.(U)
APR 79 R F CARISTI, D V TURNQUIST DAAB07-76-C-1301
UNCLASSIFIED DELET-TR-76-1301-F NL

1 OF 2
AD
A069840

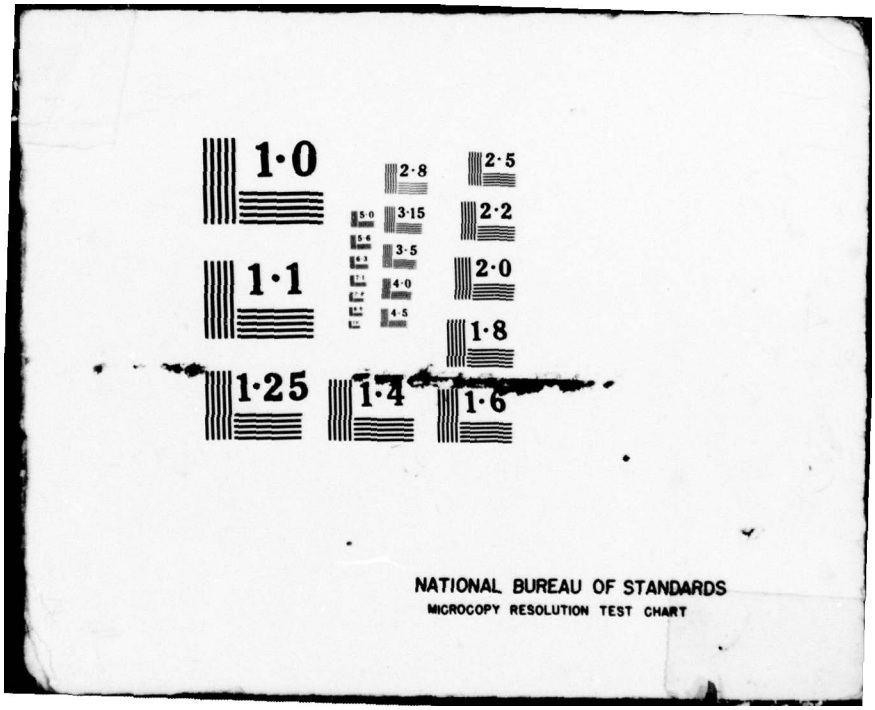
1·0
1·1
1·25
1·4
1·6
1·8
2·0
2·2
2·5
2·8
3·15
3·5
4·0
4·5
5·0
NATIONAL BUREAU OF STANDARDS
MICROCOPY RESOLUTION TEST CHART

LEVEL II

Research and Development Technical Report
DELET-TR-76-1301-F

AD A069840

REPETITIVE SERIES INTERRUPTER II

Robert F. Caristi
David V. Turnquist
EG&G INC.
35 Congress Street
Salem, Ma. 01970

April 1979

Final Report for the Period 26 January 1976 to 30 September 1978

Prepared for:
Electronics Technology & Devices Laboratory

ERADCOM
U.S. ARMY ELECTRONICS R&D COMMAND, FORT MONMOUTH, NEW JERSEY 07703

HISA-FM 195-78

NOTICES

Disclaimers

The findings in this report are not to be construed as an official Department of the Army position, unless so designated by other authorized documents.

The citation of trade names and names of manufacturers in this report is not to be construed as official Government indorsement or approval of commercial products or services referenced herein.

Disposition

Destroy this report when it is no longer needed. Do not return it to the originator.

UNCLASSIFIED

SECURITY CLASSIFICATION OF THIS PAGE (When Data Entered)

REPORT DOCUMENTATION PAGE

READ INSTRUCTIONS BEFORE COMPLETING FORM

1. REPORT NUMBER: DELET-TR-76-1301-F

2. GOVT ACCESSION NO.

3. RECIPIENT'S CATALOG NUMBER

4. TITLE (and Subtitle): REPETITIVE SERIES INTERRUPTER II.

5. TYPE OF REPORT & PERIOD COVERED: Final Report, 26 Jan 76 - 30 Sep 78

6. PERFORMING ORG. REPORT NUMBER

7. AUTHOR(s): Robert F. Caristi; David V. Turnquist

8. CONTRACT OR GRANT NUMBER(s): DAAB07-76-C-1301

9. PERFORMING ORGANIZATION NAME AND ADDRESS:
EG&G Incorporated
35 Congress Street
Salem, MA 01970

10. PROGRAM ELEMENT, PROJECT, TASK AREA & WORK UNIT NUMBERS: 612705; 1L1 62705 AH 94 E1.08

11. CONTROLLING OFFICE NAME AND ADDRESS:
US Army Electronics Technology & Devices Laboratory
ATTN: DELET-BG
Fort Monmouth, NJ 07703

12. REPORT DATE: April 1979

13. NUMBER OF PAGES: 139

14. MONITORING AGENCY NAME & ADDRESS (If different from Controlling Office): 138p.

15. SECURITY CLASS. (of this report): UNCLASSIFIED

15a. DECLASSIFICATION/DOWNGRADING SCHEDULE

16. DISTRIBUTION STATEMENT (of this Report)

Approved for Public Release; distribution unlimited

17. DISTRIBUTION STATEMENT (of the abstract entered in Block 20, if different from Report)

18. SUPPLEMENTARY NOTES

19. KEY WORDS (Continue on reverse side if necessary and identify by block number)

Series Interrupter
Gas Filled Device
Fuse
Thyratron
Magnetic Interaction Region

20. ABSTRACT (Continue on reverse side if necessary and identify by block number)

This report summarizes the results of the work performed under the Repetitive Series Interrupter Program. The fundamental aims were to obtain the information necessary to build five exploratory development RSI's designed to interrupt 1000 A at 50 kV, to construct these tubes, and to evaluate their performance under conditions simulating their intended usage.

The relatively low-voltage 10 Series of RSI's built under the initial phase of the Program were characterized for both interruption capability and (over)

→ next page

DD FORM 1 JAN 73 1473 EDITION OF 1 NOV 65 IS OBSOLETE

UNCLASSIFIED

SECURITY CLASSIFICATION OF THIS PAGE (When Data Entered)

410 029 LB

forward voltage drop. Using the 10 Series tubes, investigations were also made to determine the extent to which the self-interruption tendency of a constricted, high current gas discharge would affect the interruption process. The conclusion was that the self-interruption process in no way hindered RSI operation, and in fact operated so as to reduce the magnetic field necessary to interrupt a given discharge.

Also using the 10 Series tubes, it was shown that with appropriate keep-alive systems, the anode delay time and delay time jitter of an RSI could be made comparable to those of conventional thyratrons. It was also shown that a suitable keep-alive system applied to the control grid would cause the RSI to operate as a closed switch. Keep-alive power requirements were minimal, being of the order of tens of watts.

Typical column drops for the 10 Series tubes were of the order of 350 volts per section (20 volts/cm). The most efficient member of the Series, a "folded-channel" device designed to operate at 30 kV, was successfully operated at epy = 25 kV and ib = 18.5 A with a total tube drop of 830 volts or 3.3% of epy. This tube successfully interrupted 600 A at 20 kV with a magnetic field energy of less than 8 joules being required to achieve the interruption.

From the testing of the 10 Series of tubes, an optimum geometry for the interaction channel was inferred, and this geometry served as the base for the design of the 50 kV interrupters. These tubes were designated RSI 12, and their testing provided further information concerning channel design, forward drop and forward drop distribution, and the effects of the magnetic field risetime on the interruption process.

Tube drop was studied extensively, and it was found that a total forward drop of the order of 2% of epy was typical for an efficient interrupter. The forward drop across the discharge column was found to be uniform along the column's length during conduction. During the interruption, the drop across the column was non-uniform, but not seriously so. The column drop for the triple-section 12 Series tubes was 870 volts (16.3 volts/cm) during conduction, and the total tube drop was typically 1000 volts. During a 50 kV interruption, the average electric field in the gas was 937 volts/cm.

A typical 12 Series tube successfully interrupted 100 A at 50 kV, 180 A at 44 kV, 305 A at 26 kV, 700 A at 18 kV, and 1000 A at 15 kV. Operation at these power levels was reliable and free of restrike. The magnetic field energy delivered to the interaction channel to effect these interruptions varied from a high of 32.8 joules in the high voltage case, to a low of 1.2 joules in the high current case, indicating a strong dependence of the interrupting field on the voltage level of the interruption. The parameter believed to be important to minimize the necessary magnetic field energy for high voltage interruptions is the time derivative of the magnetic field intensity.

Techniques have been developed that effectively preclude restriking of the discharge after interruption has occurred. Normal RSI operation at pulse repetition rates approaching 10 kilohertz are considered as being feasible, as is a life of several thousand hours including several thousand interruptions.

ABBREVIATIONS AND SYMBOLS

A	Ampere(s)
B	Magnetic field required to reduce fault current to zero with a 50% probability
Crc	Capacitance of fault network
Cm	Capacitance of magnet circuit
d	Arbitrary unit of length
D	Diode in tube drop measuring circuit
Dch	Holdoff diode
eag	Peak anode to grid voltage
eb	Instantaneous anode voltage
Ebb	DC anode supply voltage
Ecc	Bias voltage
ecd	Voltage drop of interaction column (steady-state)
Ef	Cathode heater voltage
egk	Peak forward grid to cathode voltage
Em	DC supply voltage of magnet circuit
eo	Output voltage of tube drop measuring circuit
epy	Peak forward anode voltage
etd	Total voltage drop of conducting tube (steady-state tube drop)
Eres	Reservoir heater voltage
Hz	Hertz
ib	Peak forward anode current
im	Peak current through magnet coil
kV	Kilovolt(s)
kG	Kilogauss(es)
l	Active length of interaction column (per section)
Lch	Charging inductor
N	Number of turns in magnet coil
P	Gas pressure within tube
PFN	Pulse forming network

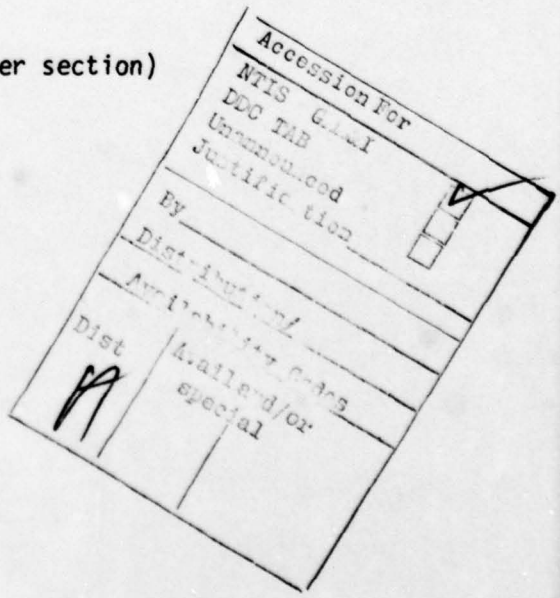

Rch	Charging resistor
Rl	Load resistance of pulse forming network
Rm	Magnet circuit damping resistance
Rrc	Load resistance of fault network
RSI	Repetitive series interrupter
t	Time
tp	Pulse width of pulse forming network
tr	Rise time of current in magnet circuit
TUT	Tube under test
V	Volts
Zn	Characteristic impedance of pulse forming network
Ω	Ohm(s)

TABLE OF CONTENTS

LIST OF ILLUSTRATIONS

LIST OF TABLES

1.0 FOREWORD

This Final Technical Report describes the results of a thirty-two month program of research and development conducted by EG&G, Inc. under ERADCOM Contract DAAB07-76C-1301, entitled "Repetitive Series Interrupter II." The report covers the period 26 January 1976 through 30 September 1978.

Phase I of the program demonstrated the feasibility of tubes operating at 15 kV. Detailed discussion of the work done under Phase I is given in the Sixth Interim Report, dated April 1978. Under Phase II, tube operation was extended to 50 kV. The Final Report, although covering the entire program, emphasizes the results of Phase II.

Mr. Murray Weiner of ERADCOM served as the Government's technical contract monitor.

The work was performed by EG&G's Electronic Components Division, 35 Congress Street, Salem, Massachusetts 01970. Mr. Robert F. Caristi was Program Engineer, and Mr. David V. Turnquist was Program Manager. The authors wish to recognize the contributions of Mr. Robert P. Simon who served as Program Engineer during Phase I of the Program.

2.0 INTRODUCTION AND SUMMARY

a. Purpose and Concerns of the RSI Program

The purpose of the Repetitive Series Interrupter II Program was to develop a gas discharge device which functioned as both a repetitively closable and openable switch at the 50 kV, 1000 A power level. In addition to thirty-two months of research and development work, the Program also entailed the actual construction of five exploratory development RSI's designed to operate under the electrical conditions given in Table 1.

A repetitively closable and openable switch is clearly useful as an automatically resettable fuse. When used in series with some component to be protected (e.g., a traveling wave tube), the RSI can be made to function as an automatically openable switch in the event of a fault within the protected device. Upon termination of fault conditions, the RSI can be made to function as an automatically closable switch so that normal system operation can be resumed.

Three mandatory characteristics of a practical RSI are thus implied: 1) the device must operate with a reasonable steady-state drop when in the conducting state; 2) the device must remain in the nonconducting state for a suitable period after receiving the command to switch off, i.e., the device must not restrike; and 3) the device must be either a) free-wheeling, i.e., automatically returnable to the conducting state, or b) retriggerable, i.e., returnable to the conducting state upon receipt of a suitable triggering command.

The work described herein was directed toward the development of an RSI based primarily on hydrogen thyratron technology and construction techniques. Such an RSI may be closed by the application of a grid pulse (as is a standard thyratron), maintained in the normally closed state by the use of a "keep-alive" current, and opened by the application of a pulsed magnetic field applied across an interaction channel built into the tube. An additional requirement is thus implied for a practical RSI device of this type, namely that the current within the RSI be extinguishable with a minimum of magnetic field energy.

Table 1. Desired Electrical Characteristics, Repetitive Series Interrupter (As Amended For Phase II).

(a)	Open Circuit Holdoff Voltage	50 kV, Minimum
(b)	Normally Closed Voltage Drop	500 V, Maximum
(c)	Peak Fault Current	1,000 A, Maximum
(d)	Normal Average Current	0.7 A, Minimum
(e)	Normal Peak Current	17 A, Maximum
(f)	Repetition Rate	1 kHz to 20 kHz (Burst Mode)
(g)	Life	1,000 Hours, Minimum
(h)	Operating Mode	Normally closed
(i)	Opening Actions	20,000 Cycles, Minimum

The principal goals of the RSI R&D Program were thus to develop an RSI which:

1. operated at 50 kV, 1000 A;
2. operated with a reasonably low steady-state drop;
3. did not restrike;
4. required a minimum of interrupting magnetic field energy;
5. was of a design lending itself to construction using established techniques and conventional materials;
6. was capable of providing a reasonable service life under applicable operating conditions.

The fundamental requirements of the Program were to obtain the information necessary to design five exploratory development RSI's, to construct these tubes, and then to evaluate their performance under conditions approximating those of Table 1.

b. Report Organization

Six experimental RSI's were built as deliverable end items under Phase I of the RSI Program. Five of the six were designed to operate at 15 kV and 300 A; the sixth was designed to operate at 30 kV and 300 A.

These tubes (designated the RSI 10 Series) were characterized during Phase II of the Program. The results of this characterization provided the information necessary to design the 50 kV, 1000 A tubes desired under Phase II. Five of the latter (designated the RSI 12 Series) were required as end items under Phase II, but a total of seven RSI 12 Series tubes were in fact built and tested. Interruption characteristics (Bq vs Ebb) and forward drops (etd) for the RSI 10 and 12 Series tubes are presented (with a minimum of discussion) in Section 3 of this report.

The remaining sections discuss in detail various aspects of RSI design and operation, and overall conclusions on the subject at hand. Section 4 covers the important matter of self-interruption ("quenching") of RSI discharge, and various effects of altering the period over which the interruption actually takes place.

Section 5 examines the subject of tube drop in depth; Section 6 discusses the techniques developed to avoid restriking of the discharge.

Section 7 considers the RSI triggering characteristics and performance at high pulse repetititon rates. Section 8 summarizes the more important experimental results and presents conclusions reached during the Program.

c. Summary of Principal Results and Conclusions

The RSI 10 and 12 Series of chuted interrupters were built and characterized for both interruption capability and total tube drop. From testing the 10 Series of tubes, an optimum interaction channel geometry was inferred; this geometry served as the base for the design of the 12 Series of 50 kV tubes.

Typical column drops for the 10 Series tubes were of the order of 350 volts per section (20 volts/cm). The most efficient member of the Series, the folded-channel RSI 10DD, operated at 25 kV, 18.5 A with a total drop of 830 volts, or 3.3% of epy. This tube successfully interrupted 600 A at 20 kV with a magnetic field energy of less than 8 joules being required to achieve the interruption.

Testing the 12 Series tubes provided further information concerning the design of efficient channel geometries. Typical total tube drops for the triple-section 12 Series interrupters were of the order of 1000 volts (2% of epy) at 18.5 A. The column drop was typically 870 volts (16.3 volts/cm).

The RSI 12C successfully interrupted 100 A at 50 kV, 180 A at 44 kV, 305 A at 26 kV, 700 A at 18 kV, and 1000 A at 15 kV. Operation at these levels was reliable and free of restrike. The magnetic field energy to achieve these interruptions varied from a high of 32.8 joules in the high voltage case, to a low of 1.2 joules in the high current case, indicating a strong dependence of the interrupting field on the voltage level of the interruption. Currents in excess of 1000 A were routinely interrupted at the 15 to 20 kV level using several of the 12 Series tubes; however, at voltages greater than about 30 kV, the interruption efficiency appeared to depend strongly on the time derivative of the magnetic field intensity. We thus believe that with a suitably designed magnetic field generator, these tubes are capable of interrupting higher power levels than those experimentally demonstrated.

The RSI has been shown to be a practical means for the repetitive interruption of high current at high voltage. It has been experimentally demonstrated that tube drops of 2% of epy can be achieved, that restriking of the discharge can be avoided, that reasonable triggering characteristics are possible, and that the device can be made to operate as a closed switch. Pulse repetition rates of 10 kHz are feasible, and a life of several thousand hours including thousands of interruptions should be achievable.

3.0 PRINCIPAL EXPERIMENTAL RESULTS

a. "Chuted" Interaction Channel Geometry

It was established during Phase I of the RSI Program that "plasma chutes" built into the walls of the interaction channel materially reduced the magnetic field required to interrupt a given discharge current at a given anode supply voltage.(1) The mechanism whereby interruption occurs is one where the IXB force drives the discharge plasma into the chutes such that recombination at wall surfaces and subsequent cessation of the discharge occurs.(2) In general, chuted RSI's are more efficient than non-chuted RSI's when each is operated under essentially the same conditions, and a device equipped with chutes on one side of the interaction channel (and none on the other) will operate more efficiently when the direction of the applied magnetic field is such that the IXB force is directed into the chutes.

Two families of chuted interrupters were designed, built, and tested under the auspices of the RSI Program. The first of these (the 10 Series) was built to investigate the relative effectiveness of various (and substantially different) chuting arrangements. The design of the second group (the 12 Series) was based on the design of the most efficient 10 Series tubes, with variations in chuting among the members of the 12 Series family being relatively minor. The principal function of the 12 Series of tubes was to serve as a vehicle to determine the feasibility of interrupting currents as high as 1000 A at anode supply voltages up to 50 kV.

b. Tube Designs and Experimental Results

(1) Experimental Apparatus and Technique

(a) Determination of Magnetic Field Required for Interruption (B_q)

The circuit of Figure 1 was typically used to determine the magnetic field required for current interruption. The TUT was triggered directly and its holdoff section was actively employed, as opposed to relying on a series thyratron to provide holdoff capability.

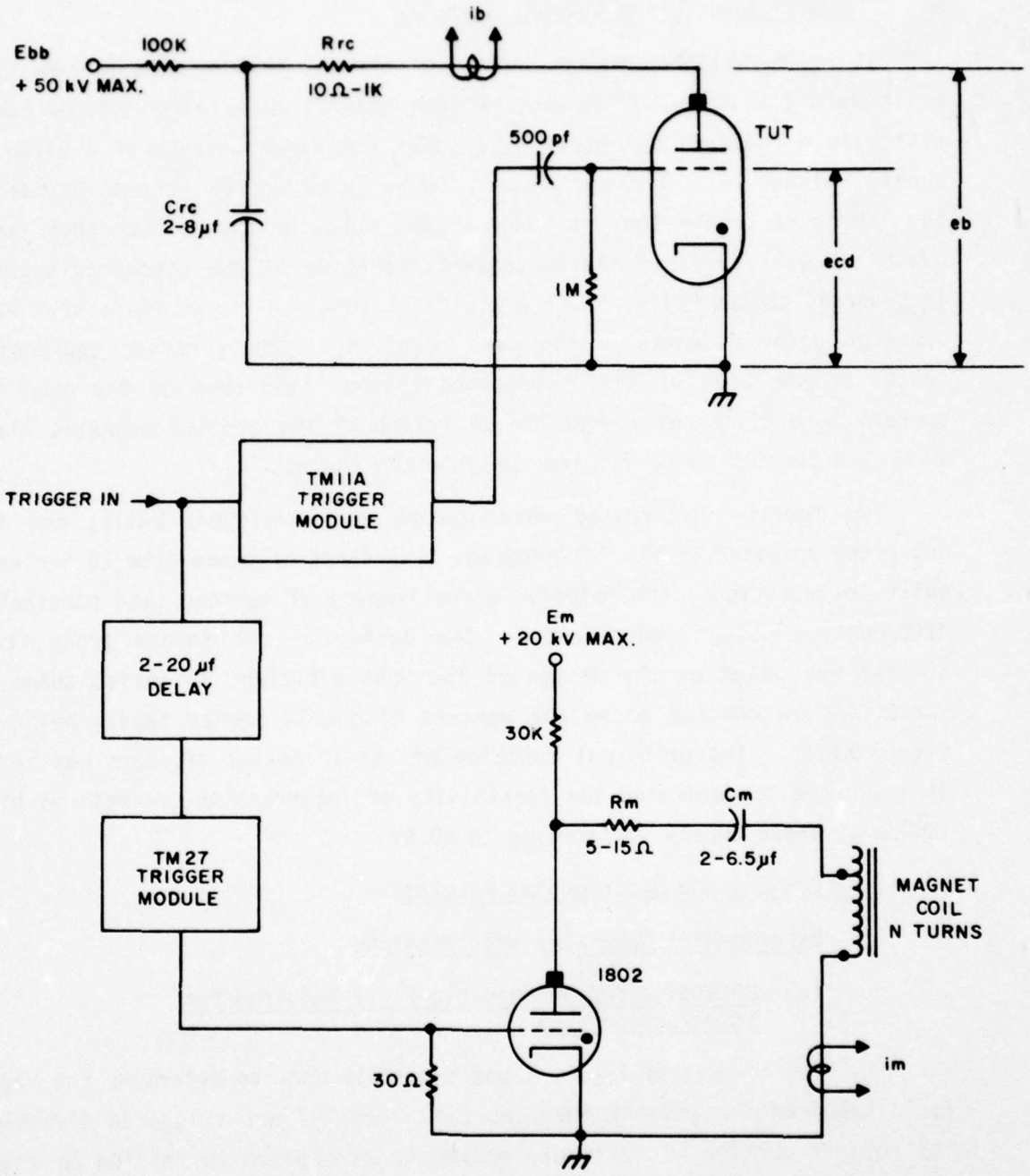

Figure 1. Circuit Used to Determine Magnetic Field Required for Interruption. The fault current may be varied independently of Ebb by varying Rrc, and the duration of the fault may be varied by changing the electronically generated delay. The number of turns in the magnet coil, N, was adjustable from 1 to 20.

The DC anode voltage of the TUT, Ebb, could be varied at will, as could TUT hydrogen pressure P. Fault circuit load resistor Rrc, magnet circuit capacitor Cm, and magnet circuit damping resistor Rm, could be readily adjusted as desired. Rm was generally set to provide a somewhat underdamped current waveform in the magnet circuit, thus eventually establishing a negative voltage at the anode of the 1802 thyratron to ensure its recovery.

Number of turns, N, of the magnet coil was adjustable to permit alteration of magnetic field rise time tr. Connections to the coil were reversible to permit changing the direction of the IXB force in the RSI's interaction region.

The peak current in the TUT, ib, was monitored by means of a calibrated current measuring transformer placed in the anode lead of the TUT; the transformer thus monitored the sum of the cathode current and any current which flowed through the grid and out of the anode-grid region.

Peak magnet current im, to which the peak magnetic field is proportional, was monitored using a calibrated current measuring transformer as shown in Figure 1. Independent testing had established that level of im for which the magnet core saturated; that current level was avoided.

A time delay was introduced, as shown in Figure 1, such that the magnetic field was not applied to the interaction region until 2-20 microseconds after initiation of discharge within the TUT.

The instantaneous anode voltage of the TUT, eb, and the voltage drop of the interaction column were monitored using calibrated and frequency-compensated high voltage probes.

Observation of eb and ib provided an indication of the effect of the magnetic field on the discharge. Magnet supply voltage, Em, was adjusted until the magnetic field required for interruption, Bq, was established. Bq was defined as being that field for which the current in the TUT was alternately extinguished or nearly extinguished since it was found that this condition could be achieved with reasonable regularity and independently of other operating conditions.

An arbitrary but representative sample of the data taken with the circuit of Figure 1 is shown in Figure 2, where the upper, center, and lower traces represent eb, im, and ib, respectively. Note that eb is initially equal to epy, drops to etd upon triggering of the RSI, and then returns to high voltage when ib is extinguished by the magnetic field. Voltage eb does not return to epy because ib has removed some of the charge from Crc, and the charging resistor (30K) is too large to permit a rapid recharge of Crc. Notice also from Figure 2 that the trailing edges of both eb and ib have finite slopes; this implies that the RSI actually passed through an operating region wherein its incremental impedance assumed discrete values. Thus the RSI is neither a short nor an open circuit during its opening transition.

The RSI appears to have changed its state prior to the peak of the magnetic field. This observation implied that decreasing the rise time of the magnetic field would improve the switching efficiency of the RSI; subsequent testing verified this supposition.

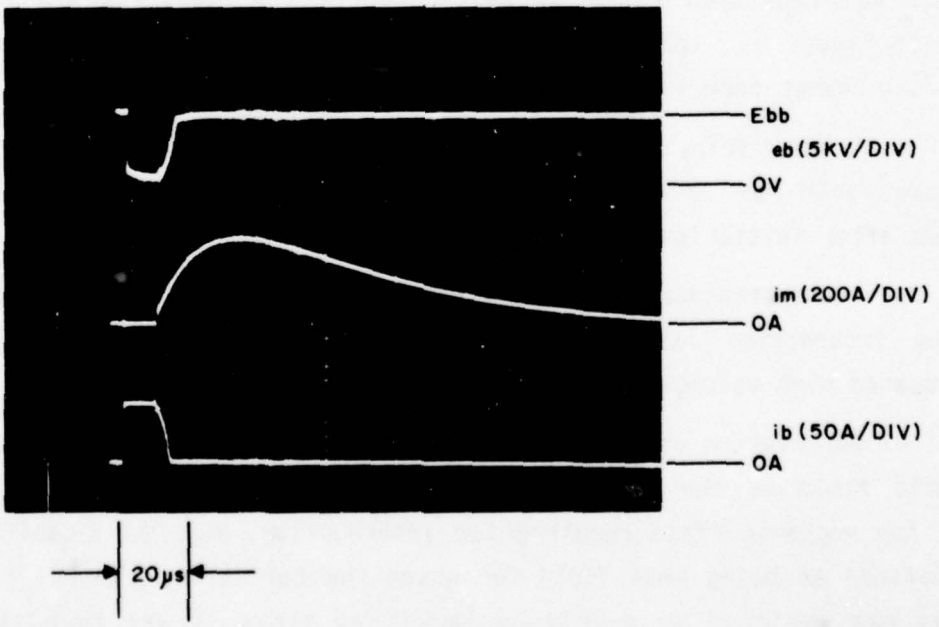

Figure 2. Typical RSI Waveforms During Interruption. Note that the waveforms of eb and ib have a finite slope during the interruption. In the case shown, the interruption takes place in about five microseconds.

(b) Determination of Steady-State Tube Drop (etd)

Figure 3 shows the circuit used to determine etd, the steady-state tube drop. Anode supply voltage Ebb was continuously varied at will up to 20 kV and two different pulse forming networks were used. One network had an impedance of 42 ohms and a pulse width of 1 μsec for investigations of etd at normal thyratron current levels. The other had an impedance of 600 ohms and a pulse width of about 7 μsec for investigations of etd at the current levels appropriate for "normal" operation of an RSI. In each case, load resistor R1 was chosen to provide a slightly negative voltage at the anode of the TUT after the main discharge of the PFN. Peak tube current ib was monitored in the same manner as the circuit of Figure 1, and the tube drop measurements were taken at the time corresponding to the midpoint of the current pulse.

The network shown within the dotted lines in Figure 3 was used in conjunction with a calibrated and frequency-compensated probe and an oscilloscope to obtain the actual tube drop data. Measurement of eb, the instantaneous voltage across the TUT, is complicated by the fact that prior to triggering the TUT, eb is equal to peak forward anode voltage epy. After triggering and commutation, eb is equal to steady-state tube drop etd, which is materially less than epy. Thus one is faced with a measurements situation where the dynamic range of the measuring scheme is of great importance. Previous experience with a high voltage probe located directly at the anode of the TUT showed that such probes may be voltage sensitive, i.e., the attenuation of the probe may be a function of the voltages being measured. Furthermore, the oscilloscope sensitivity which is appropriate for accurate determination of etd results in severe overdriving of the oscilloscope vertical amplifier in the presence of a signal corresponding to epy.

To overcome these problems, diode D (Figure 3) was used in conjunction with diode bias supply Ecc (a positive voltage), and a 15 K diode load resistor as shown. (The 0.1 μF capacitor served only as a filter.) For values of eb greater than Ecc (e.g., eb = epy), measuring circuit output voltage eo was equal to Ecc because the diode was biased off. For values of eb less than Ecc (e.g., eb = etd), eo was equal to eb because the diode was biased on (the diode drop was neglected). By varying Ecc from zero to large

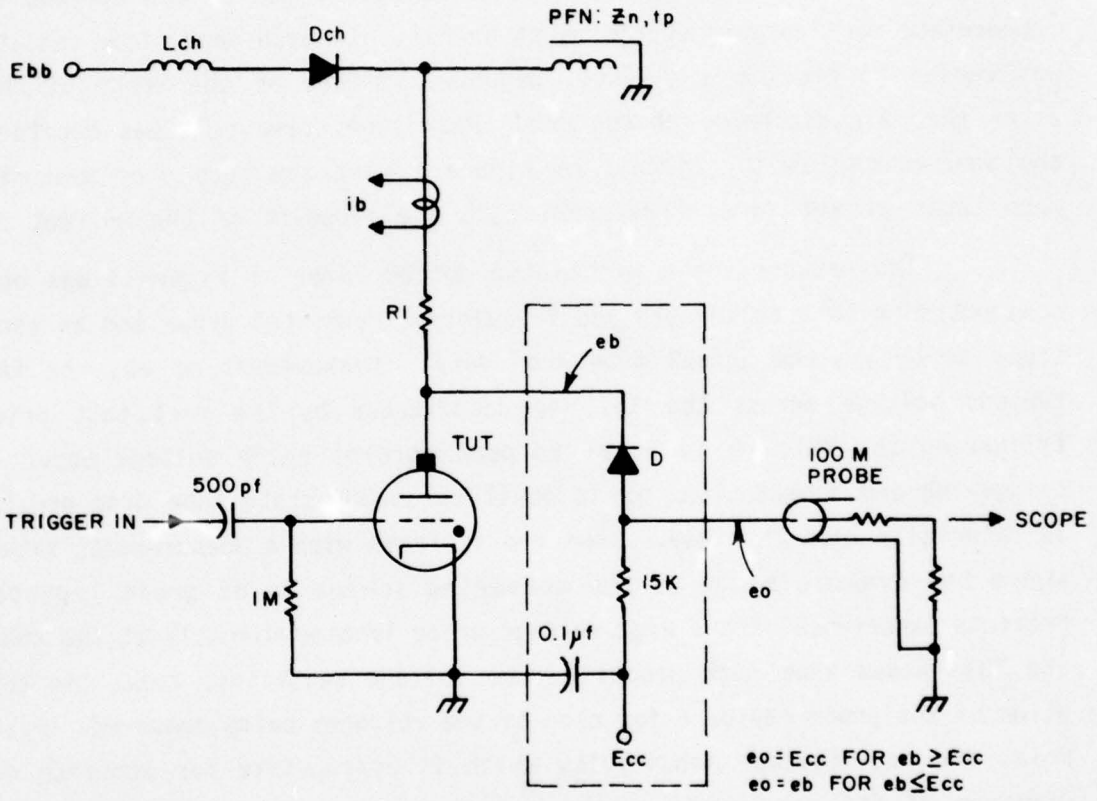

Figure 3. Circuit Used to Determine the Steady-State Tube Drop. The network shown within the dotted lines was contrived to permit accurate measurement of etd despite the effects of the relatively high voltage, epy.

positive values, while observing the waveform of eo, that level of Ecc which was adequately high to reliably measure etd could be determined, since higher values of Ecc would result in no change in the portion of the waveform of eo which corresponded to etd.

Representative data obtained in this fashion are shown by the oscillograms of Figure 4. The upper traces show the waveform of eo and the lower traces show the tube current. Note from Figure 4(a) that the entire waveform of eo (including the negative portion, which is of no particular interest) produces only about 1 cm of oscilloscope deflection. Thus oscilloscope sensitivity may be increased by an order of magnitude without overdriving the amplifier during the time of interest. In Figures 4(a) and 4(b), a bias voltage of 1600 volts and a tube drop of 800 volts can be discerned. Furthermore, the probe never "sees" a voltage greater than 1600 volts during the period of interest, despite the fact that epy was 25 kV for the case shown. The technique described here is thus suitable for accurate measurements of etd in the presence of high values of initial anode voltage.

At various times during the course of the investigation, the circuits shown in Figures 1 and 3 were modified as required to meet the needs of circumstances, but at no time did the essence of the apparatus deviate from that discussed above.

(2) RSI 10 Series - Design and Data

(a) Channel Geometry and Holdoff Sections

The geometry of the interaction region of the RSI 10 Series is shown in Figure 5. All interaction channels were made of ceramic (95% alumina), machined in the "green" state, and then subjected to high-temperature curing. Types A, B, and C had in common a bore diameter of 0.300 inch. Type A had both long (0.500 inch) and short (0.250 inch) chutes; Type B had 0.750 chutes on one side of the bore and none on the other; and Type C was similar to Type A except that the total number of chutes in Type C was one-half that of Type A. Types D and E were similar to Types A and B, respectively, except that the bores of the former tubes were 0.150 inch as opposed to 0.300 inch. Type DD was similar to Type D except that its total length was twice that of Type D (12 inches as opposed to 6 inches for Type D and also 6 inches for Types A, B, C, and E).

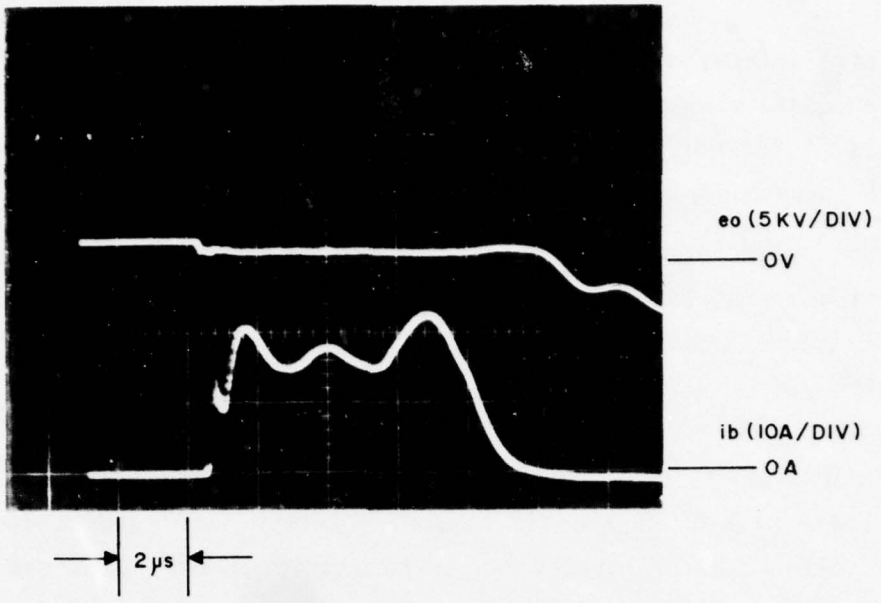

(a)

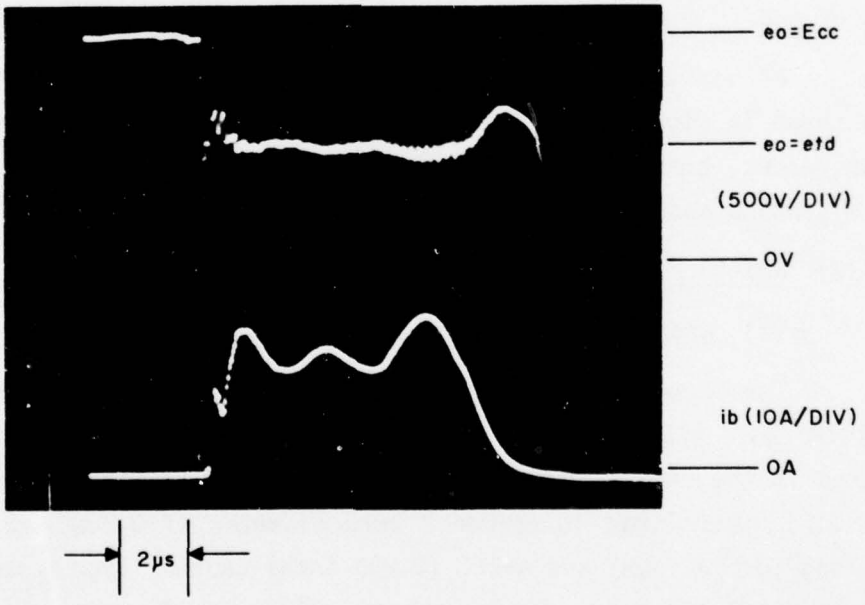

(b)

Figure 4. Typical Tube Drop Waveforms. The values reported for etd are those corresponding to the central peak of the current pulse.

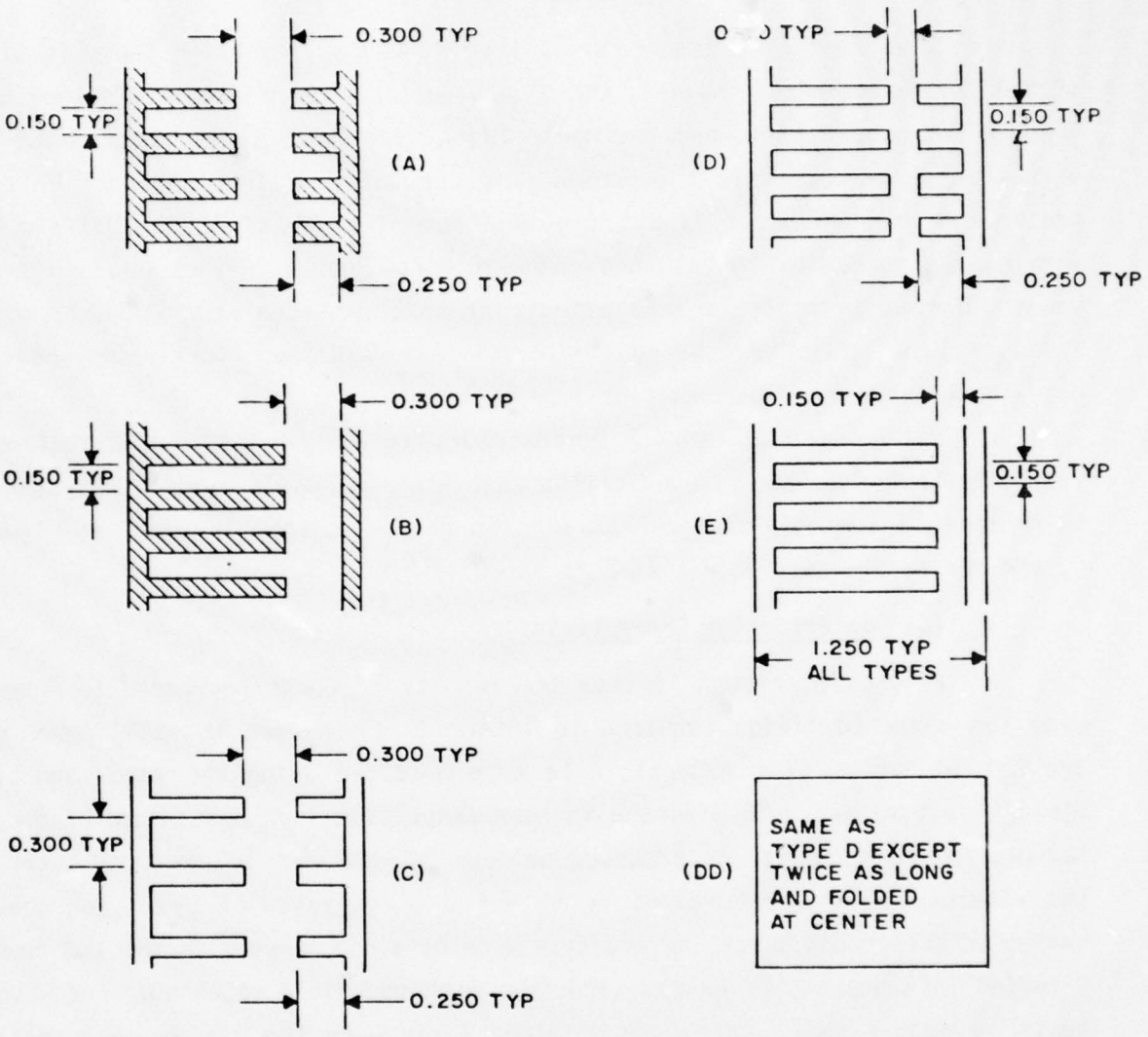

DIMENSIONS ARE IN INCHES
ALL WALL THICKNESSES ARE 0.100
ALL COLUMNS EXCEPT DD ARE 6.1 INCHES LONG

Figure 5. Interaction Channel Geometry - RSI 10 Series. The various channel segments were machined from 95% alumina and then fused together to form a gas tight structure.

All tubes except DD were equipped with a holdoff section similar to that of a standard EG&G Type HY-6. RSI 10DD was equipped with a holdoff section specifically designed to operate with epy = 30 kV.

When testing a tube such as Type A, and by reversing the direction of the IXB force in the channel, the discharge could be driven into either the long or the short chutes as desired. With Type B, the discharge could be driven into the chutes in the presence of the wall, or into the wall in the presence of the chutes. Type C provided some insight as to the effects of varying the number of chutes when compared with Type A. Types D and E provided information regarding the effects of bore diameter when compared with Types A and B. Type DD (the double-length tube) was specifically designed to operate reliably at higher voltage levels.

All of the 10 and 12 Series tubes were equipped with a cathode-reservoir-heater assembly identical to that used in EG&G's Type 7322 hydrogen thyratron. The single-section RSI 10A (in cross-section) is shown in Figure 6, and the triple-section RSI 12A2 is shown as Figure 7.

(b) Interruption Characteristics

Figures 8 through 16 show the results of tests performed to determine the magnetic fields required to interrupt discharges in each member of the RSI 10 Series. In general, data were obtained using the same magnetic field rise time and tube pressure in each case. The load resistance of fault network Rrc (Figure 1) was adjusted between 20 ohms and 100 ohms to observe the effects of different values of ib for a given value of Ebb. For tubes having both long and short chutes, data were obtained first with the IXB force directed into one set of chutes, and then with the field reversed. For tubes having a smooth wall, data were obtained first with the IXB force directed into the chutes, and then with the field reversed such that the IXB force was directed against a smooth surface. (The RSI 10E showed evidence of arcing in the interaction channel when the IXB force was directed against the smooth surface; therefore, meaningful data for this tube in this mode could not be obtained.) As will be discussed further in this section, it became evident that the tubes performed better with IXB directed into the short chutes (or away from the smooth surface in tubes so equipped), so the data as shown in Figures 8 through 16 are in general more complete for these favored modes of operation.

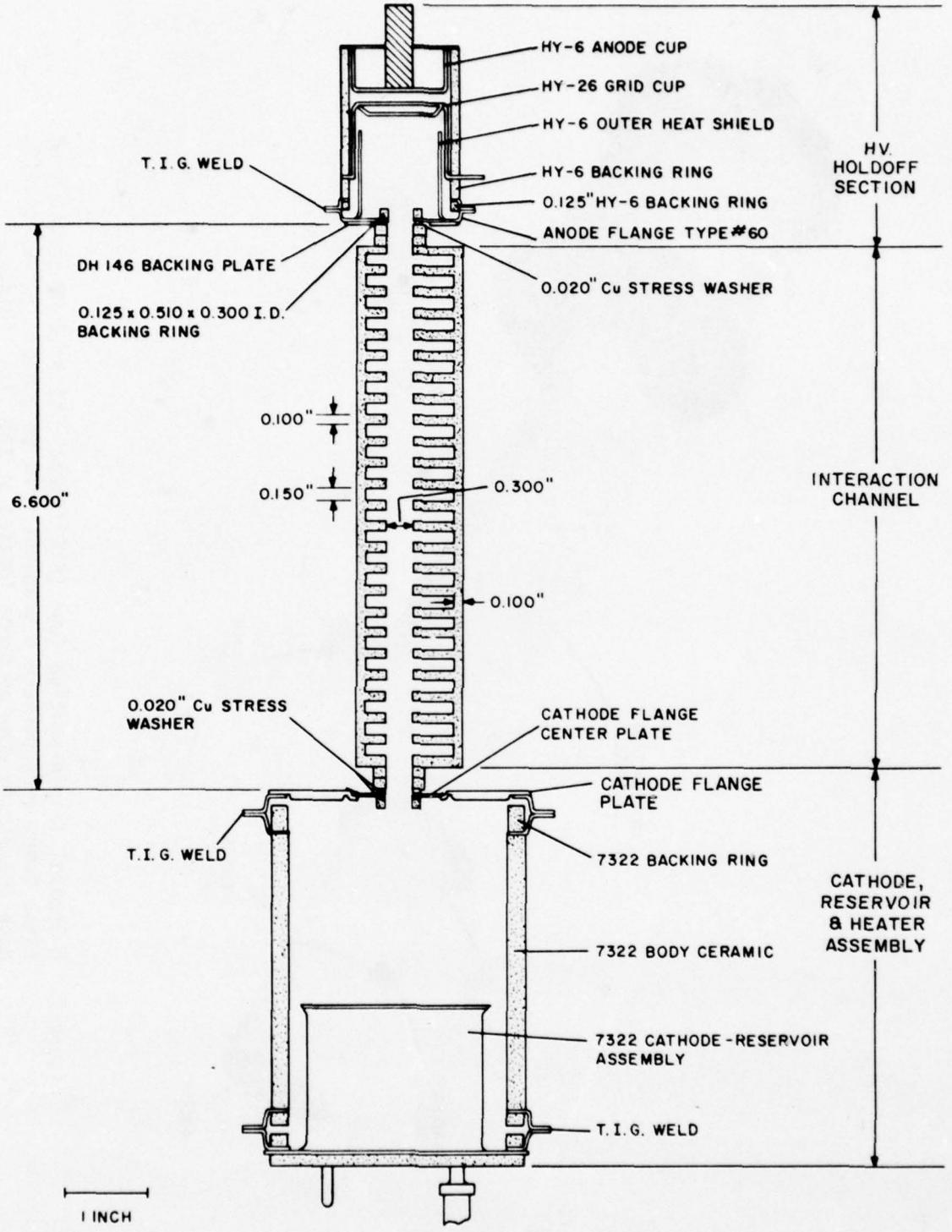

Figure 6. A Typical Single-Section Tube (RSI 10A). The magnetic field was applied in the direction perpendicular to the page.

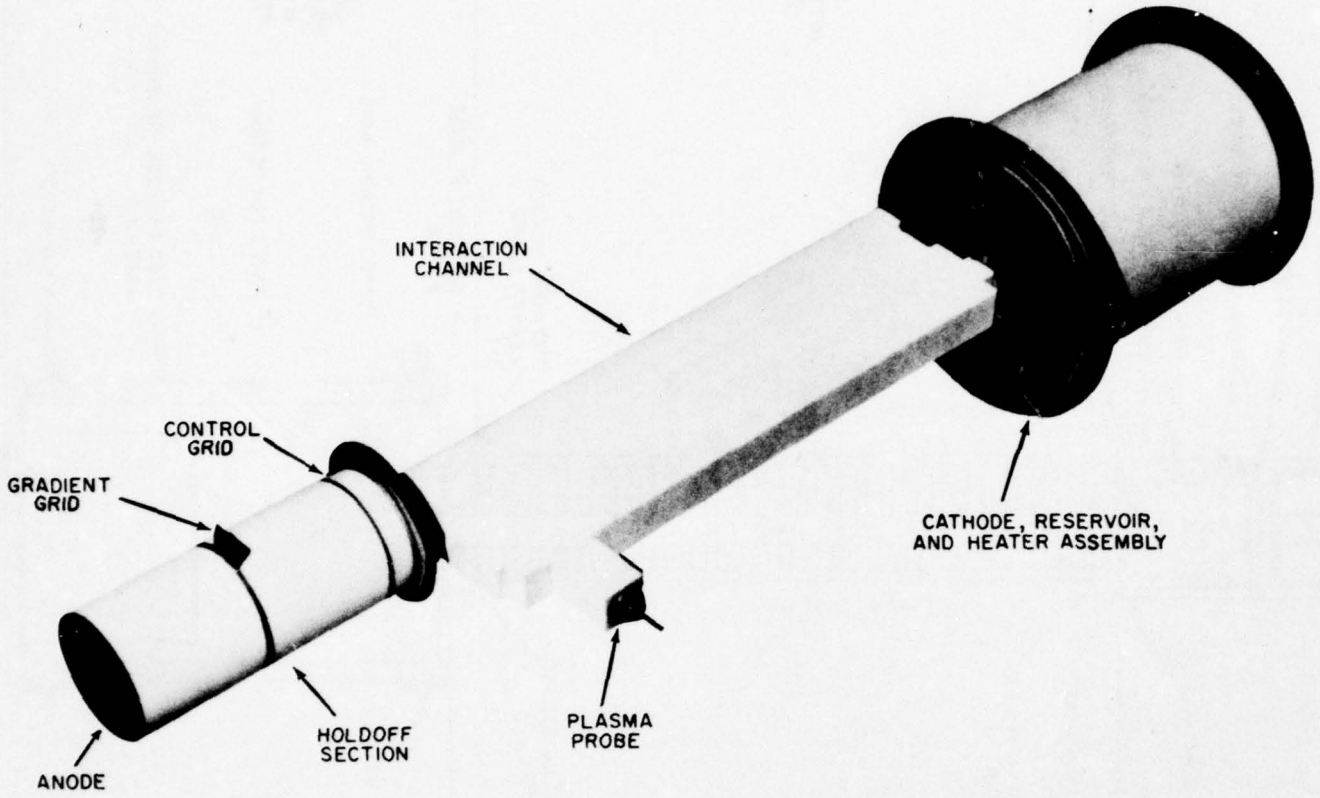

Figure 7. A Typical Triple-Section Tube (RSI 12A2). The holdoff sections of these tubes incorporated a gradient grid to achieve 50 kV holdoff. Note the plasma viewing probe located at the first fold.

(c) Tube Drop

Typical values for ecd, the steady-state drop across the interaction column, were found to average about 300 volts for Types A, B, C, and E. A typical value for Type D was 425 volts, while that for Type DD (twice the column length of Type D but otherwise identical) was about 850 volts when measured under the same conditions. Subsequent (and more accurate) measurements of ecd for the DD tube showed an average column drop of 800 volts. For most tubes, ecd decreases with decreasing pressure over the pressure range of interest, but the change in ecd with pressure is not a dominant aspect of RSI operation.

As the most efficient (and highest voltage) interrupter among the 10 Series tubes, the RSI 10DD was the logical choice for use as a vehicle to study etd, the steady-state tube drop.

Figure 17 shows etd as a function of tube pressure for various values of epy and ib, where a relatively low impedance line has been used to permit values of ib more in keeping with usual thyratron operating conditions. Table 2 shows the same type of data for the high impedance line which provides relatively low values of ib specific to RSI application. Figure 17 and Table 2 show a small decrease in etd with decreasing pressure, but the absolute values of etd are higher in the high current case. These characteristics are emphasized in Figure 18 which shows etd as a function of tube pressure for both the high and low impedance cases. To generate Figure 18, etd was averaged over voltage at each value of P shown - a valid procedure since the currents corresponding to each impedance level differ significantly. Also in Figure 18, the curve for the low impedance case is shown only for the lower pressure region (the region of interest) owing to the relative paucity of data at high P and low Zn as shown in Figure 17. (At high pressure and low Zn, the tube would go into continuous conduction at high epy. To include only low epy data in Figure 18 would unduly weight the average of etd toward low voltage operation.)

Two conclusions can be reached from Figure 17. First, over the current and pressure ranges under consideration (3-18 A for high Zn; 70-300 A for low Zn), etd increases measurably but not significantly with increasing current; second, as the tabulation in Figure 18 emphasizes, etd also increases with increasing pressure to a measurable but not significant extent.

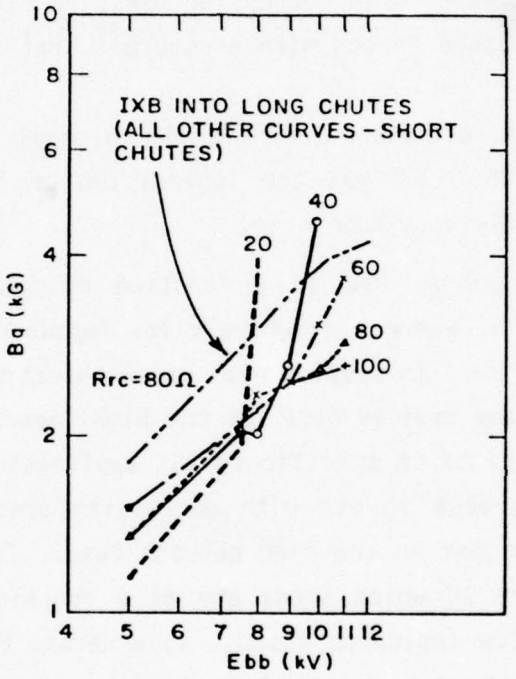

Figure 8. Interruption Characteristics - RSI 10A (P = 300 Microns, N = 10). Note that directing the IXB force into the short chutes provides lower Bq.

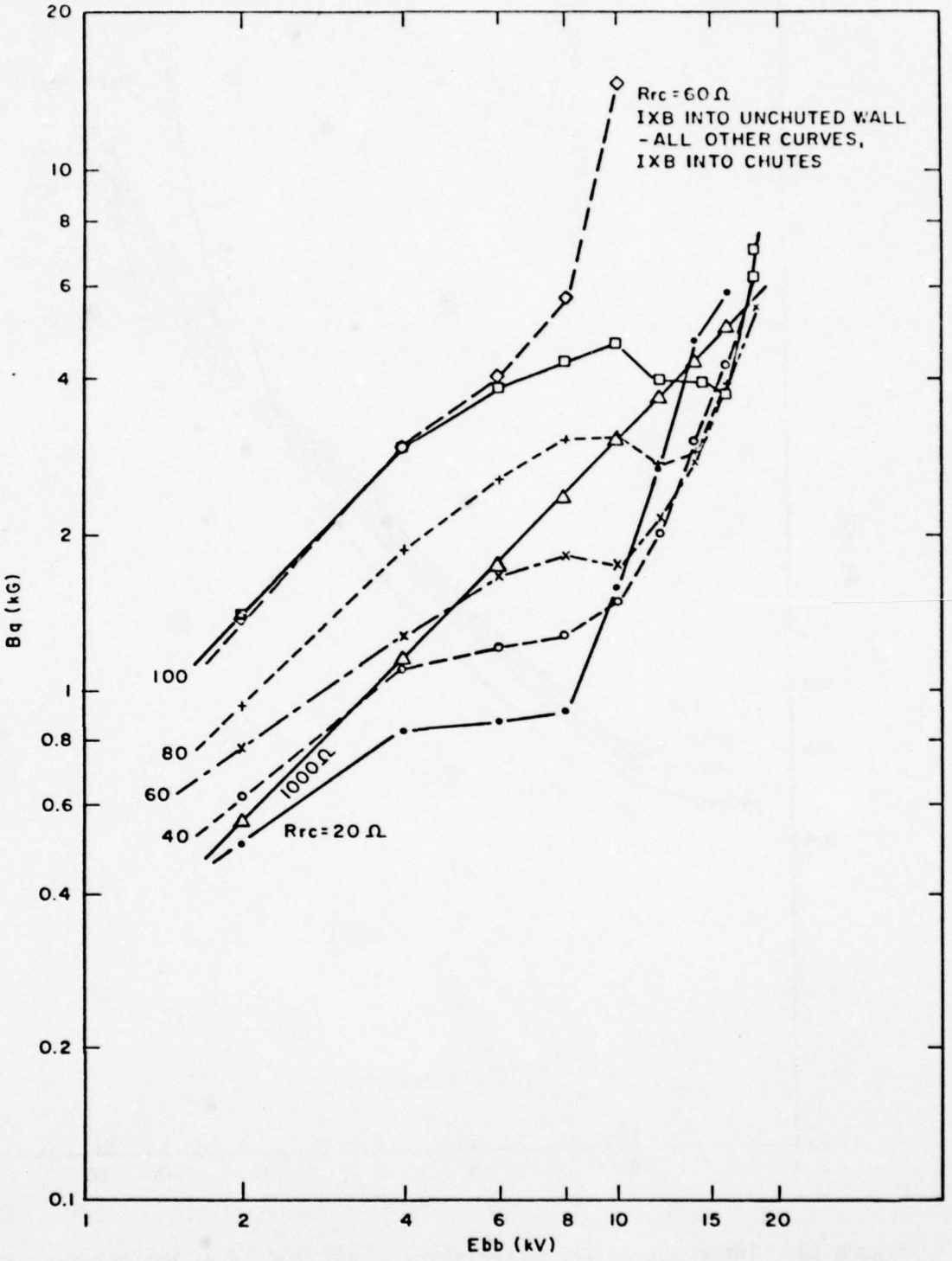

Figure 9. Interruption Characteristics - RSI 10B (P = 300 Microns, N = 10). The relationship between Bq and Ebb is nearly linear at low currents.

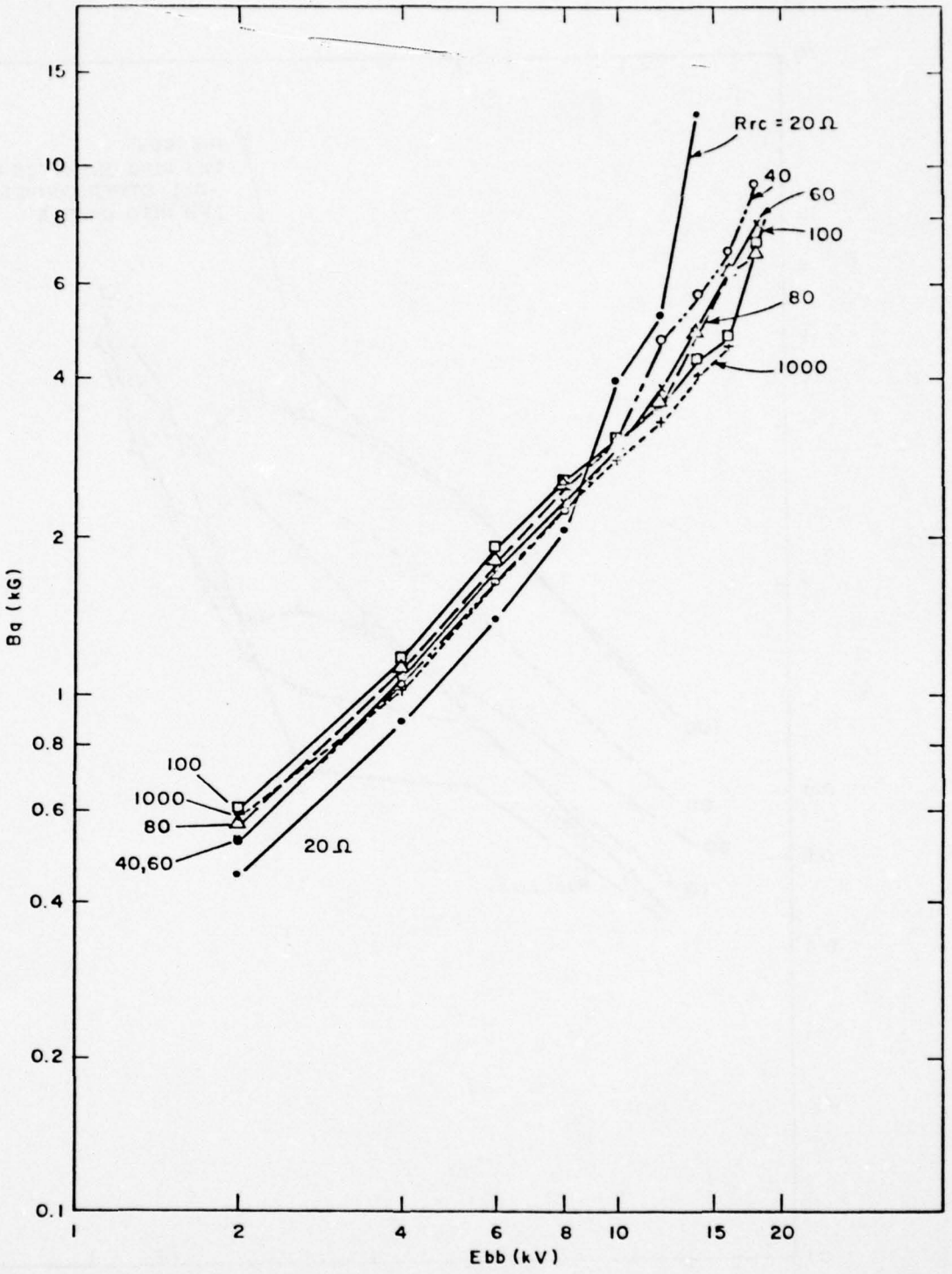

Figure 10. Interruption Characteristics - RSI 10C (P = 300 Microns, N = 10, IXB into Short Chutes). This relatively wide-bore tube with relatively few chutes was one of the least efficient of the 10 Series tubes.

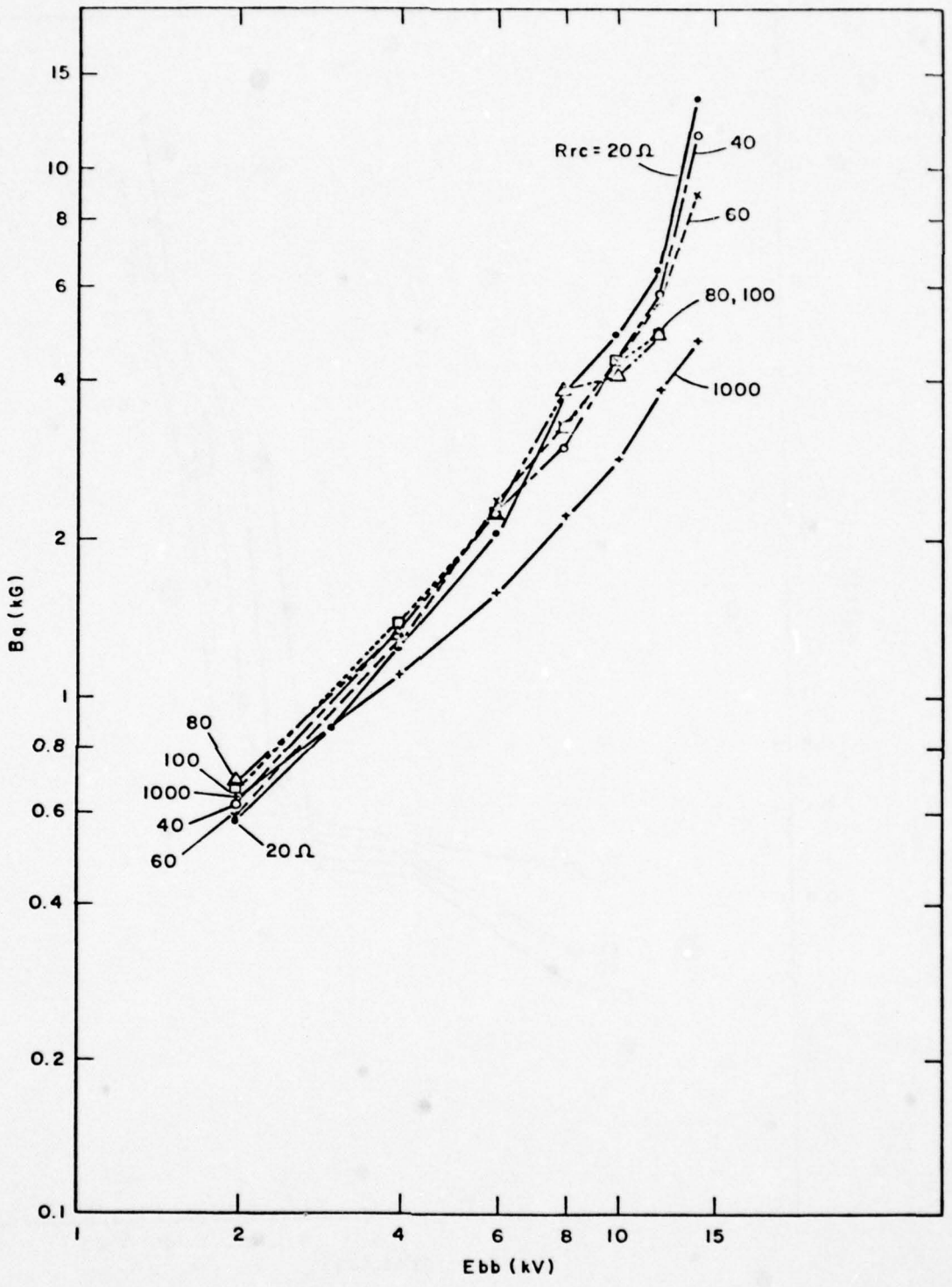

Figure 11. Interruption Characteristics - RSI 10C (P = 300 Microns, N = 10, IXB into Long Chutes).

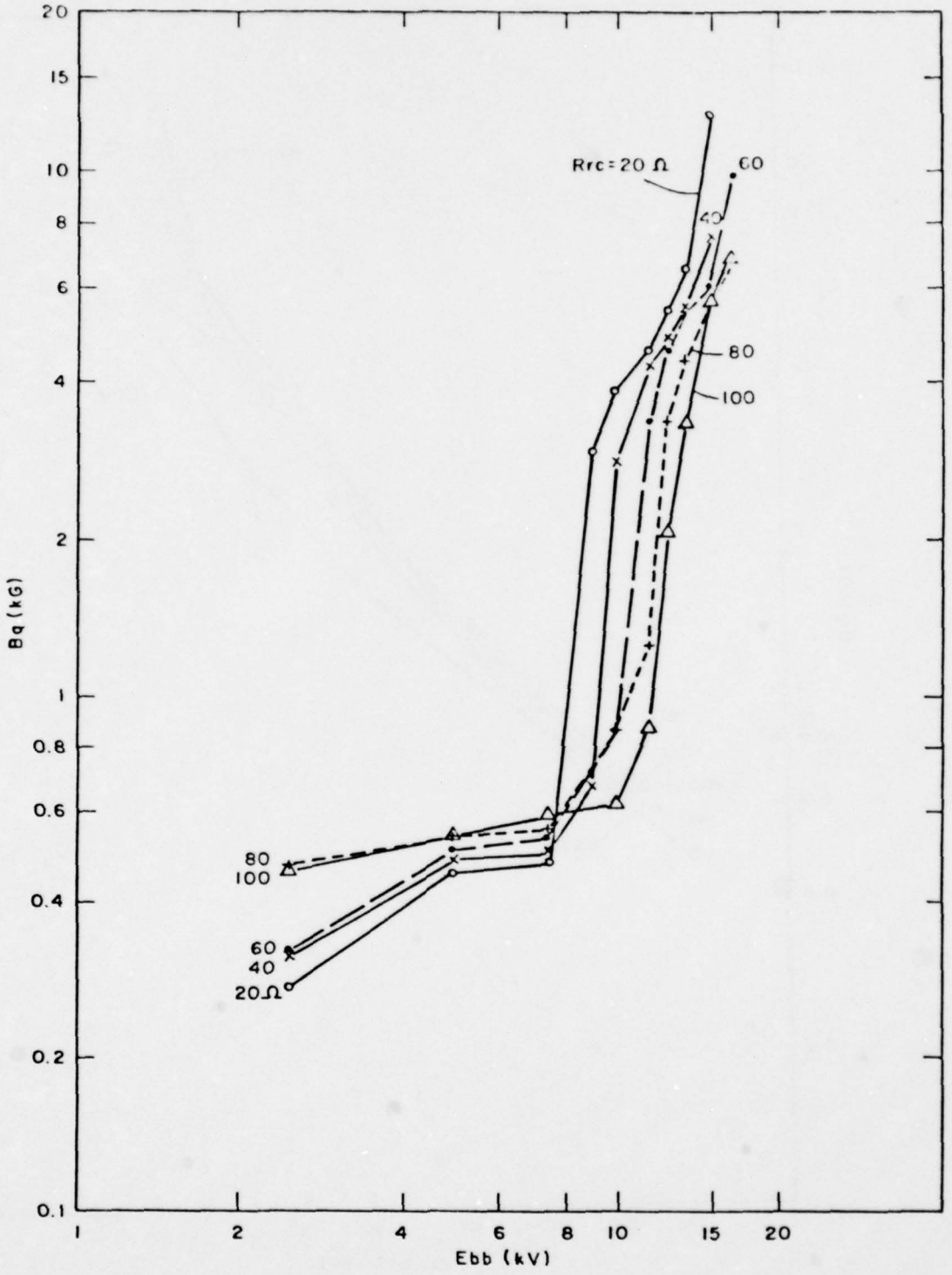

Figure 12. Interruption Characteristics - RSI 10D (P = 300 Microns, N = 10, IXB into Short Chutes). The characteristics of the Type D tube are representative of most of the 10 and 12 Series RSI's.

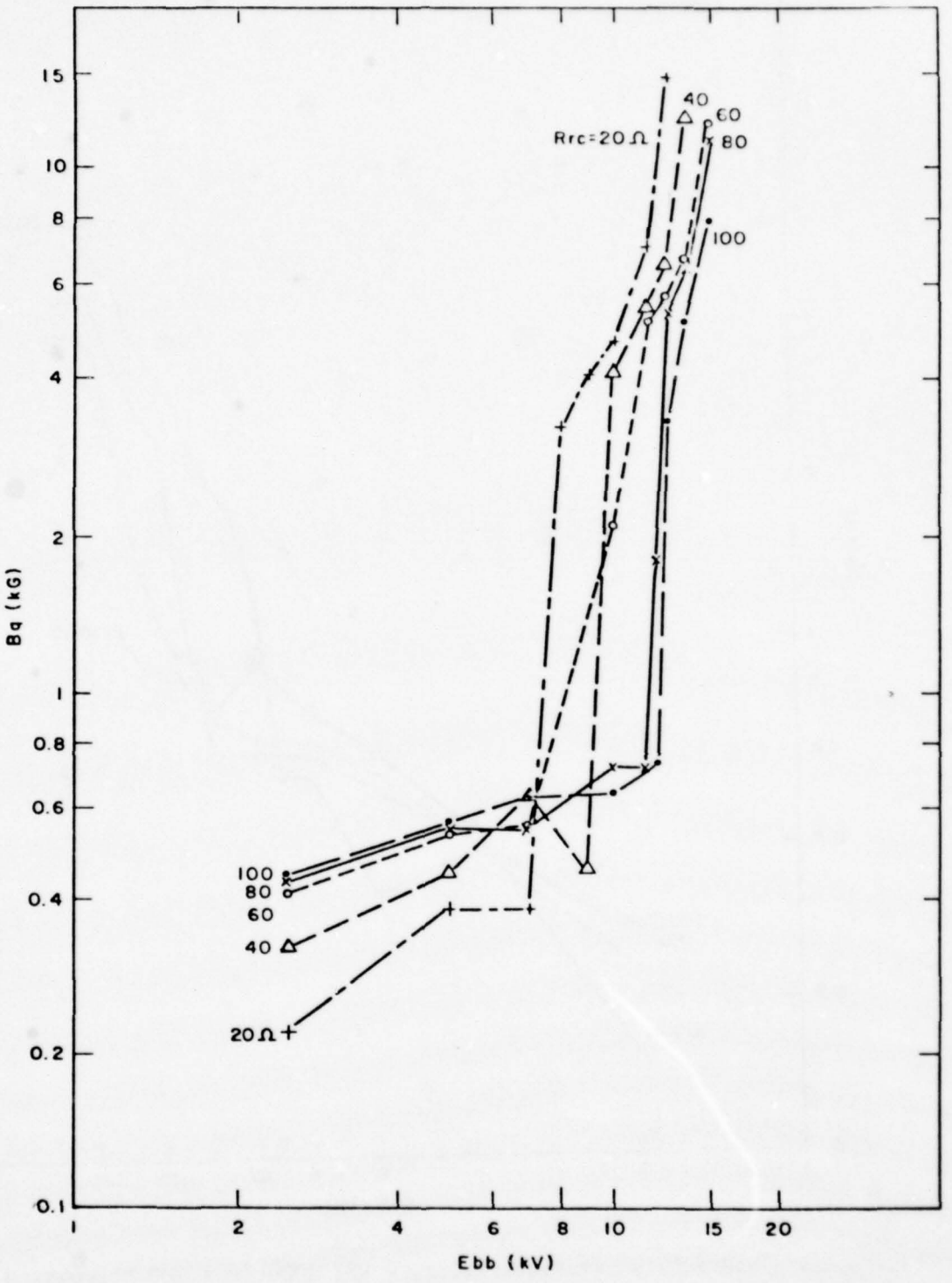

Figure 13. Interruption Characteristics - RSI 10D (P = 300 Microns, N = 10, IXB into Long Chutes).

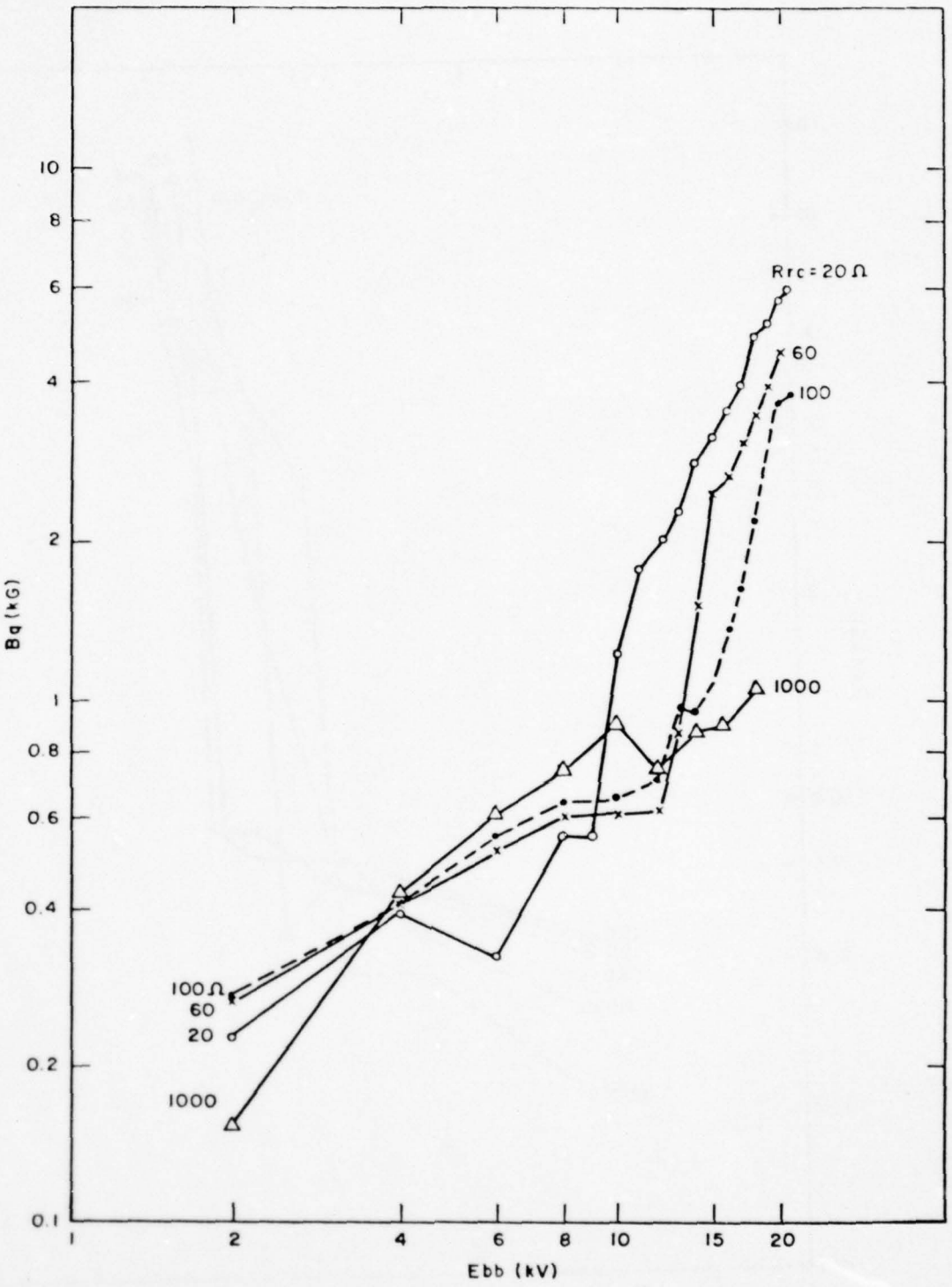

Figure 14. Interruption Characteristics - RSI 10DD (P = 300 Microns, N = 10, IXB into Short Chutes). With its long, folded interaction channel, the RSI 10DD was the most efficient of the 10 Series tubes. This tube successfully interrupted 600 A at 20 kV.

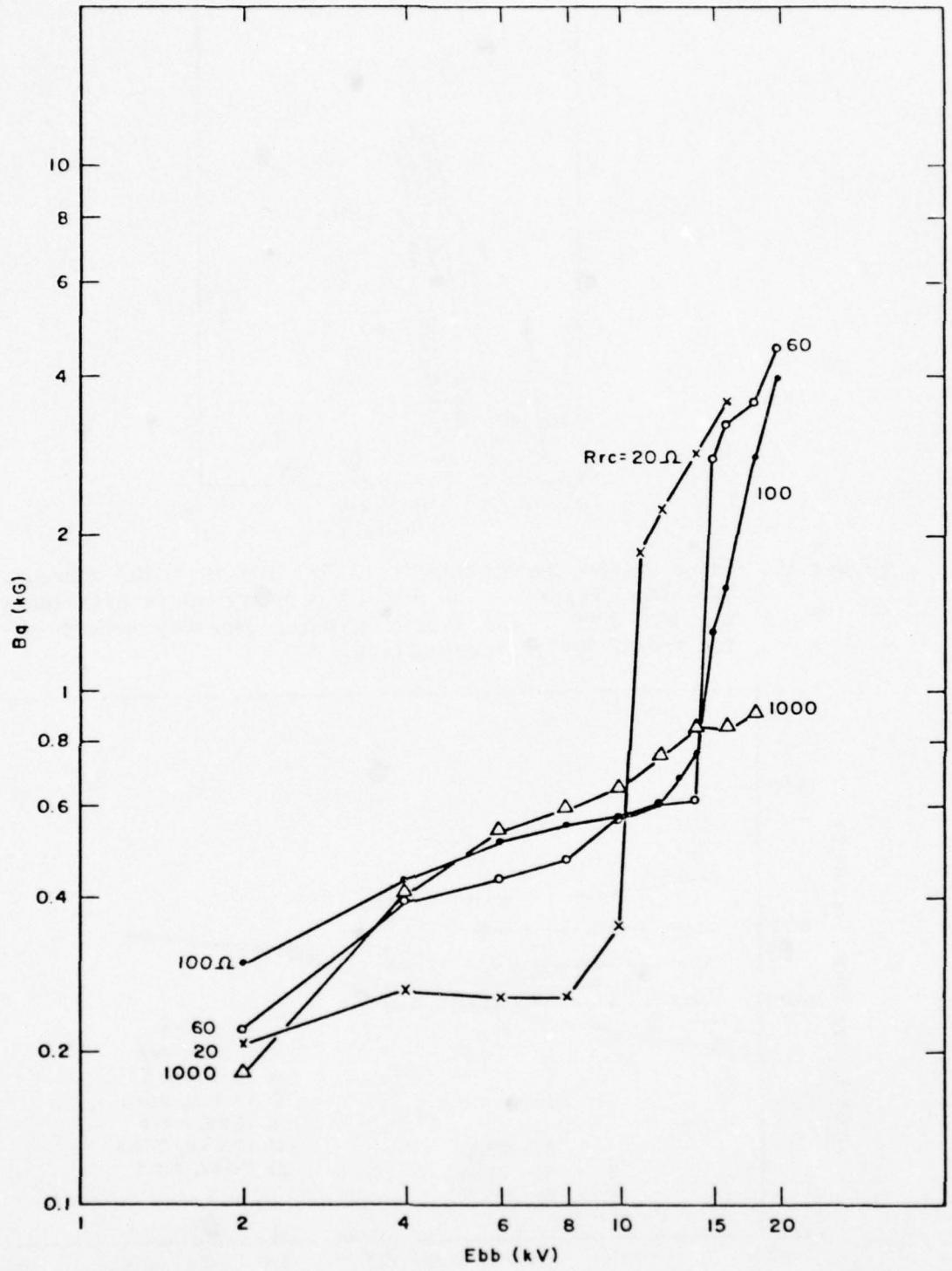

Figure 15. Interruption Characteristics - RSI 10DD (P = 300 Microns, N = 10, IXB into Long Chutes).

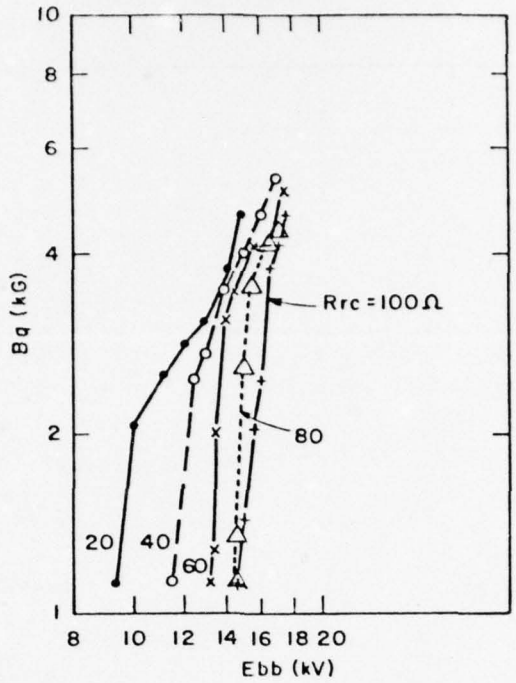

Figure 16. Interruption Characteristics - RSI 10E (P = 300 Microns, N = 10, IXB into Chutes). The RSI 10E was second in efficiency only to the RSI 10DD. The Type E channel geometry served as the base for the 12 Series interrupters.

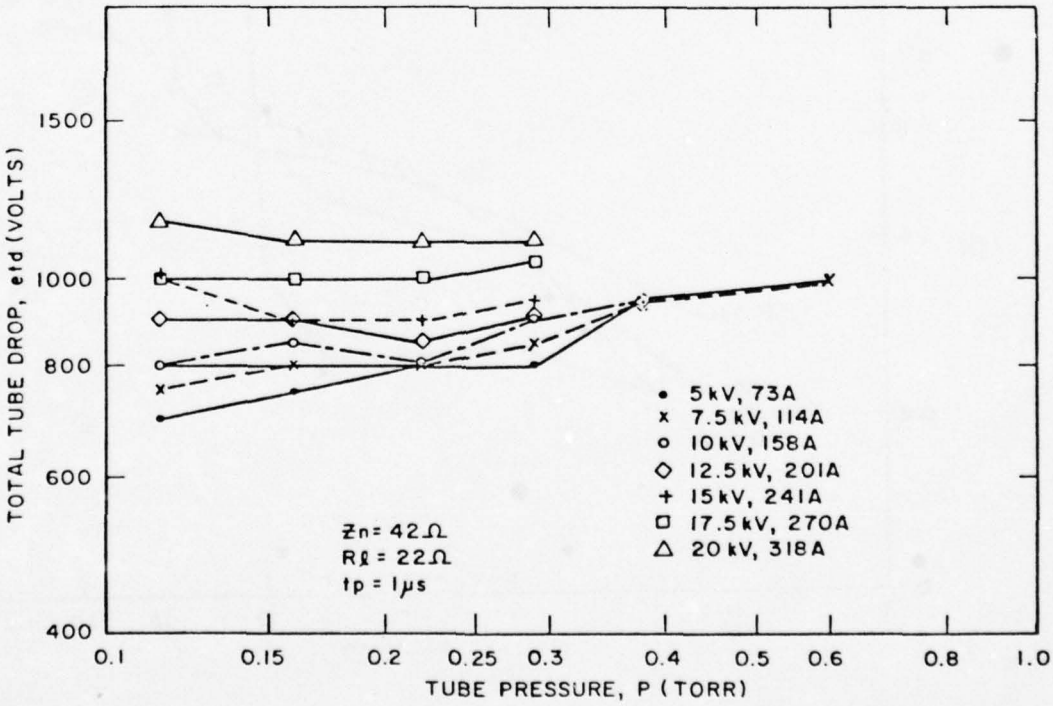

Figure 17. Total Tube Drop as a Function of Pressure at Various Peak Anode Currents - RSI 10DD. The pressure dependence of etd is of little consequence when compared with current dependence.

Table 2. Total Tube Drop, etd, of RSI 10DD. Zn = 600Ω, Rl = 500Ω.

Tube Pressure (microns)	epy (kV)	etd (volts)	ib (amps)	Tube Pressure (microns)	epy (kV)	etd (volts)	ib (amps)
115	5.0	950	3.4	380	5.0	950	3.3
	7.5	900	5.6		7.5	920	5.6
	10.0	825	7.5		10.0	920	7.4
	12.5	810	9.6		12.5	920	9.6
	15.0	800	11.5		15.0	920	11.5
	17.5	800	13.5		17.5	920	13.0
	20.0	800	15.5		20.0	920	15.0
	22.5	750	16.5		22.5	900	16.5
	25.0	800	18.5		25.0	900	18.5
160	5.0	920	3.4	480	5.0	1000	3.4
	7.5	900	5.6		7.5	1000	5.4
	10.0	880	7.4		10.0	970	7.2
	12.5	840	9.6		12.5	960	9.6
	15.0	810	11.4		15.0	960	11.5
	17.5	800	13.0		17.5	950	13.0
	20.0	790	15.5		20.0	950	15.0
	22.5	810	16.5		22.5	940	16.5
	25.0	810	18.5		25.0	930	18.5
222	5.0	900	3.4	600	5.0	1050	3.3
	7.5	880	5.6		7.5	1000	5.4
	10.0	920	7.4		10.0	1000	7.2
	12.5	900	9.4		12.5	1000	9.4
	15.0	860	11.2		15.0	1000	11.5
	17.5	850	13.0		17.5	1000	13.0
	20.0	810	15.0		20.0	1000	15.0
	22.5	810	17.0		22.5	970	16.5
	25.0	810	18.0		25.0	—	—
290	5.0	920	3.4				
	7.5	900	5.4				
	10.0	920	7.2				
	12.5	920	9.4				
	15.0	890	11.1				
	17.5	900	13.5				
	20.0	850	15.0				
	22.5	870	16.5				
	25.0	900	18.5				

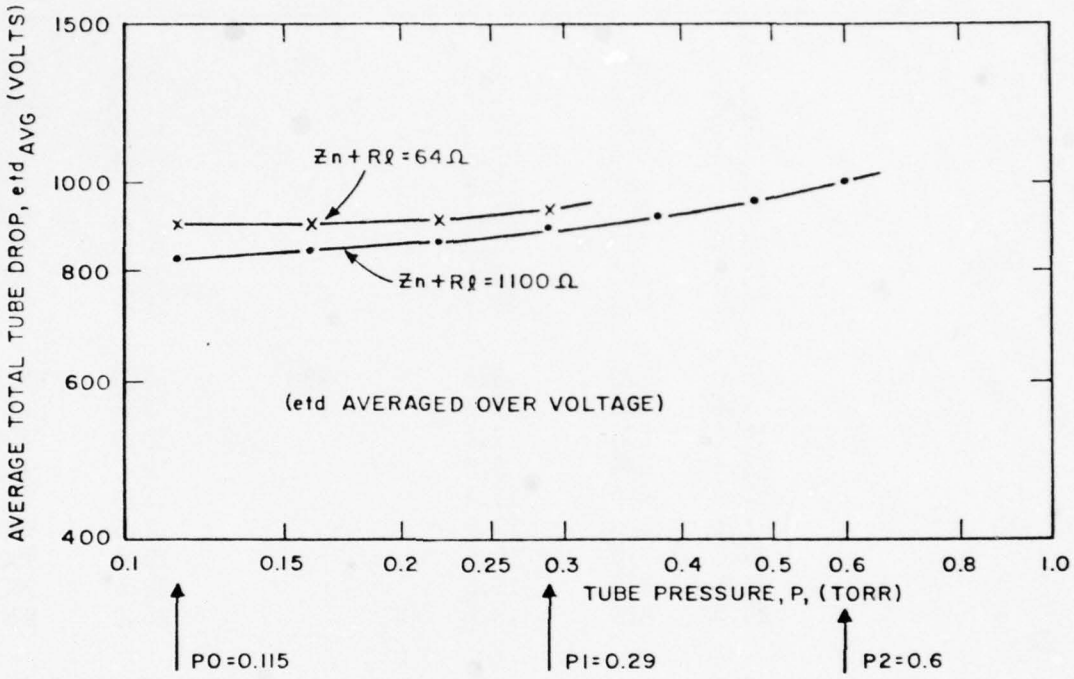

$$\frac{P1}{P0} = 2.5 \qquad \frac{etd_{AVG}\,|_{P1}}{etd_{AVG}\,|_{P0}} = \frac{940}{900} = 1.04 \quad \text{at } Z_n + R_\ell = 64\,\Omega$$

$$\frac{P2}{P0} = 5.2 \qquad \frac{etd_{AVG}\,|_{P2}}{etd_{AVG}\,|_{P0}} = \frac{1002}{826} = 1.21 \quad \text{at } Z_n + R_\ell = 1100\,\Omega$$

Figure 18. Total Tube Drop Averaged Over Voltage as a Function of Pressure - RSI 10DD.

The current sensitivity of etd (as opposed to voltage sensitivity) is illustrated in Figure 19, which shows etd as a function of epy for high and low ib at two typical operating pressures. In the low impedance case, etd increases with increasing epy (and ib), but in the high impedance case, etd decreases with increasing epy. The conclusion is that an optimum ib exists for minimum etd, and this optimum ib lies somewhere between about 20 and 70 A for the values of P of interest.

For the RSI application, the normal ib is of the order of 20 A. To maintain Bq at a reasonable level, and to ensure that the RSI can withstand the anticipated epy, the column length and geometry are variable only to a limited extent. An important consideration is thus the ratio of etd to epy, which serves as a measure of the effectiveness of the RSI as a closed switch. Figure 20 shows this ratio for the RSI 10DD for both the high and the low current cases, with the tube drop averaged over the pressure values of interest. The increase in etd at high currents is reflected in the curve of Figure 20 which corresponds to the high current case, but in the low current case (which applies for RSI "normal" operation), etd is still in the current region where increases in ib reduce etd. Hence etd/epy continues to decrease materially with increasing epy. The overall conclusion from Figure 20 is that tube drops of only a few percent are feasible for an RSI which operates at high epy with a low Bq

(d) Data Evaluation

Modes of Operation

Many observations and conclusions result from a perusal of the various interruption curves of Figures 8 through 16, so it is well to examine a representative set of curves in detail.

Figure 21 shows again the interruption characteristic for the RSI 10D with the IXB force directed into the short chutes. The curves have been sectioned into regions for purposes of the discussion that follows.

The RSI operated in at least two modes (Regions 1 and 3, Figure 21), separated by a transition region (Region 2) wherein Bq increased rapidly with increasing Ebb and also became heavily current-dependent. In the lower power

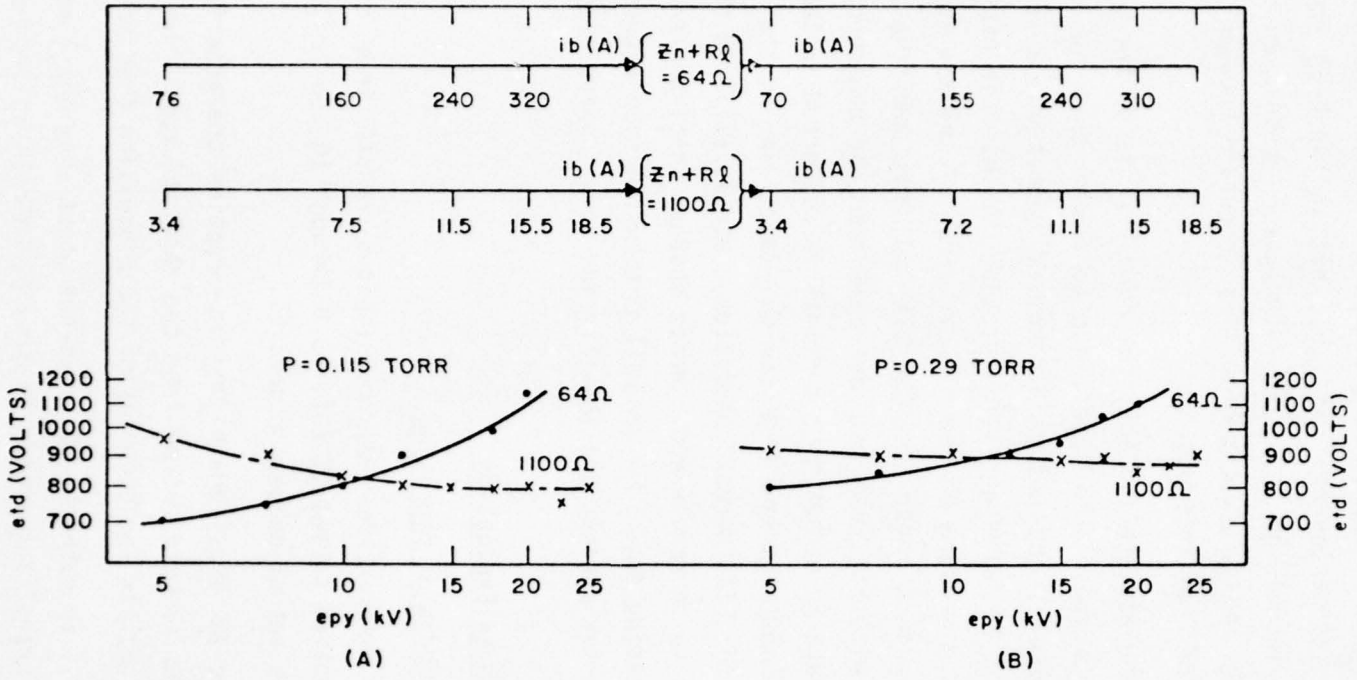

Figure 19. Total Tube Drop as a Function of epy - RSI 10DD. An optimum ib for minimum etd is seen to exist in the region between 20 and 70 A.

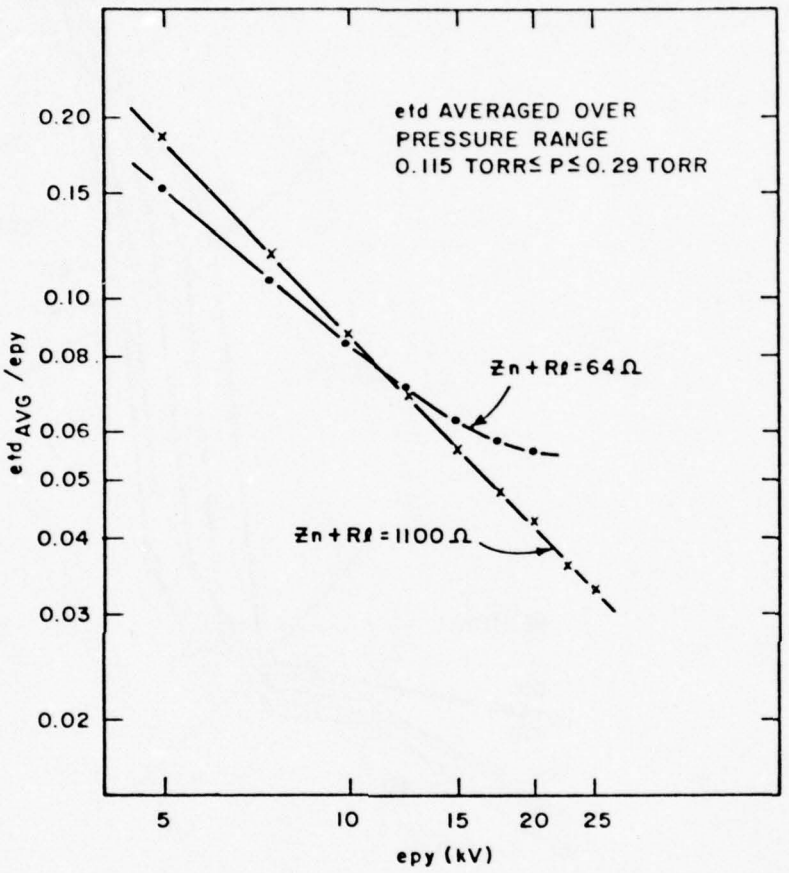

Figure 20. Ratio of etd to epy as a Function of epy - RSI 10DD. This ratio serves as a measure of the effectiveness of the RSI as a closed switch. For the high impedance case, etd is still decreasing with increasing ib, so ratio etd/epy continues to decrease with increasing epy.

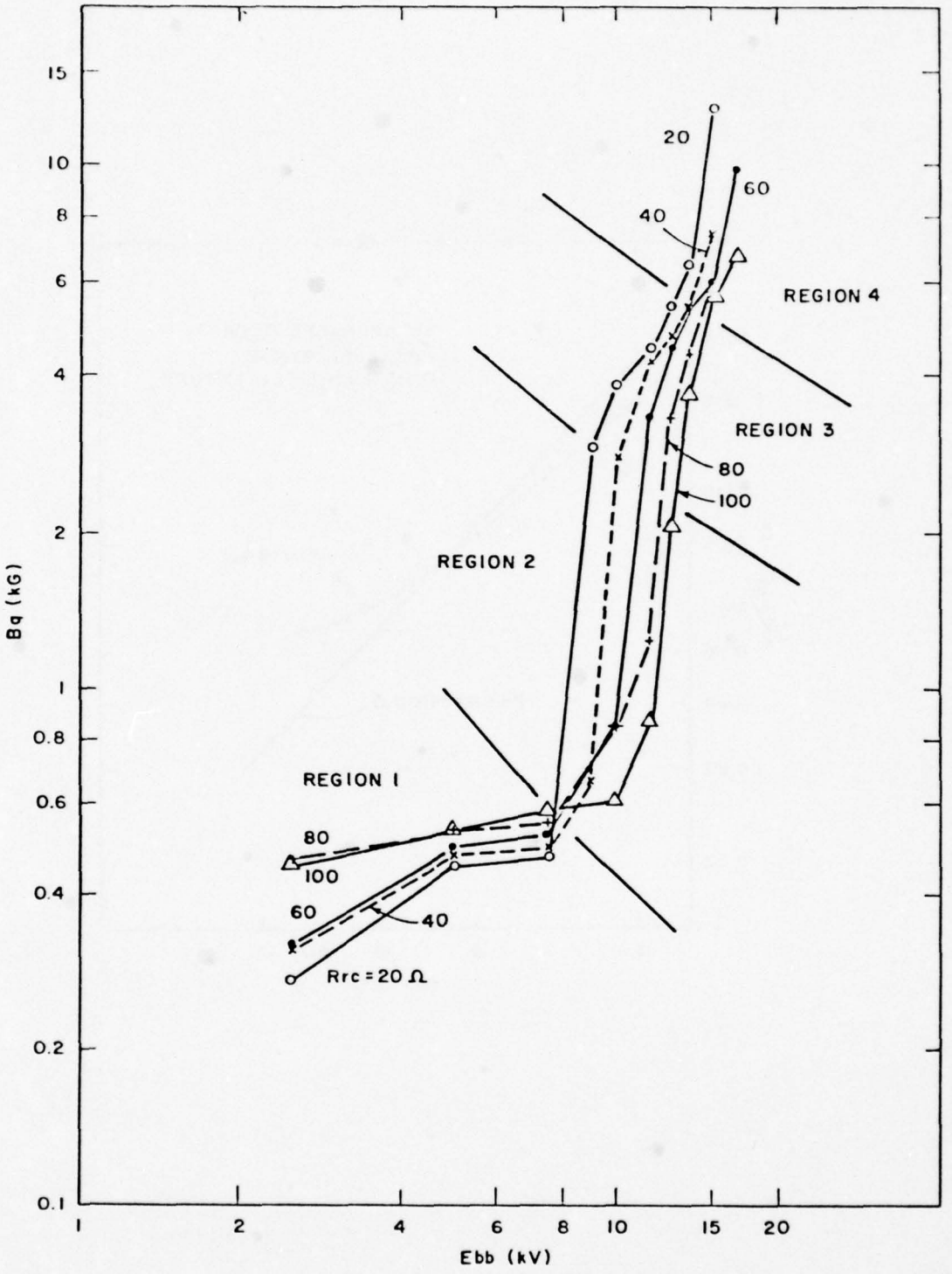

Figure 21. Interruption Characteristics - RSI 10D (P = 300 Microns, N = 10, IXB into Short Chutes). In Region 1, higher currents are more readily interrupted than lower currents, while in Region 3, the reverse is true.

region (Region 1), operation at higher currents reduced the field required to interrupt the discharge at a given Ebb, while in the higher power and transition regions (Regions 2 and 3), the reverse was true. In Regions 1 and 3, the curves exhibit a definable slope and stable operation (repeatable Bq) was readily achievable, but in Region 4, stable operation was difficult to achieve and the tube showed some evidence of arcing in the interaction channel. Various trends exhibited by the RSI 10D, shown in Figure 21, were repeatable for this tube and were also in evidence to varying degrees for each member of the RSI 10 family, as examination of Figures 8 through 16 shows.

Effect of Tube Pressure

The overall shape of the interruption characteristic of Figure 21 strongly suggested that "thin-channel quenching," i.e., the self-interruption of an aperture-bound gas discharge, was a significant factor in the operation of these tubes. This was particularly evident at low Ebb (Region 1, Figure 21) in that for a given Ebb, higher currents were more readily interrupted than were lower currents. At higher Ebb, the electric field was sufficient to cause an immediate "restriking" of the discharge after a self-quench. This theory was supported by the data of Figure 22 which show the interruption characteristic for the RSI 10D (a typical 10 Series tube) with pressure as a parameter. Note from Figure 22 that Bq is heavily pressure dependent in the low-Ebb region, with higher pressure requiring a higher magnetic field to achieve interruption. Such a pressure dependence for Bq is consistent with the self-interruption process.

Although thin-channel quenching is not the only mechanism that can be invoked to explain the pressure sensitivity of the interruption process, it is clear that the tendency of a constricted discharge to self-interrupt plays a significant role in the operation of these tubes. The self-interruption process is discussed in Section 4.0

Effects of Various Chuting Arrangements on Bq

Figure 23 shows a comparison of the performance of several 10 Series RSI's when the IXB force was directed in one case into the long chutes, and in another case into the short chutes. A comparison was also made for the RSI

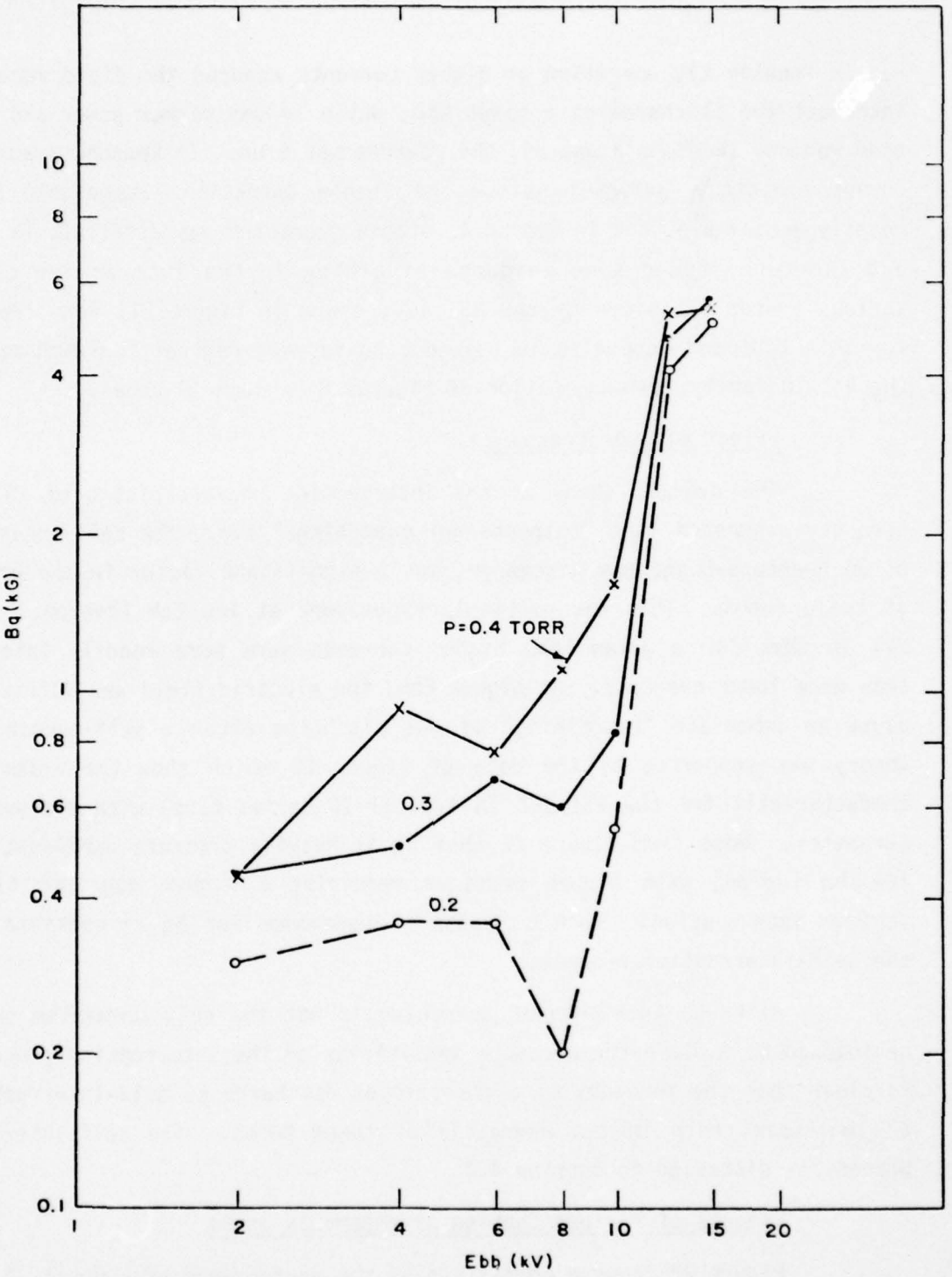

Figure 22. Interruption Characteristics with Pressure as a Parameter - RSI 10D (Rrc = 60Ω, N = 10, IXB into Short Chutes). The interrupting magnetic field is heavily pressure-dependent in the low voltage region.

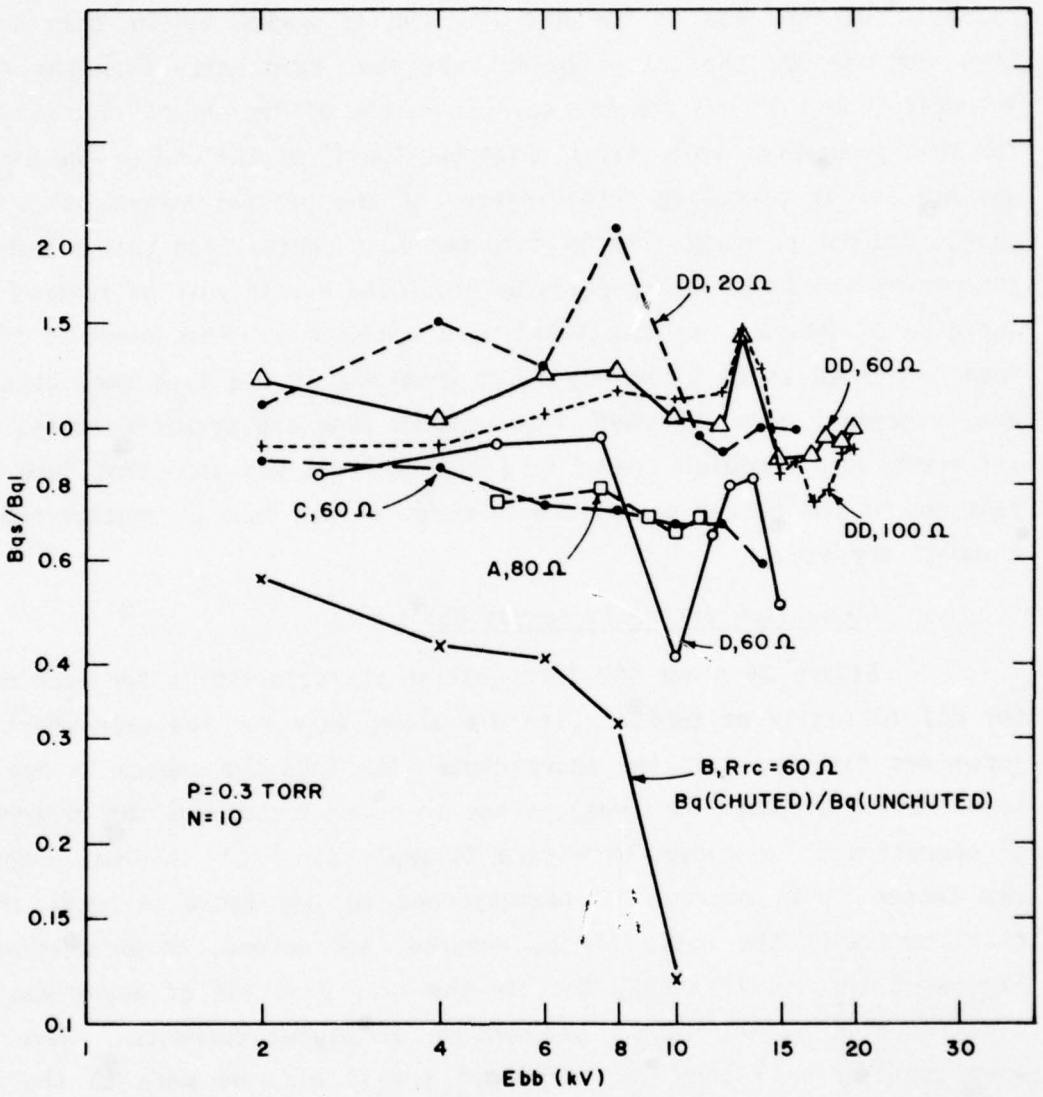

Figure 23. Effect of Various Chuting Arrangements on the Magnetic Field Required for Interruption. Bqs is the field required with IXB directed into the short chutes, and Bql is the field required with IXB directed into the long chutes. In general, the shorter chutes required lower Bq.

10B, which had both chuted and unchuted (smooth) surfaces. For all tubes except RSI 10DD, the ratio of Bqs to Bql (as defined in Figure 23) was less than unity, implying that the short chutes "worked better" than the long chutes. In the case of the RSI 10B, chutes worked better than no chutes. Even for the DD, the ratio Bqs/Bql was less than unity over the region of interest (Ebb > 15 kV) for the several values of Rrc shown. Two explanations for this phenomenon are: first, that the "wall" at the end of the short chute was helpful in promoting recombination of the plasma; second, that the discharge did not penetrate deeply into the long chutes, and that plasma trapped therein hindered the interruption by providing a reservoir of ionized gas. In the case of Tube B, the effect was most pronounced. This might at first have been construed as being merely representative of the fact that chuted tubes are in general more efficient interrupters than are unchuted tubes, but when all tubes were compared (refer to Figure 24), it was seen that Tube B was in fact one of the better overall performers, as was Tube E, another tube having a smooth surface.

Comparison of the 10 Series RSI's

Figure 24 shows the interruption characteristics for each member of the RSI 10 family of tubes. Data are shown only for the case where the IXB force was directed into the short chutes (or into the chutes in the case of tubes having unchuted surfaces), since in general this was the preferred mode of operation. The curves of Figure 24 apply for Rrc = 20 ohms. This value was chosen first because it corresponded to the fault currents that were consistent with the goals of the Program, and second, as an examination of Figures 8 through 16 shows, because the true behavior of any given tube is best revealed by the tube's performance at higher currents. Nevertheless, when considering Figure 24, reference should also be made to the detailed curves for the tubes in question, since marked differences do exist as a function of fault current for any given tube.

From Figure 24, the RSI 10DD clearly emerged as the most successful of the 10 Series tubes. This tube had successfully interrupted 600 A at 20 kV with a magnetic field energy of less than 8 joules. Under non-fault conditions, the DD had been operated at 25 kV, 18.5 A with a total tube drop of 830 volts, or 3.3% of epy.

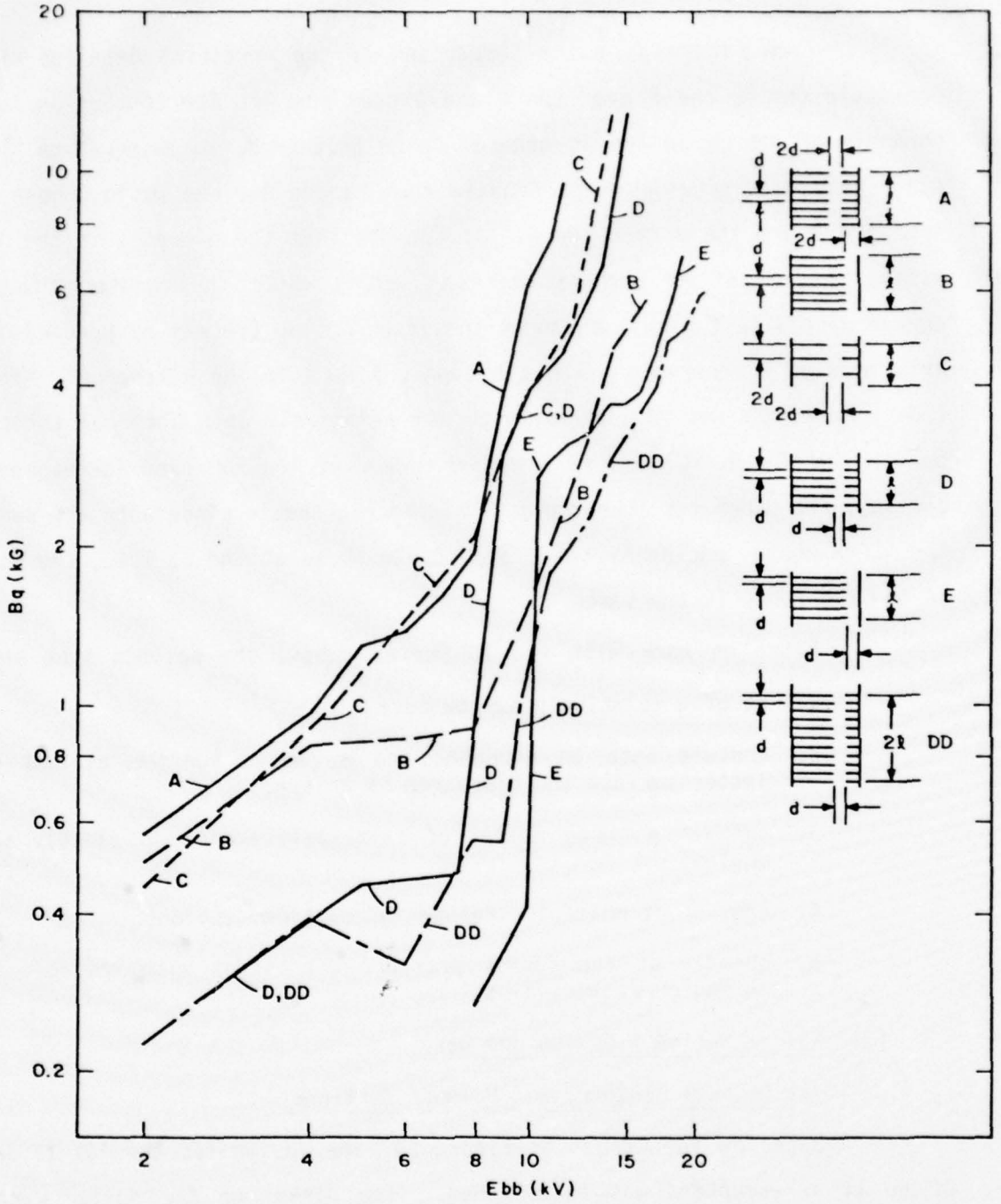

Figure 24. Interruption Characteristics - RSI 10 Series (P = 300 Microns, N = 10, Rrc = 20Ω, IXB into Short Chutes for Chuted Tubes, IXB into Chutes for Tubes with a Smooth Wall). Type DD was the most efficient of the 10 Series tubes, and Type E was the most efficient among those tubes having but a single (unfolded) interaction section.

From Figure 24 and a comparison of the pertinent detailed curves, one would choose the E over the B and D over the A. The conclusion is that channels of narrow ID are in general to be preferred, an observation that is consistent with previous data. Again from Figure 24, one would choose the E over the D and the B over the A. It appears that the presence in the interaction channel of an unchuted surface, along which the uninterrupted discharge most likely flows, enhances the interruption process by precluding the existence of a reservoir which can supply plasma to the discharge. Finally, from Figures 10 and 24, the C, with its relatively open internal structure, behaves as though it were an unchuted tube. At low Ebb (and correspondingly low ib), the C behaves like the D. This is reasonable since both the bore and the inter-chute spacing of the C are double those of the D; i.e., the scaling of the two tubes is the same.

Based on work with the 10 Series tubes, the optimum tube should:

1. be of a relatively narrow bore;
2. contain both an unchuted and a chuted surface against which latter surface the discharge is driven;
3. contain a large number of relatively short and closely spaced chutes;
4. consist of multiple, folded interaction sections;
5. operate at the lowest pressure consistent with reliable triggering characteristics.

(3) RSI 12 Series - Design and Data

(a) Channel Geometry and Holdoff Sections

Based on the curves of Figure 24, the design for the RSI 12 Series of 50 kV interrupters was established. The bases for the design were the relative performances of 10 Series Types E and DD relative to those of the

other 10 Series tubes. Type E showed that one wall should be smooth, while Type DD established that multiple, folded interaction sections better utilized the available magnetic field while simultaneously allowing operation at higher Ebb for a given electric field in the interaction region. The conclusion was that a Type EEE tube would meet the requirements for an efficient interrupter capable of operating at 50 kV.

Figure 25 shows in schematic form the channel geometries which were finally chosen for the RSI 12 Series of 50 kV tubes. Each tube was a triple-section design (folded twice), with each section being 7 inches long (E = 937 V/cm during interruption and 23 V/cm during conduction). A chute wall thickness of 0.75 inch (dimension "t" in Figure 25) was the minimum consistent with ease and reliability of fabrication, and this minimum thickness was chosen to achieve the maximum number of chutes over the length per section, l.

Six geometries are indicated in the tabulation of Figure 25. The dimensions of interest for each tube type are D, the diameter of the bore; x, the depth of the chute; y, the height of the chute; and z, the width of the chute. The tabulation calls out these dimensions; the more important points are discussed below.

Tube Type A was the base tube for the 12 Series. It was patterned after the most efficient of the single-section 10 Series tubes, the RSI 10E.

All tubes except the B had a bore diameter of 0.150 inch; this diameter worked well with the RSI 10E, the forerunner of this series, as well as with other 10 Series tubes. Type B had a bore of 0.100 inch, since in general smaller bores lower Bq. A bore of 0.100 inch was still well above the self-quenching current density limit for the RSI "normal" current of 17 A.

All tubes except Type C had a chute depth of 0.250 inch, which corresponded to the "short" chutes of the 10 Series. The purpose of the 0.150 inch chute depth in Type C was to determine if the "end of chute wall" aided in interruption.

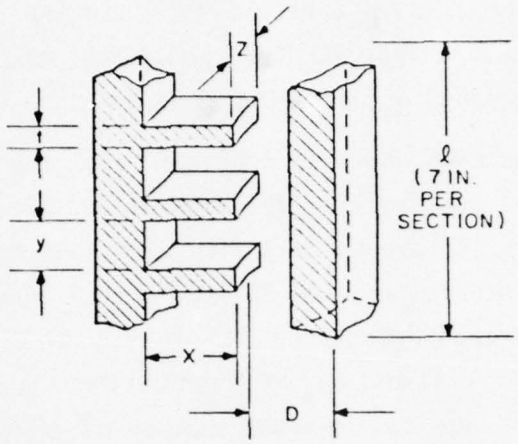

Type	D	x	y	z	Notes
A	0.150	0.250	0.150	0.300	Base Tube
B	0.100	0.250	0.150	0.300	Small Diameter
C	0.150	0.150	0.150	0.300	"End Wall"
D	0.150	0.250	0.100	0.300	Maximum Chutes
E	0.150	0.250	0.125	0.300	Chutes at 45°
F	0.150	0.250	0.150	0.150	Minimum Reservoir

- All dimensions in inches.
- All sections 7 inches long (l).
- Three sections per tube (31).

Figure. 25. Interaction Channel Geometry - RSI 12 Series. Type A geometry was the base of 12 Series, with various other geometries being only minor departures in those directions expected to lower Bq.

All tubes except Types D and E had a chute height of 0.150 inch. This was the same height as in the RSI 10E and other 10 Series tubes. The purpose of the 0.100 inch chute height in Type D was to determine whether increasing the number of chutes reduced Bq.

Type 12E was a special case obviously chosen to determine whether altering the channel geometry to accommodate the assumed trajectory of the electrons would reduce Bq.

All tubes except Type F had a chute width of 0.300 inch, the same width as in the 10 Series of tubes. The purpose of the 0.150 inch chute width in Type F was to determine whether minimizing the possible plasma reservoirs would lower Bq.

The approach used in the design of the RSI 12 Series of tubes was conservative in that "safe" dimensions were used throughout; i.e., all "base" dimensions were known to have worked satisfactorily in the past, and in those cases where dimensions were changed, the change was in a direction believed to reduce Bq.

Figure 26 shows the holdoff section design that was chosen for the 12 Series of tubes. The design was based on that of the 30 kV holdoff section incorporated into the RSI 10DD, with consideration given to the cost advantages that accrue when standard production components are used. To achieve a 50 kV holdoff capability, a gradient grid was required, and an E-E spacing of 0.140 inch was used. (A spacing of 0.138 inch had been successfully employed with the 30 kV holdoff section of the RSI 10DD, and both designs were operable over the same pressure range.)

The grid-grid baffle spacing shown in Figure 26 is 0.106 inch, which value was that of the RSI 10DD. Various apertures shown in Figure 26 were chosen to have a calculated self-quenching current of 420 A - several times the limit imposed by the 12 Series interaction channels.

As shown in Figure 26, in one case the apertures in the gradient grid were offset with respect to one another in accordance with standard practice; in the other, they were located in line. The rationale for the in-line aperture arrangement was to determine if such a scheme might result in improved triggering characteristics or reduced steady-state drop without materially degrading the forward holdoff characteristic of the structure as a

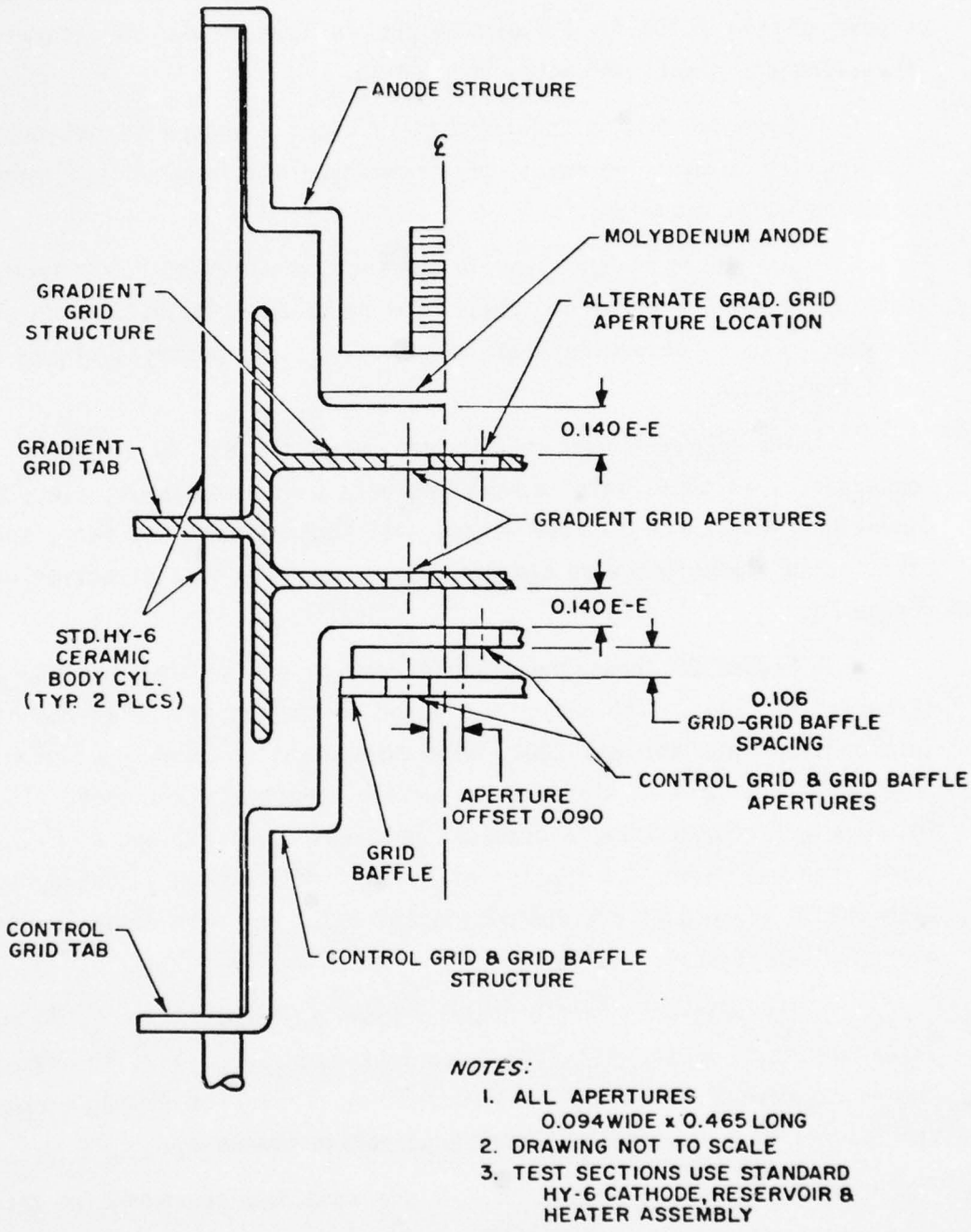

Figure 26. Fifty Kilovolt Holdoff Section Designed for the 12 Series Tubes. As expected, the offset gradient grid apertures provided the better holdoff characteristic.

whole. Two test vehicles (designated RSI 13A and 13B) were built and tested to verify the efficacy of the basic holdoff section design. The 13A was built with the gradient grid apertures offset, and the 13B with the apertures in line. Both tubes had standard EG&G Type HY-6 cathode-reservoir assemblies.

The 13A and 13B performed well, and had, in fact, nearly identical triggering characteristics and steady-state drops. As expected, the 13A (offset apertures) provided the better holdoff characteristic, with epy greater than 50 kV being achievable at pressures well above the minimum required for reliable triggering. The 13A-type of holdoff section was chosen for the 12 Series tubes, all of which successfully held off 50 kV as shown in Figure 27.

(b) Interruption Characteristics

The RSI 12's were tested in substantially the same manner as were the RSI 10's, with the only significant difference being that the RSI 12's were operated at higher Ebb. The first 12 Series tube to be completed and tested was the RSI 12A. This tube suffered mechanical damage during its fabrication, and subsequently developed a leak. A duplicate Type A (designated RSI 12A2) was later built and tested, and the interruption data included in this report for the Type A geometry are those corresponding to the RSI 12A2.

It was first verified that the 12 Series tubes would operate most efficiently when the discharge was driven into the chuted wall (as opposed to the smooth wall), and also that the general trends observed for the 10 Series devices would also be in evidence for the 12 Series tubes. Representative data of this nature for the RSI 12C are shown in Figure 28. Note from Figure 28 that the chuting materially reduced Bq at any given values of Ebb and Rrc, and that the general shape of the interruption characteristic is substantially the same as that found to be typical for the 10 Series tubes, with the similarity extending to all operating regions.

Figures 29 through 34 show the interruption characteristics for each member of the RSI 12 family for various values of Rrc, N, and Eres with IXB directed into the chutes.

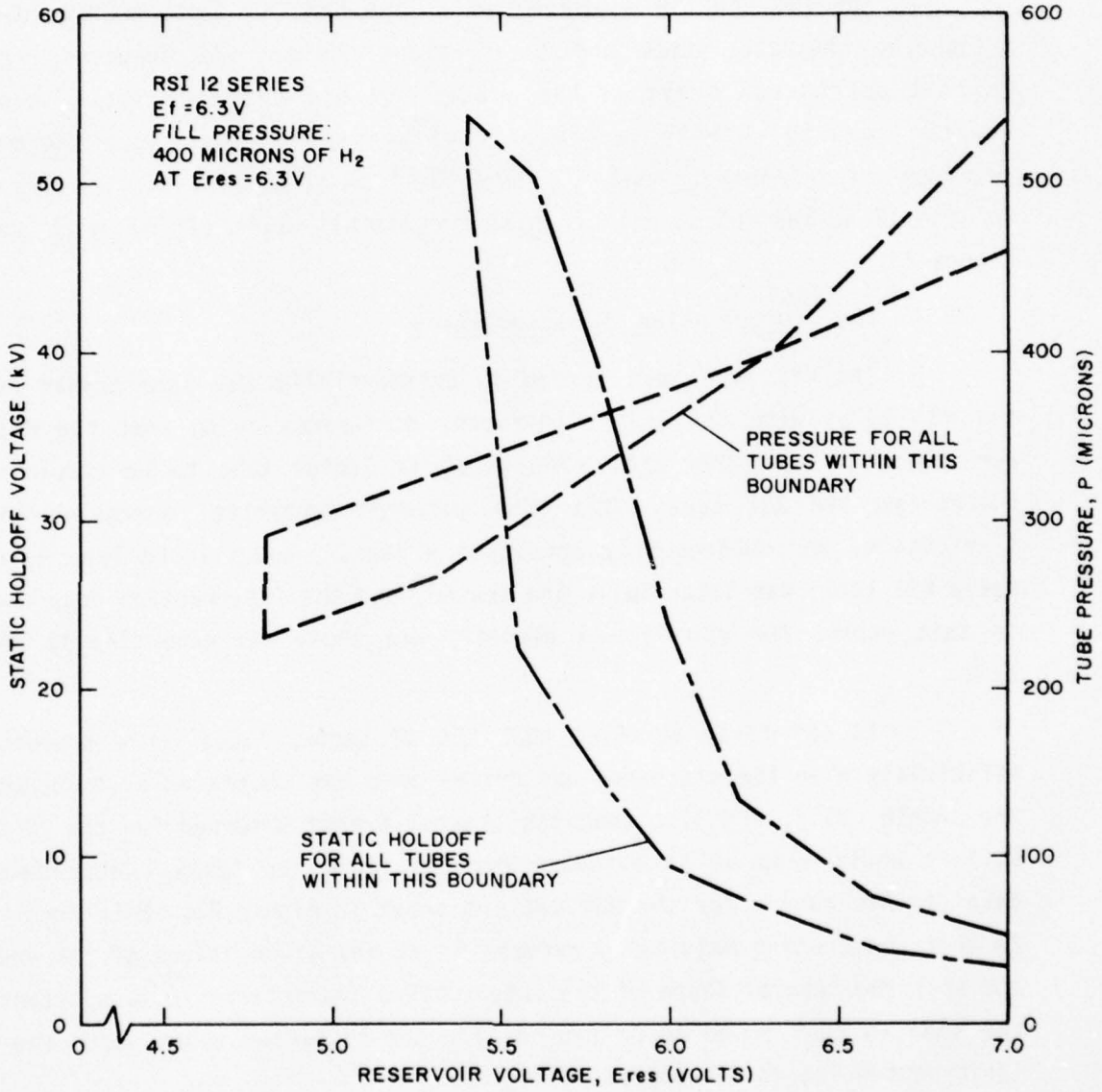

Figure 27. Static Holdoff Characteristics - RSI 12 Series. All tubes successfully held off at least 50 kV at reasonable gas pressures.

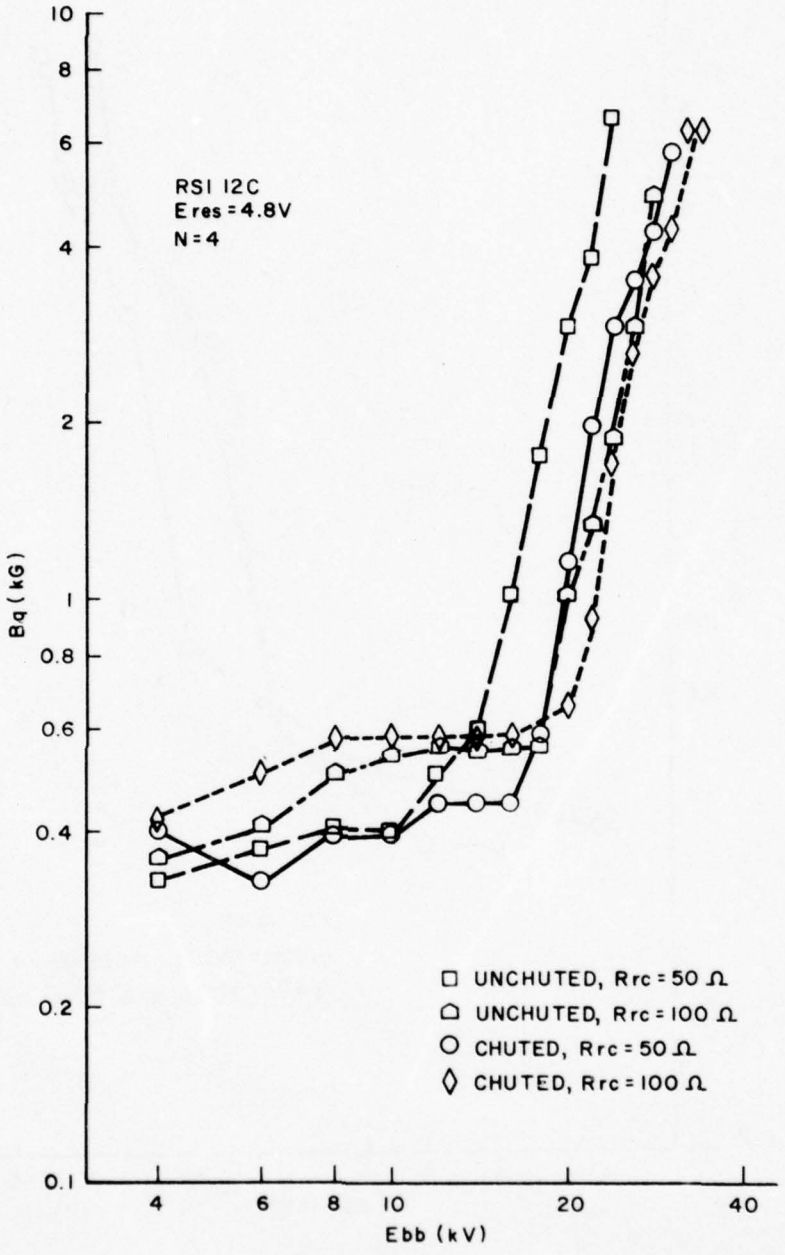

Figure 28. Interruption Characteristics - RSI 12C. Directing IXB into the chutes again provided the lower Bq. The overall shape of the interruption characteristics is similar to that observed for the 10 Series of tubes.

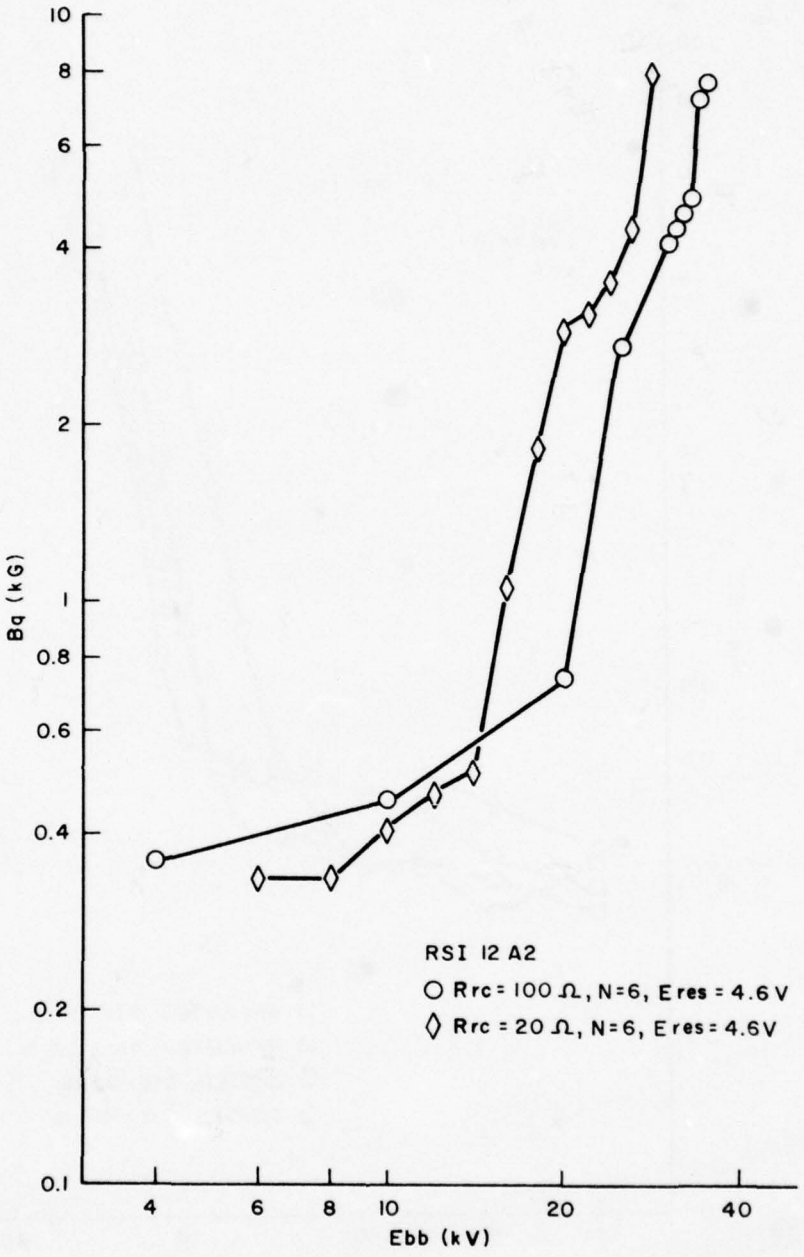

Figure 29. Interruption Characteristics - RSI 12A2. To preclude the possibility of damage to the RSI's before a comparison of various interruption characteristics could be made, Ebb was limited to 35 kV. Data are shown here and in Figures 30 through 38 only for IXB directed into the chutes.

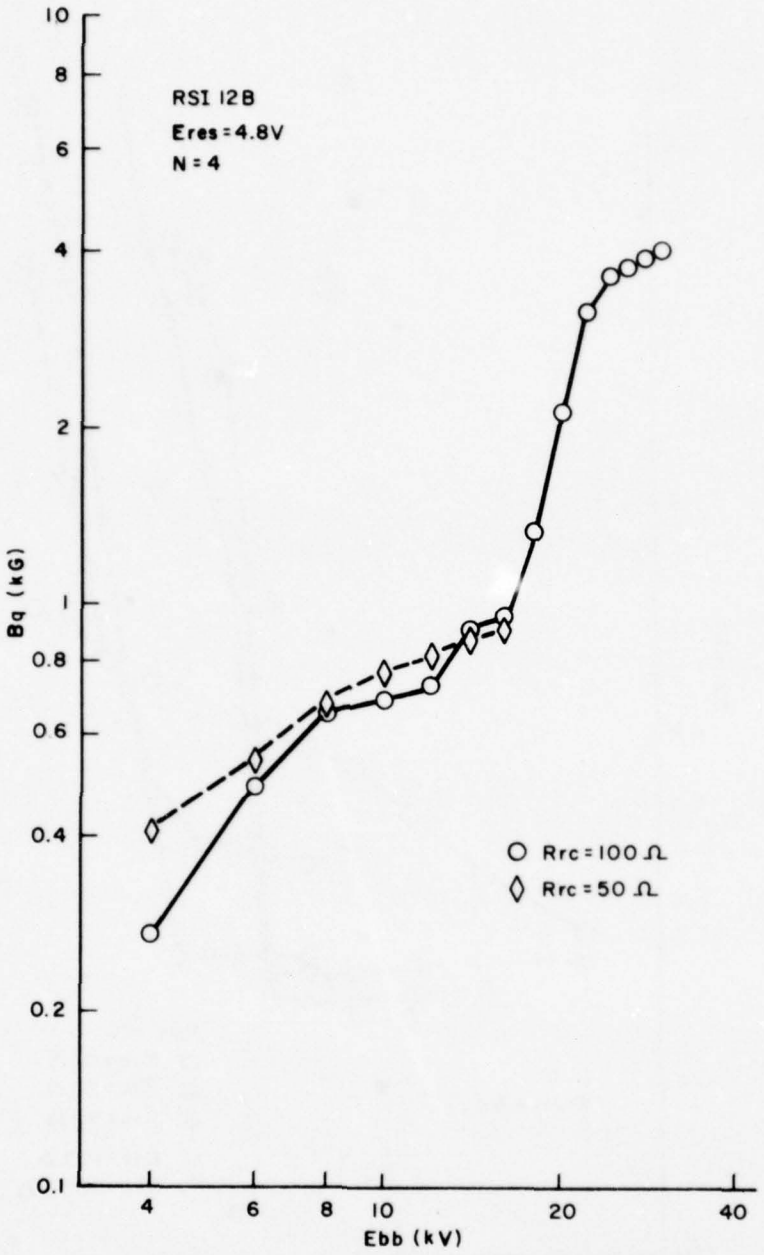

Figure 30. Interruption Characteristics - RSI 12B. Because of its relatively narrow bore, this tube would operate satisfactorily only at a relatively high pressure compared to the other 12 Series tubes. The 12B was the least efficient of the 12 Series designs. (Refer also to Figure 35.)

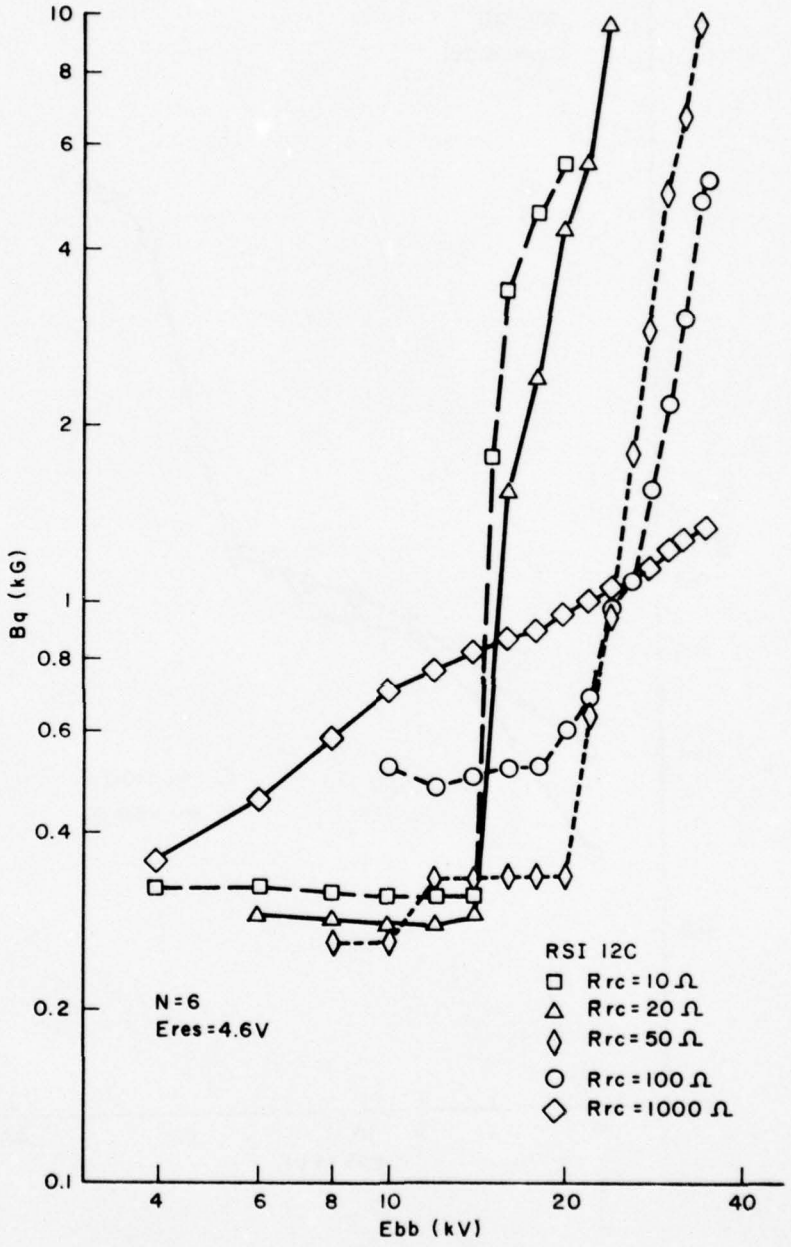

Figure 31. Interruption Characteristics - RSI 12C. This tube was later operated with epy = 50 kV (Figure 36).

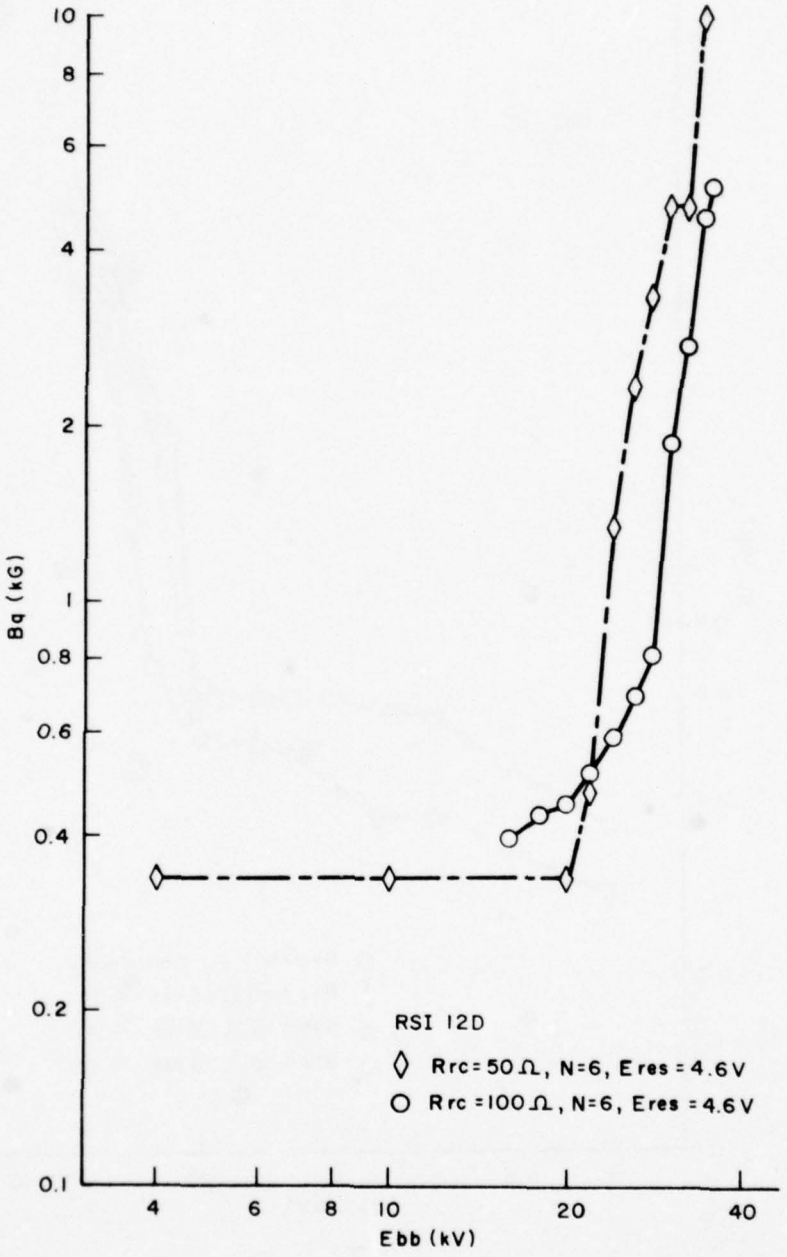

Figure 32. Interruption Characteristics - RSI 12D. This tube had the largest number of chutes and was one of the most efficient of the 12 Series tubes.

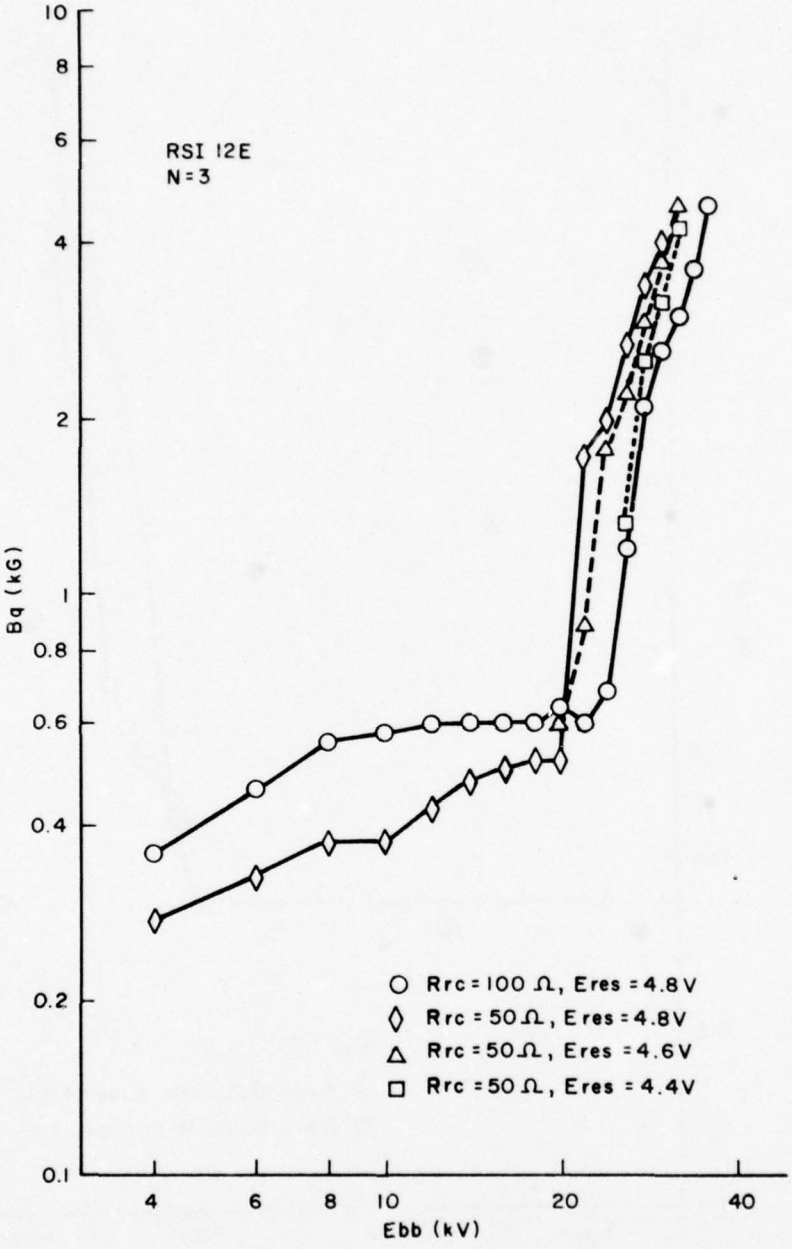

Figure 33. Interruption Characteristics - RSI 12E. This tube was built with the chutes set at an angle to accommodate the assumed trajectory of the electrons during interruption.

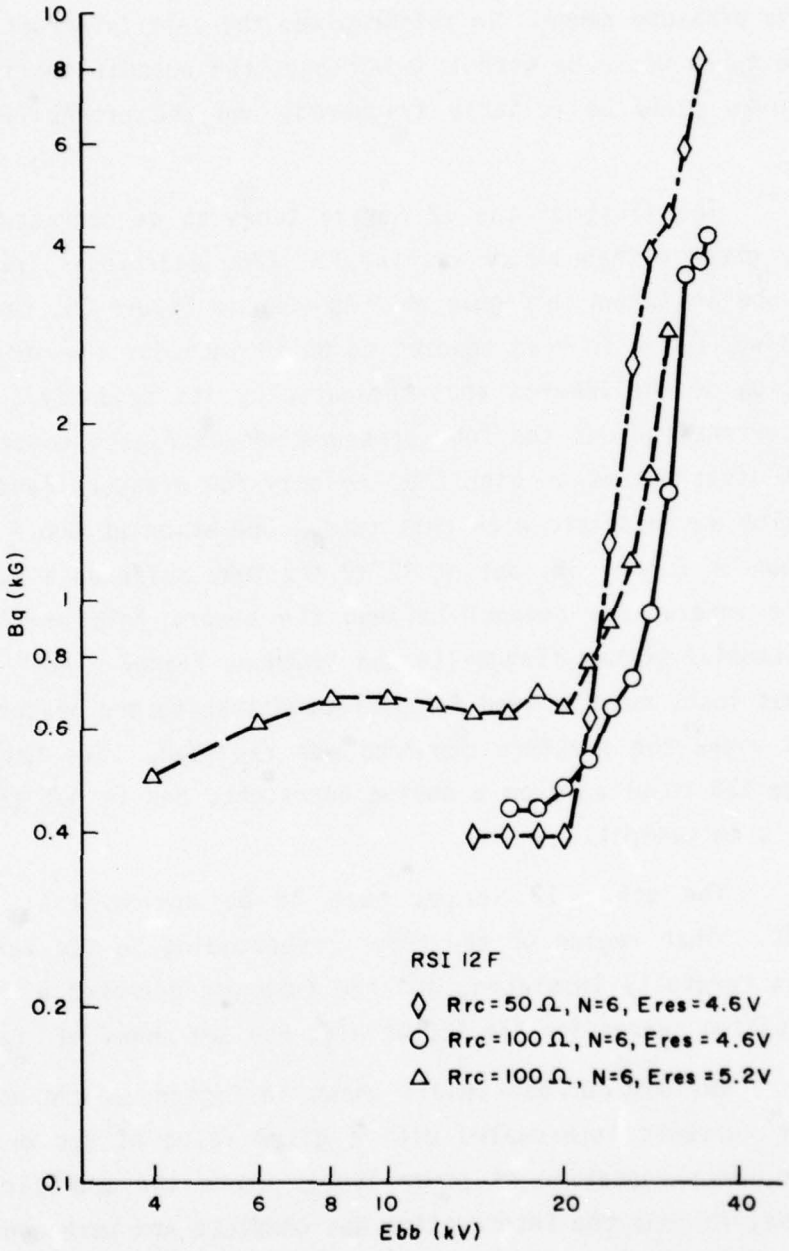

Figure 34. Interruption Characteristics - RSI 12F. This tube was built to minimize possible plasma reservoirs by minimizing the width of the chutes. It was one of the most efficient 12 Series tubes.

In general, the 12 Series tubes operated best at hydrogen pressures between 200 and 250 microns and the curves of Figures 29 through 34 correspond to this pressure range. In this regime, the self-interruption characteristics of the tubes could be used to advantage, the holdoff sections performed well, the tubes could be reliably triggered, and the probability of restrike was low.

The first of the 12 Series tubes to be operated with Ebb significantly greater than 35 kV was the RSI 12B; additional interruption data for this tube are shown in Figure 35. As seen in Figure 25, the bore diameter for Type B was 0.100 inch as opposed to 0.150 inch for the other 12 Series tubes. Operation of the 12B was thus dominated by its tendency to self-interrupt at high currents unless the tube pressure was increased considerably. This led to holdoff problems at high Ebb, so only low pressure (and somewhat erratic) operation was possible with this tube. Operation at Ebb = 40 kV was achieved as shown in Figure 35, but at 42 kV the tube suffered a puncture through the ceramic interaction channel between the second fold of the channel and the low-potential bottom flange (termed "cathode flange plate" in Figure 6). The tube was lost, but the need for increased spacing and better insulation in the region where the puncture occurred was realized. *The failure* mode observed for the 12B resulted from a design oversight, and is not an inherent property of RSI's in general.

The other 12 Series tube to be operated at high Ebb was the RSI 12C. That region of the tube corresponding to the failure point of the 12B was carefully insulated, and the tube was operated with Ebb up to 50 kV. Interruption curves for the 12C at high Ebb are shown in Figure 36.

Various current levels shown in Figure 36 are not necessarily the highest currents interrupted with a given value of Rrc or Ebb.* They are, however, representative of power levels where the operation of the tube was flawless, in that the interruption was complete and permanent. Representative oscillograms showing such performance are given in Figure 37. Figure 37(a)

---

*The values of ib shown in Figure 36 are measured values. They cannot be calculated from Ebb and Rrc without a knowledge of etd. The tube drop is a function of ib; and at high ib, etd is significant.

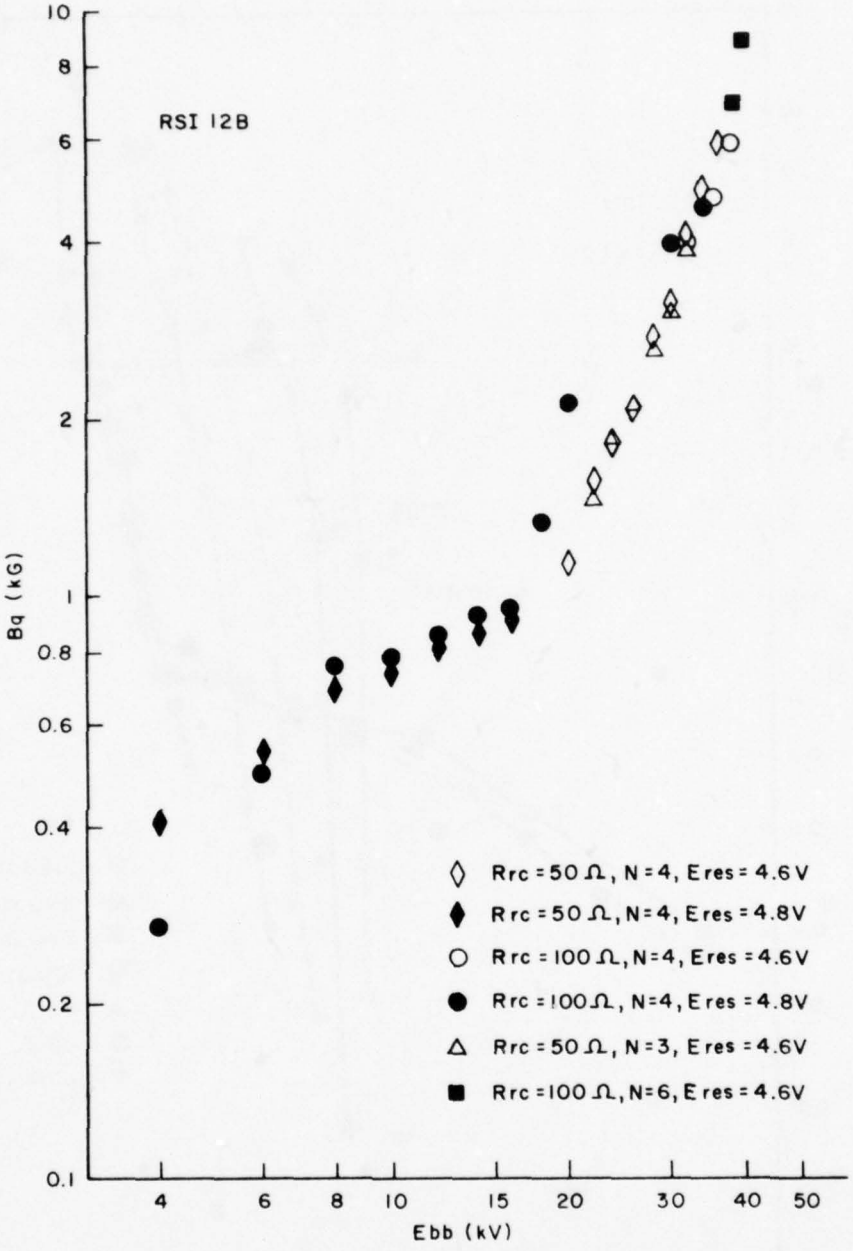

Figure 35. Interruption Characteristics - RSI 12B. By reducing the operating pressure of this thin-bore tube to capitalize on its tendency to self-interrupt, several hundred amperes were interrupted at Ebb = 40 kV. Operation was erratic however, and at Ebb = 42 kV the device failed due to a puncture of the ceramic interaction channel.

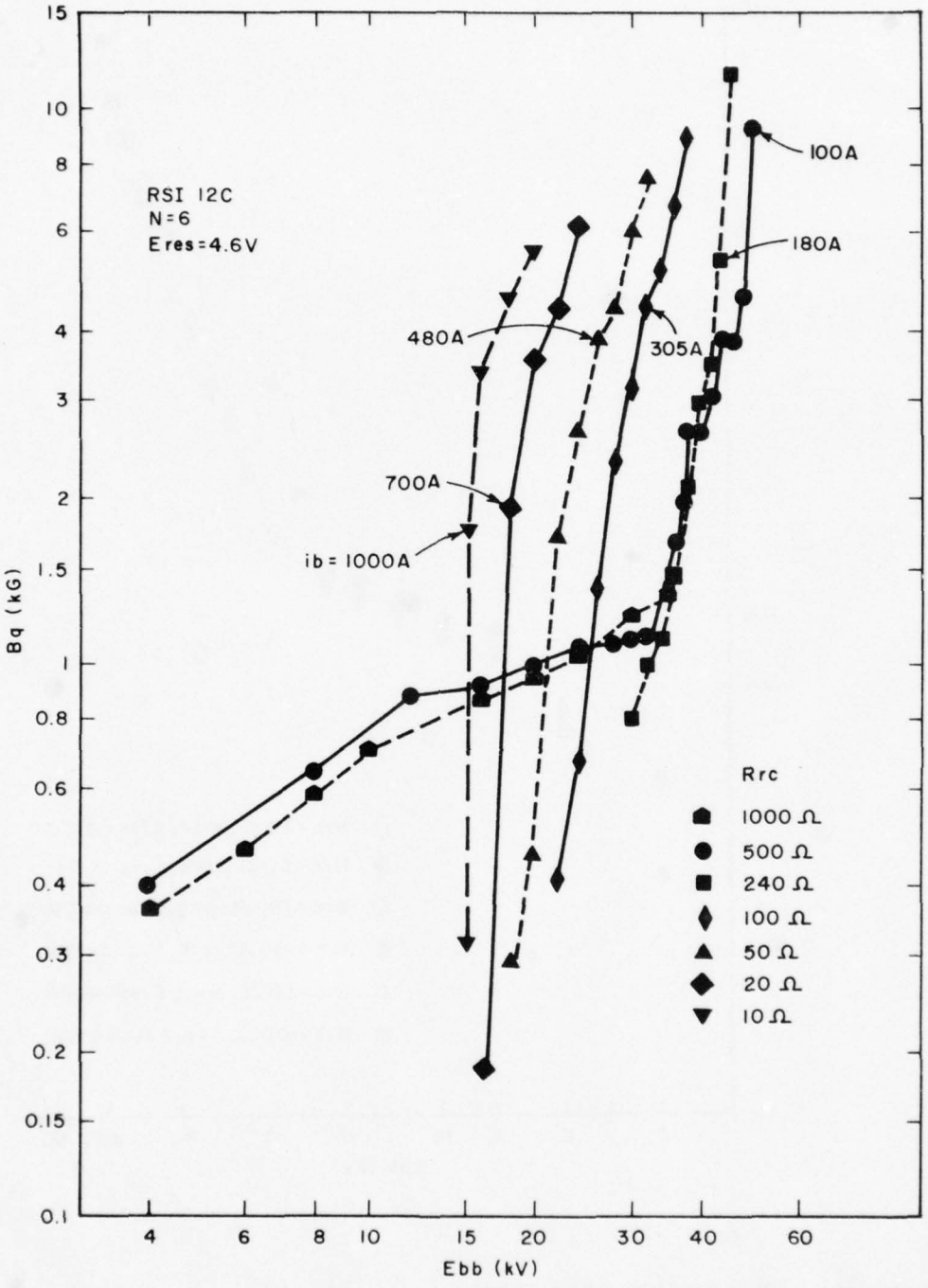

Figure 36. Interruption Characteristics - RSI 12C. This tube successfully interrupted 100 A at 50 kV, 480 A at 26 kV, and 1000 A at 15 kV.

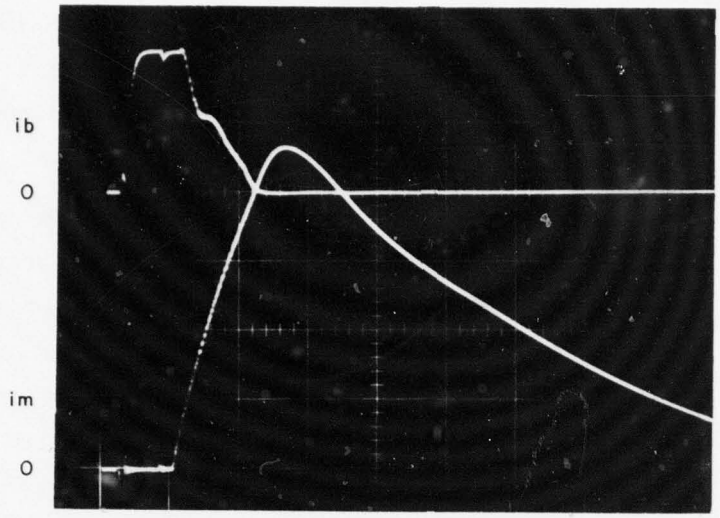

(a)

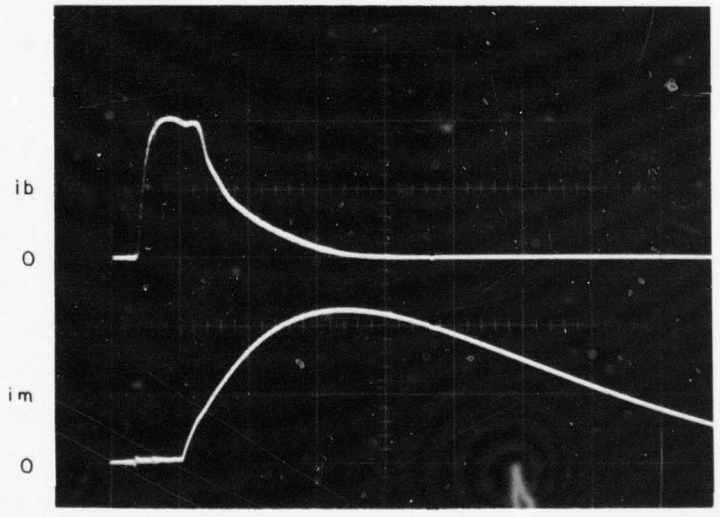

(b)

Figure 37. Oscillograms Showing the Interruption of 100 A at 50 kV and 1000 A at 15 kV. The load power interrupted is 5 megawatts in the 50 kV case but only 10 megawatts in the 1000 A case owing to the high tube drop under the high current condition. Note from the waveform of im in the high voltage case that saturation of the magnet core is imminent.

shows the interruption of 100 A at 50 kV and Figure 37(b) shows 1000 A at 15 kV. Note the total absence of restrike in Figure 37. Note also (Figure 37(a)), that saturation of the magnet core is imminent as evidenced by the distortion in the waveform of im.

Table 3 gives the calculated interruption efficiency in terms of interrupted megawatts at the load per joule of magnetic field energy delivered to the interaction channel. Calculations were made for each value of ib and Rrc indicated in Figure 36. Table 3 indicates that for the cases shown the load power varies by a factor only slightly more than two, the current by a decade, and Ebb by roughly a factor of three. Yet the interruption efficiency increases from 0.15 in the high voltage case to 8.33 in the low voltage case (a factor of 56), and does so despite the ten-fold increase in tube current. Table 3 shows that the interruption efficiency is dominated by Ebb and that the functional dependence is strongly nonlinear. This, of course, accounts for the general shape of the interruption characteristics of Figure 36 and suggests that the simultaneous interruption of 50 kV and 1000 A is not readily accomplished.

(c) Tube Drop

Measurements were made to determine total tube drop etd for each tube as a function of tube pressure and tube current. The results of this effort are given in Table 4 which shows etd as a function of tube pressure with the tube current held constant at 9A, and in Table 5 which shows etd as a function of tube current with Eres = 5.2 V (P = 305-340 microns). As was the case with the 10 Series tubes, the tube drop increased with increasing pressure (Table 4), but the pressure dependence of etd was not a dominant aspect in the operation of these tubes. Similarly (from Table 5), etd decreased with increasing current (over the range of ib investigated) as had previously been observed for the 10 Series tubes.

The overall significance of the tube drop measurements is discussed further below; the tube drop in general is discussed in Section 5.0.

Table 3. Typical Interruption Efficiencies - RSI 12C.

Ebb (kV)	ib (A)	Load Power (Megawatts) (Note 1)	Interrupting Energy (Joules) (Note 2)	Interruption Efficiency (Megawatts/Joule)
50	100	5.0	32.8	0.15
44	180	7.8	11.3	0.69
32	305	9.3	7.77	1.20
26	480	11.5	5.83	1.97
18	700	9.8	1.43	6.85
15	1000	10.0	1.20	8.33

Notes: (1) The load power is materially less than the product of Ebb and ib because of the high tube drop at high ib.

(2) Calculated energy delivered to the interaction channel. The energy in the magnetic field was found from the relation $1/2 \frac{Bq^2}{\mu_o} V$ where μ_o is the permeability of free space and volume V is the total volume of the interaction channel (gas and ceramic).

Table 4. Steady-State Tube Drop (etd) as a Function of Tube Pressure (P) (RSI 12 Series, ib = 9A).

RSI 12A2		RSI 12B	
P (Microns)	etd (Volts)	P (Microns)	etd (Volts)
210	890	230	1350
260	990	270	1310
320	1020	315	1310
375	1090		

RSI 12C		RSI 12D	
P (Microns)	etd (Volts)	P (Microns)	etd (Volts)
230	980	250	920
270	1110	280	1000
340	1020	310	1040
360	1110	330	1090

RSI 12E		RSI 12F	
P (Microns)	etd (Volts)	P (Microns)	etd (Volts)
240	1025	260	960
270	1025	280	990
310	1090	305	1010
360	1125	350	1070

Table 5. Steady-State Tube Drop (etd) as a Function of Tube Current (ib) (RSI 12 Series*, P = 305-340 Microns)

ib (Amps)	RSI 12B etd (Volts)	RSI 12C etd (Volts)	RSI 12D etd (Volts)
3	1400	1100	1015
6	1400	1080	1010
9	1330	1030	980
12	1250	1000	950
18	1150	910	900

ib (Amps)	RSI 12E etd (Volts)	RSI 12F etd (Volts)
3	1100	1110
6	1075	1050
9	1040	1000
12	1010	970
18	910	900

TUBE DROPS AVERAGED OVER CURRENT

RSI 12B - 1306V
RSI 12C - 1024V
RSI 12D - 971V
RSI 12E - 1027V
RSI 12F - 1006V

*Data not taken for RSI 12A2.

(d) Data Evaluation

Tube Drop

The total tube drops observed for the 12 Series tubes (as shown in Tables 4 and 5) were typically 900 to 1100 volts under non-fault conditions, except for narrow-bore Type B which typically operated with etd = 1300 volts. Neglecting Type B, and assuming an average value for etd of 1000 volts, the total of the holdoff and cathode section drops (130 volts) may be subtracted from this average to estimate the drop across the 21-inch column as 870 volts, and thus infer an electric field of 16.3 volts/cm. This is in fair agreement with the "rule-of-thumb" figure derived for the 10 Series tubes (20 volts/cm) as described in Section 5.0.

Under fault current conditions, etd rises dramatically and beneficially. Consider, for example, RSI 12C which operated with etd = 910 volts at a "normal" current of 18 A, as shown in Table 5. At ib = 1000 A, etd increased to 5 kV, and as shown by the data of Table 3, this increase in etd significantly limited the instantaneous power delivered to the load before the actual interruption occurred. However, the benefit derived through this mechanism becomes less significant as Ebb is increased.

Channel Geometry

Figure 38 shows the interruption characteristics typical of the 12 Series tubes with Rrc = 100 ohms. Most of the 12 Series testing was done with Eres = 4.6 volts since this value provided the experimentally determined optimum tube pressure of 200 - 250 microns. Similarly, it was experimentally determined that N = 6 turns provided the best compromise (in terms of interrupting capability) between the peak magnetic current and the magnetic field rise time within the constraints imposed by the existing magnet circuit.

As previously discussed, Type A geometry was the base for the 12 Series tubes. Each of the other tube series had been designed with a deviation from the Type A geometry that was expected to improve the efficiency of that particular device with respect to that of the 12 A. As the curves of

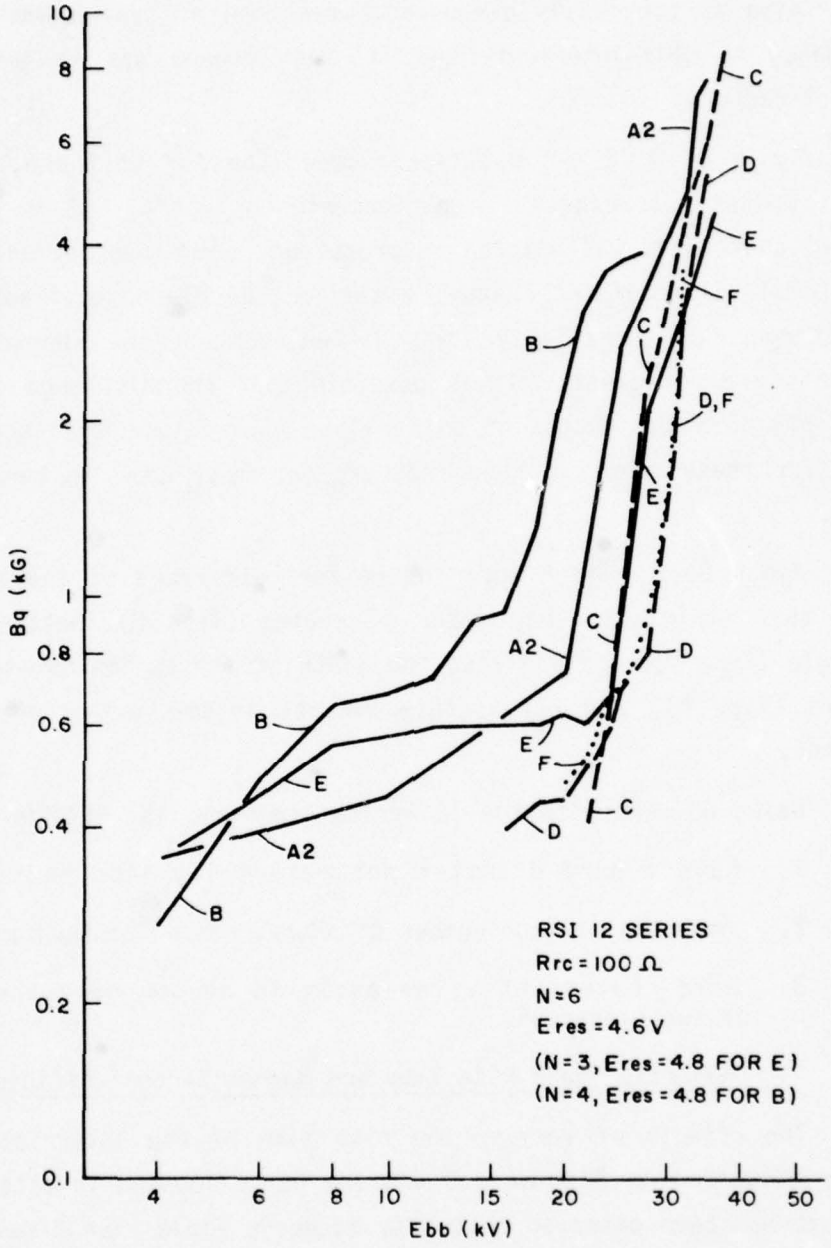

Figure 38. Interruption Characteristics - RSI 12 Series. Except for narrow-bore Type B, the characteristics of the various tubes did not differ widely in the high voltage region. Type A was the base design for the Series, with each variation expected to provide lower Bq. For Types C, D, E and F, the expected improvement was observed.

Figure 38 show, this expectation was realized in every case except that of Type B. Also as previously discussed, operation of Type B was dominated by its tendency to self-interrupt, and its performance was in general erratic and unsatisfactory.

Types C, D, E and F out-performed Type A. Of these, Type C (with its short chutes) was closest in performance to Type A. It is probable that the end-of-chute wall was helpful in promoting recombination, and/or that the smaller total volume of the channel minimized the plasma available to sustain the discharge. Alternatively, the differences in the characteristics of these tubes are not great. It is possible that the discharge did not penetrate deeply into the chutes of either Type A or C, and that the differences observed for these tubes in Figure 38 are not meaningful in terms of channel geometry.

Types D, E, and F were the better performers of the series. This suggests that maximizing the number of chutes (Type D), setting the chutes at an angle (Type E), and limiting the width of the chutes to minimize plasma reservoirs (Type F), are all useful concepts in the design of an efficient interrupter.

Based on work with the 12 Series geometry, the optimum tube should:

1. have a bore diameter not materially less than 0.150 inch;
2. contain a maximum number of short, narrow chutes; and
3. have chutes set at an angle to accommodate the trajectory of the electrons.

Magnetic Field Rise Time and Magnet Circuit Efficiency

The effects of varying the rise time of the interrupting magnetic field are discussed in Section 4.0 and are not discussed in detail here. In general, it has been observed that fast magnetic field rise times are in fact beneficial in reducing Bq, and become more so at high Ebb. This phenomenon was not extensively studied, and no attempt was made to establish any functional dependence of Bq on dB/dt. During the 12 Series testing, however, it was determined that for the existing magnet circuit, N = 6 turns was an

optimum operating condition when the RSI's were operated at Ebb greater than about 30 kV. (N = 6 did not provide the maximum field.) The 12 Series tubes could have interrupted higher currents at high Ebb (over 30 kV) had the magnet circuit been capable of generating higher dB/dt.

When the energy actually delivered to the interaction channel is compared with that stored in the magnet circuit capacitor, it is found that the magnet circuit typically operated with an efficiency of only 2 to 3 percent. Delivery of 10 joules to the RSI thus required the dissipation of 400 joules on the average. Such energy levels, although frequently available at high power installations, are clearly an undesirable requirement.

The overall conclusion is that a need exists for improvement in the design of the magnet circuit, both to increase dB/dt and also to increase circuit efficiency. This is a straightforward engineering task that does not involve changes in the RSI design as it presently stands.

c. Data Summary and Conclusions

The 10 and 12 Series of chuted interrupters were built and characterized for both interruption capability and total tube drop. From the 10 Series testing, it was confirmed that tubes of a relatively narrow bore were preferred over wider bore tubes because of their superior interruption efficiency and despite their somewhat higher voltage drop. It was also determined that "plasma reservoirs" should be avoided; i.e., the better channel geometries were found to be those wherein the channels contained both an unchuted and a chuted surface, against which latter surface the discharge was driven. It was also found that the channel should contain a large number of relatively short and closely spaced chutes, that the tube should be operated at the lowest pressure consistent with reliable triggering characteristics, and that multiple, folded interaction channels were both efficient and capable of working at high Ebb.

Typical column drops were of the order of 350 volts per section (20 volts/cm) for the 10 Series tubes. The most efficient of the series, the folded-channel RSI 10DD, operated at 25 kV, 18.5 A with a total drop of 830 volts, or 3.3% of epy. This tube successfully interrupted 600 A at 20 kV with a magnetic field energy of less than 8 joules being required to achieve the interruption.

From testing the 12 Series tubes, it was further determined that the optimum tube should have a bore diameter not materially less than 0.150 inch; contain a maximum number of short, narrow chutes; and also that the chutes should be set at an angle to accommodate the trajectory of the electrons.

Typical total tube drops for the triple-section 12 Series tubes were of the order of 1000 volts (2% of epy) under non-fault current conditions (18.5 A). The column drop was typically 870 volts (16.3 volts/cm).

The RSI 12C successfully interrupted 100 A at 50 kV, 180 A at 44 kV, 305 A at 26 kV, 700 A at 18 kV, and 1000 A at 15 kV. Operation at these levels was reliable and free of restrike. The magnetic field energy necessary to achieve these interruptions varied from a high of 32.8 joules in the high voltage case, to a low of 1.2 joules in the high current case. This indicates a strong dependence of Bq on Ebb. This is consistent with earlier work on unchuted interrupters[3]. Currents well in excess of 1000 A were routinely interrupted at low Ebb with several of the 12 Series tubes. At high Ebb, the interruption capabilities of the 12 Series tubes appeared to depend strongly on dB/dt. These tubes are capable of interrupting even higher currents at high Ebb given a suitably designed magnetic field generator.

4.0 SELF-INTERRUPTION AND THE EFFECTS OF INTERRUPTION TIME

The phenomenon of self-interruption in the geometrically constricted regions of a gas discharge has been widely observed and is a fundamental consideration in the design of hydrogen thyratrons.[4] As regards the RSI, the period encompassing the actual interruption of the discharge is a parameter of considerable import. This section treats each of these considerations to the extent that each affects the design of a viable high voltage, high current interrupter.

a. Self-Interruption

As the degree of ionization and the current density increase within a geometrically constricted discharge channel, a point is reached where the available gas can no longer support further increases in current density. The discharge current is thus limited to a value consistent with the cross-sectional area and initial pressure within the channel. This effect is widely observed when high currents are passed through the grid apertures of hydrogen thyratrons, and the terms "grid quenching," "thin channel quenching," and simply "quenching" have been coined to refer to the phenomenon. For normal thyratron operating pressures and pulse widths (300 to 400 microns, 5 μsec) a fairly reproducible maximum current density of the order of 10,000 A per square inch has been empirically determined. Conversely, at a given gas pressure, a minimum current density is required to sustain a stable discharge. There exists, therefore, a limited current-pressure-time characteristic for a discharge channel of any given geometry.

When designing a standard thyratron, one selects a geometry for the grid and grid baffle structures such that the quenching limit is avoided, and considerations other than grid quenching usually set the upper bound on anode current. For efficient RSI's, typical interaction channel diameters are of the order of 0.1 to 0.2 inch, these values being representative of a good compromise between the magnetic field necessary to achieve interruption, Bq, and the column drop during conduction, ecd. With dimensions of this order being appropriate for the channel, it follows that the channel is the most constricted region in the tube. As such, the channel determines the quenching-limited anode current for the device, and for a channel having a

typical diameter of 0.15 inch, the maximum current before quenching may be readily calculated to be 177 A. This current level prompts two observations. First, it is well above the normal (nonfault) current of the RSI as given in the technical guidelines for this Program (17 A), and well above the peak current to be a likely requirement for many RSI applications, particularly those at higher voltages where thin channels are most likely to be in order. Second, such a current level is well below the maximum fault current set by the guidelines (1000 A), and well below any reasonable maximum fault current that one might wish to interrupt.

From the first observation, one concludes that for even relatively small bore RSI's, the normal peak current will not be adversely affected by quenching phenomena, at least for normal pulse widths (less than 10 μsec). From the second observation, one concludes that self-quenching effects might arise under fault conditions. Furthermore, if such were the case, the effect would undoubtedly be to aid in the interruption and thus serve to lower Bq.

Self-quenching effects were investigated experimentally for three reasons:

1. To establish empirically that the RSI long interaction channel did not give rise to a materially lower current density for quenching than that commonly observed for the relatively short lengths applicable to thyratron grid structures.

2. To determine at least the minimum quench-limited, current-pressure relationship based on long pulses, the assumption being that at a given pressure, shorter pulses of even higher current levels could be passed by the channel.

3. To determine if self-interruption by the quenching mechanism would in fact decrease the magnetic field required for interruption.

(1) Self-Interruption Data

Data were obtained for two representative devices, the RSI 10DD and the RSI 13A. With its 0.15-inch diameter, 13-inch long, folded interaction channel, the 10DD is representative of chuted interrupters. The 13A was the holdoff section design chosen for the 12 Series of tubes, and as a gradient grid device, it contained a plurality of apertures through which the discharge was constrained to pass.

Figure 39 (a) shows the behavior of the RSI 10DD when operated at a relatively high pressure of 780 microns and subjected to a 340 A (peak) capacitor discharge having a time constant of 150 μsec. After about 4 μsec, the discharge became unstable and remained so until the current decayed to about one-half of its initial value. Figure 39 (b) shows the response when the peak was limited to 260 A. The time to the onset of the instability increased to about 12 μsec, and the instability ceased at a higher value of tube current than that of Figure 39 (a). Finally, in Figure 39 (c), the peak current was limited to a value of about 200 A such that the instability failed to appear.

Figure 40 shows the behavior of the tube when subjected to discharges of 150 A, 60 A, and 40 A at the relatively low pressure of 250 microns. Note from Figure 40 (b) that the tube consistently and permanently self-interrupts at currents of 40 A or higher (each oscillogram is a time exposure showing several discharges), and from Figure 40 (c) that, for an initial current of 40 A, the tube conducts without fault. It is not clear that the mechanisms at play in Figure 40 are those prevailing in Figure 39, but general conclusions may be drawn as follows:

1. An inverse relationship exists between peak current and the time to an instability or interruption.

2. Major (and sometimes permanent) self-interruptions occur at low pressure but not at high pressure.

3. Both the short- and long-term conduction characteristics are greatly enhanced by operation at high pressure.

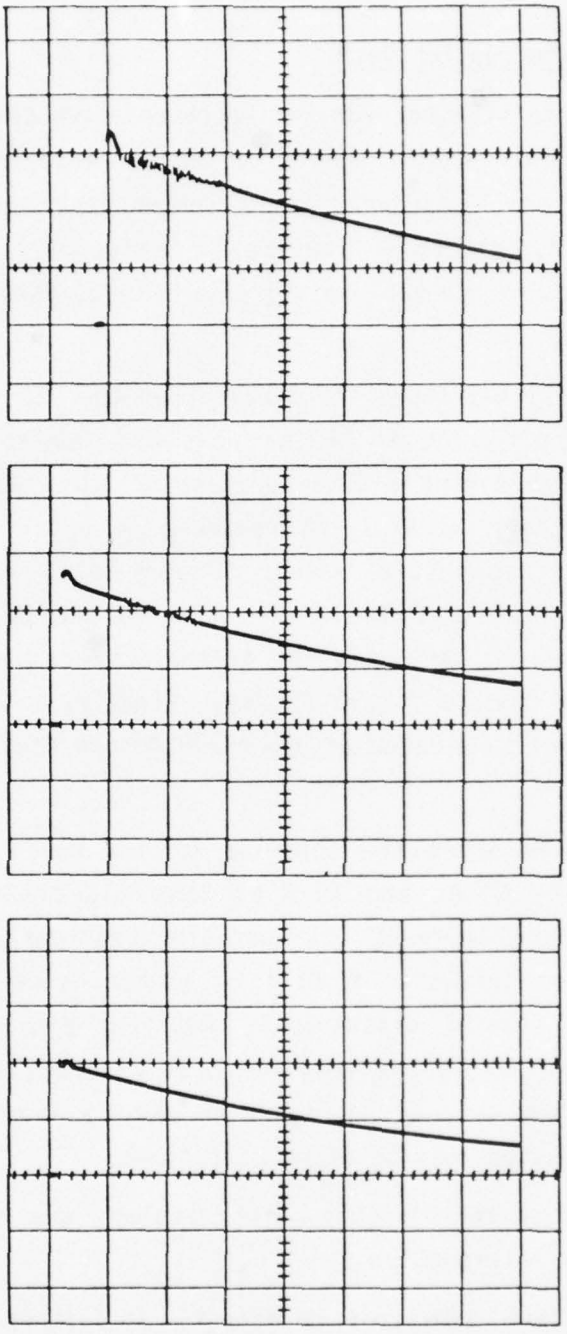

Figure 39. Effects of Thin-Channel Quenching at High Pressure — RSI 10DD. The discharge is stable at early times even for ib well above the quenching threshold.

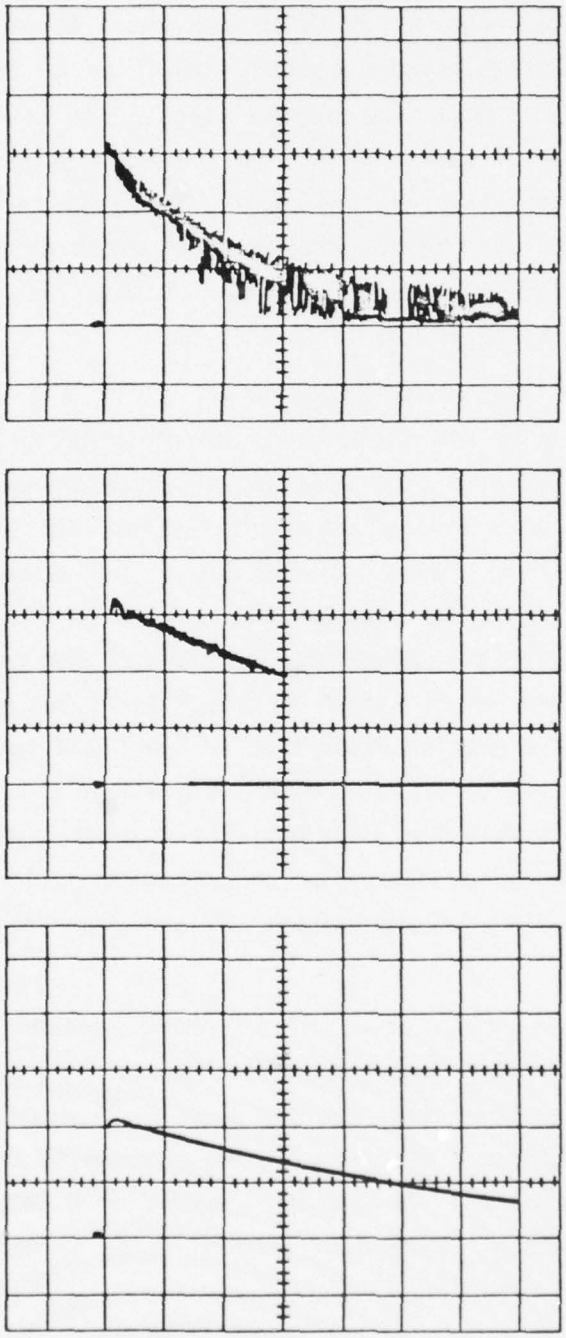

(a) 50A/DIV
50μS/DIV
P = 250 MICRONS
RSI 10DD

(b) 20A/DIV
20μS/DIV
P = 250 MICRONS
RSI 10DD

(c) 20A/DIV
20μS/DIV
P = 250 MICRONS
RSI 10DD

Figure 40. Effects of Thin-Channel Quenching at Low Pressure — RSI 10DD. A permanent self-interruption can occur.

Data of the general nature shown in Figures 39 and 40 were generated for the tube over the pressure range of 250 to 600 microns. At each pressure, an initial peak current was established such that operation at lower initial peaks was free of all types of conduction instabilities. The results of this effort appear in Figure 41, which shows the maximum long-term anode current as a function of tube pressure over the pressure range investigated. The data of Figure 41 apply to long-pulse conditions, and thus represent extremely harsh operating conditions for the tube. The DD tube will easily pass a 300 A, 1 μsec current pulse at a pressure as low as 150 microns.

For the RSI 10DD, the cross-sectional area of the interaction channel (0.0177 sq. inch) is by far the minimum area presented to the discharge. At a normal thyratron operating pressure of 400 microns and a pulse width of a few microseconds, one would expect quenching instabilities to occur at a current of about 0.0177 sq. inch x 10,000 A/sq. inch equal to 177 A. From Figure 16 at P = 400 microns, the maximum safe current is 115 A, and this value applies under the long-pulse conditions described. The conclusion is that even for long pulses, the extra length of the interaction channel does not greatly alter the self-interruption properties of the RSI from those which normally apply to the grid region of a standard thyratron. A significant consideration is that for double the required RSI "normal" peak current according to the technical guidelines for the Program (2 x 17 A), no instabilities occur even for long pulses and even at the very low pressure of 250 microns.

Figure 42 shows quenching data (of a nature similar to that of Figure 41) for the RSI 13 A, a gradient grid device designed to operate at 50 kV, and as such, contains a total of four apertures, each of which has an area of 0.042 sq. inch. At a pressure of 400 microns, the maximum "safe" long-term current is 110 A as opposed to the "theoretical" value of 0.042 sq. inch x 10,000 A/sq. inch equal to 420 A. Such a difference is of no consequence in terms of RSI performance.

The overall conclusion to be drawn from the data collected on thin channel quenching as thus far discussed is that the phenomenon in no way hinders RSI performance as presently contemplated. Furthermore, the phenomenon actually functions to an advantage, as discussed below.

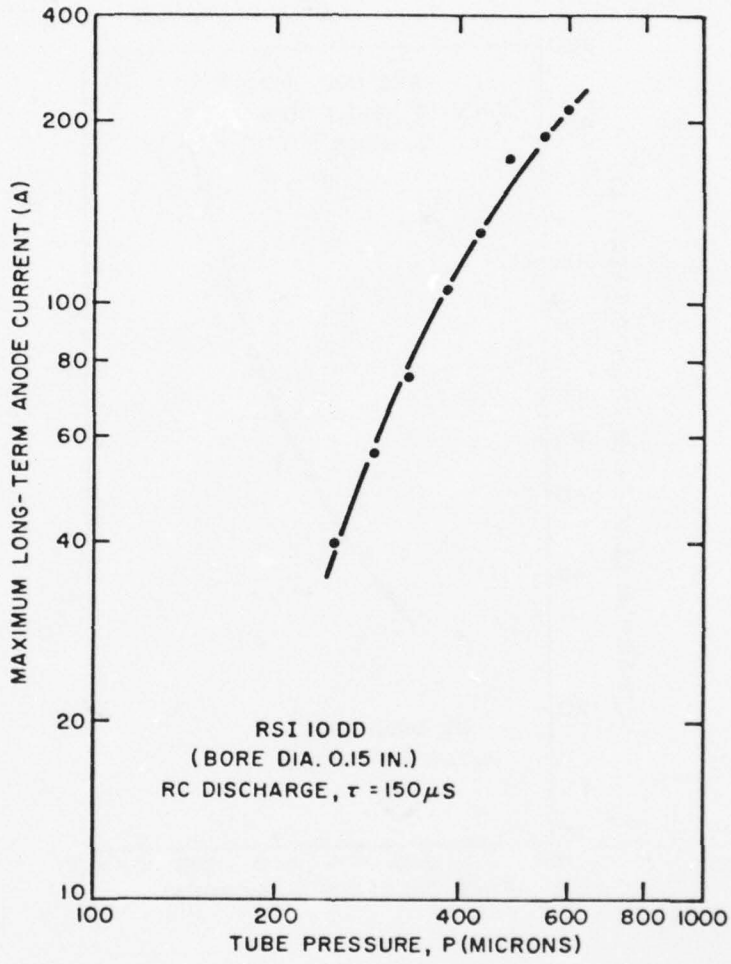

Figure 41. Maximum Long-Term Current Without Self-Interruption — RSI 10DD. For double the required RSI "normal" current, no instabilities occurred even for long pulses at low pressure.

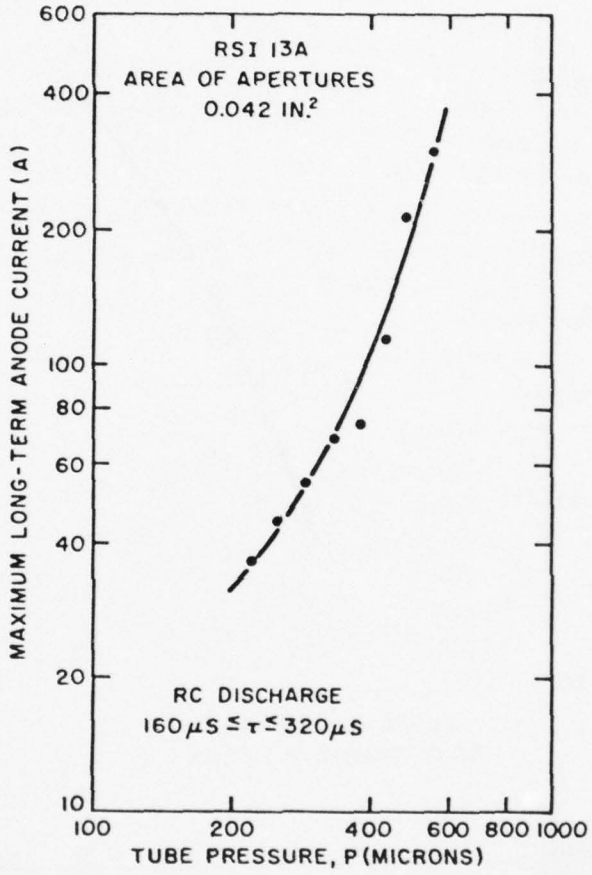

Figure 42. Maximum Long-Term Current Without Self-Interruption — RSI 13A.

(2) Effects of the Self-Interruption Process on Bq

From the foregoing discussion on the self-interruption process, it follows that a reduction in Bq is to be expected when an RSI is operated under conditions where self-interruption is likely to occur. Except for the L di/dt voltages which might be generated as a result of rapid self-interruption, such an assist to the magnetic field may be viewed as being a beneficial phenomenon. This effect was investigated as shown in Figures 43 and 44 and the expected decrease in Bq did occur. Figure 43(a) shows a 40 A discharge being interrupted at a pressure of 250 microns with a required magnet current of 18 A peak. When the pressure is increased to 600 microns (Figure 43(b)), the same magnet current fails to interrupt the discharge. From Figure 43(c), the peak magnet current required to interrupt the discharge at high pressure is 55 A, or about three times the value required for the low pressure case. From Figure 44(a), a 50 A magnet current is required to interrupt a 200 A discharge at low pressure, while from Figure 44(b), a 150 A magnet current is required to interrupt the same current at high pressure. Thus the factor of three reduction in Bq for the pressures investigated is seen to prevail over a factor of five in tube current. The self-interruption process may be invoked to explain previously reported cases where higher currents were more easily interrupted than were lower currents, and also is a partial explanation of the previously reported general observation that reducing the tube pressure leads to reduced Bq.

b. Effects of Interruption Time

The interruption process is inherently rapid when compared with the time scale of interest in most RSI applications. The time required for the field to penetrate the plasma has been calculated by Thomas et al.[5] to be of the order of 10^{-7} to 10^{-6} sec for devices of the class under consideration in this Program. Experimental work has shown that the RSI responds to the magnetic field on a microsecond time scale.

From the viewpoint of minimum energy being deposited in the series load being protected by the RSI, it is desirable that interruption occurs with all deliberate speed. It will be shown later, however, that a considerable margin of safety exists in this regard.

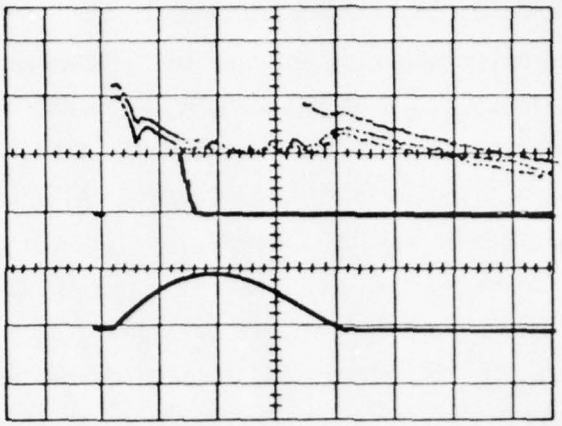

(a)

ib, 20A/DIV

im, 20A/DIV
t, 20μS/DIV
P = 250 MICRONS
RSI 10DD

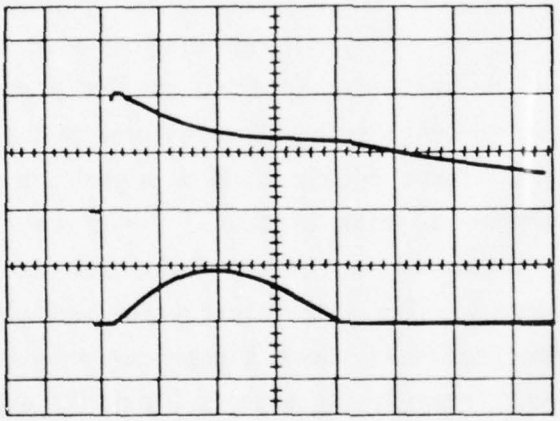

(b)

ib, 20A/DIV

im, 20A/DIV
t, 20μS/DIV
P = 600 MICRONS
RSI 10DD

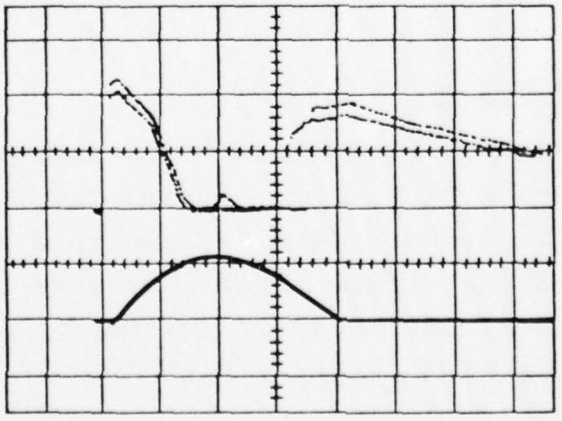

(c)

ib, 20A/DIV

im, 50A/DIV
t, 20μS/DIV
P = 600 MICRONS
RSI 10DD

Figure 43. Effect of Self-Interruption on Bq in a Low-Current Case – RSI 10DD. At high pressure, Bq is increased by a factor of three.

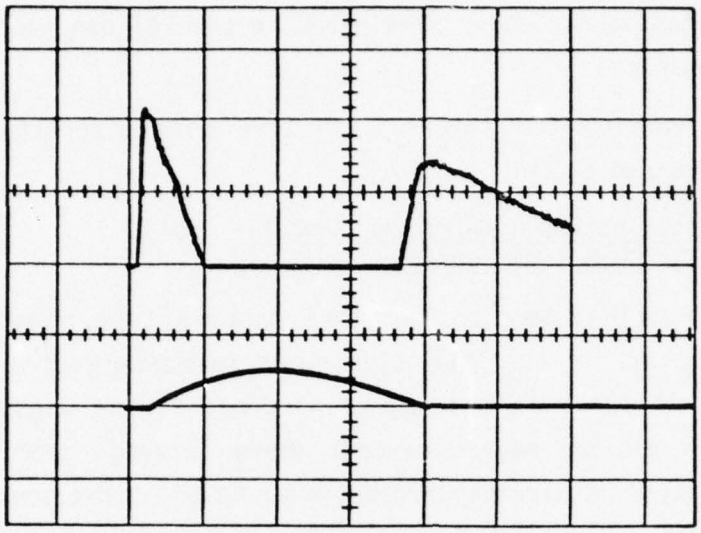

(a)

ib, 100A/DIV

im, 100A/DIV
t, 20μS/DIV
P = 250 MICRONS
RSI 10DD

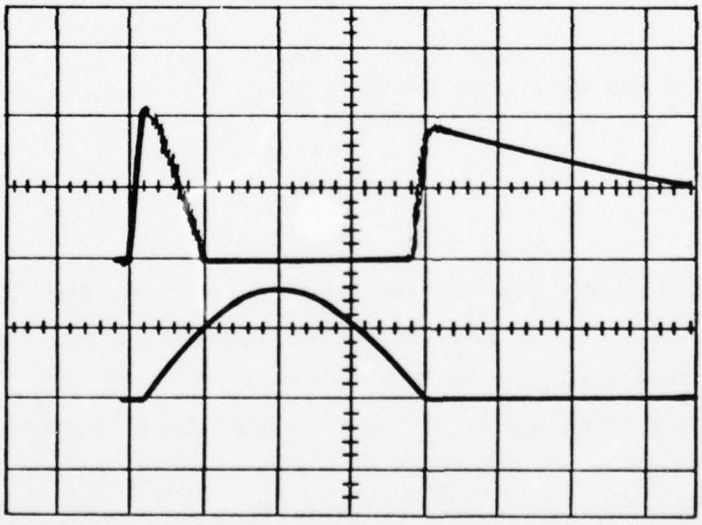

(b)

ib, 100A/DIV

im, 100A/DIV
t, 20μS/DIV
P = 600 MICRONS
RSI 10DD

Figure 44. Effect of Self-Interruption on Bq in a High-Current Case — RSI 10DD. At high pressure, Bq is again increased by a factor of three.

Rapid switching is also desirable from the viewpoint of dissipation within the RSI, both at its anode and within the interaction region. During interruption, the instantaneous power dissipated in the RSI can easily amount to several tens of megawatts.

The effects of varying the interruption time both experimentally and theoretically are discussed below.

(1) Effect of Interruption Time on the Magnetic Field Required to Achieve Interruption

The most practical way to vary the interruption time with the experimental apparatus is to vary the electrical parameters of the magnet circuit: the number of turns in the magnet winding, N; the magnet circuit damping resistor, Rm; and the magnet circuit energy storage capacitor, Cm. Magnetic field intensity B is directly proportional to the first power of both N and the magnet current. Since nearly all of the applied magnetomotive force is used to overcome the reluctance of the air gap,

$$HL = NI$$

where L is the length of the gap. But $H = B/u$, so

$$B = uNI/L.$$

It is difficult to calculate the instantaneous current in the RSI during interruption as a function of the interrupting magnetic field, but it is reasonable to assume that the form of the solution would be such that high dB/dt would encourage the interruption process. Experimental support for this appears in Figure 45 which shows waveforms of anode current, column drop, and magnet current for a case where im was slightly less than that value which would provide complete and relatively abrupt interruption. All waveforms were observed at the same sweep speed. The anode current does not always decrease with increasing B, with a substantial fraction of the interruption taking place during the very rapid initial rise of magnet current from zero to about

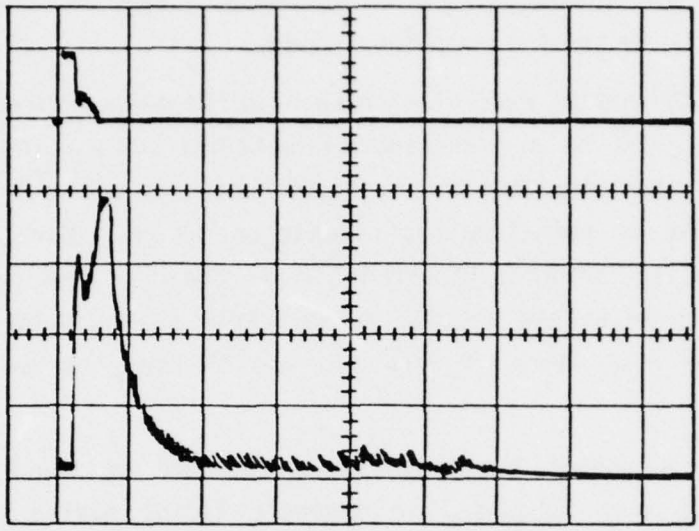

(a)

ib, 200A/DIV

UPPER FLANGE,
5kV/DIV
t, 100μS/DIV
Ebb = 20kV
P = 330 MICRONS
RSI 12A

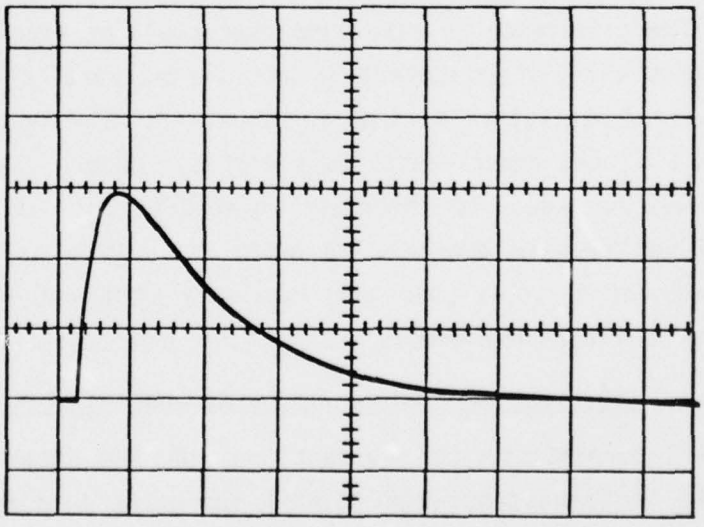

(b)

im, 100A/DIV
t, 100μS/DIV

Figure 45. Effect of Magnetic Field Rise Time on the Interruption Process — RSI 12A1. The anode current does not always decrease with increasing magnetic field, suggesting that dB/dt is a significant factor in the interruption process. (It is known that the core was below saturation.)

40 A. Furthermore, since only a slight increase in im was required to cause a totally abrupt interruption, it is strongly suspected that dB/dt is a significant factor in the interruption process.

The high initial rate of rise seen in the magnet current waveform of Figure 45(b) was due to a transient characteristic only of the particular circuit in use at the time that the waveforms were recorded, and in general is not representative of normal magnet circuit operation. More typical magnet current waveforms are shown in Figure 46, where the rise time has been altered by setting N and Rm at the values shown. From the oscillograms of Figure 46(a) and 46(b), rise times of about 15 and 35 μsec, respectively, may be inferred.

Figure 47 shows the relative performance of the RSI 12A1 (as a function of Ebb) when subjected to magnetic fields having in general the shapes shown in Figure 46, and also shows previously reported data of a similar nature for RSI's 10D and 10DD. For the data shown in Figure 47, the effect of reducing the magnetic field rise time is to lower Bq only at the higher values of Ebb, and to have little (or the opposite) effect at the lower values of Ebb. The difference in rise time that could be readily effected by altering the magnet circuit parameters is not large, particularly when compared with the second derivative evident in Figure 45. The overall conclusion is that for high Ebb, the experimental data largely support the theoretically based argument that Bq should be inversely related to tr, but the dependence is complex, and not readily amenable to analysis. As a practical matter, interruption times of 2 to 5 μsec are regularly observed when relatively slow-rising magnetic fields are used.

(2) Effect of Interruption Time on Discharge Channel Heating

During interruption, the current through the interaction channel decreases and the voltage across the channel increases in time synchronism. Observations of ib and ecd for interruption times of one microsecond to several tens of microseconds revealed no irregularities in this pattern of operation. It is thus clear that significant energy is deposited in the interaction channel during the interruption process, and it follows that the

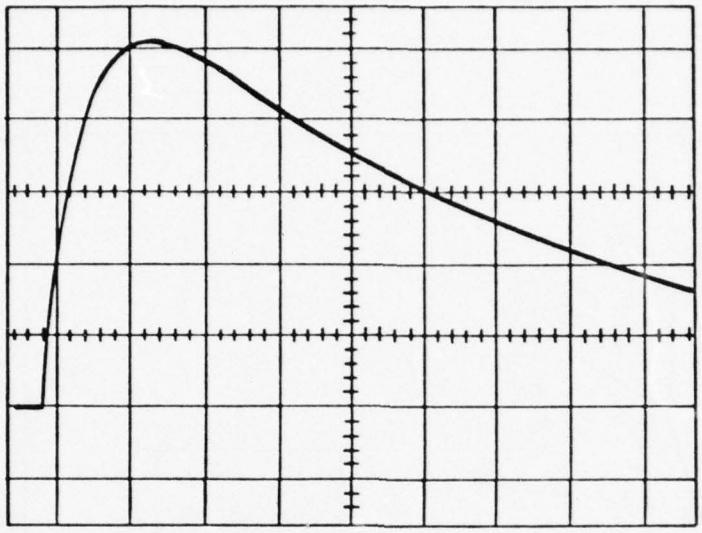

(a)

20A/DIV
20μS/DIV
N = 10
Rm = 20Ω

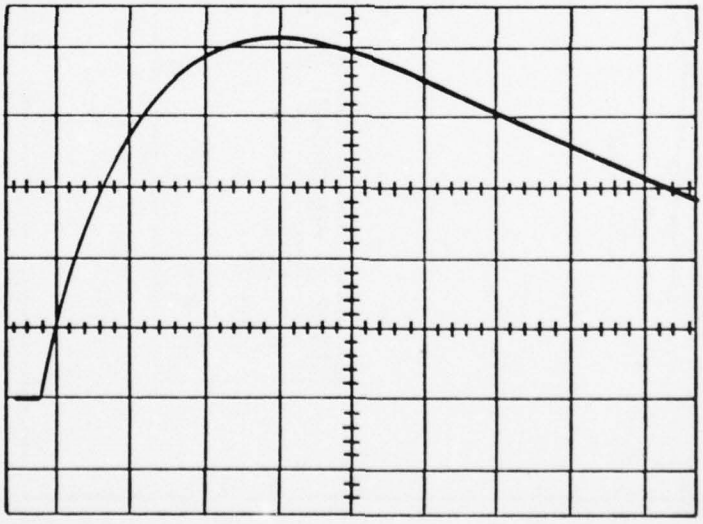

(b)

20A/DIV
20μS/DIV
N = 20
Rm = 25Ω

Figure 46. Typical Magnet Current Waveforms for Differing N and Rm.

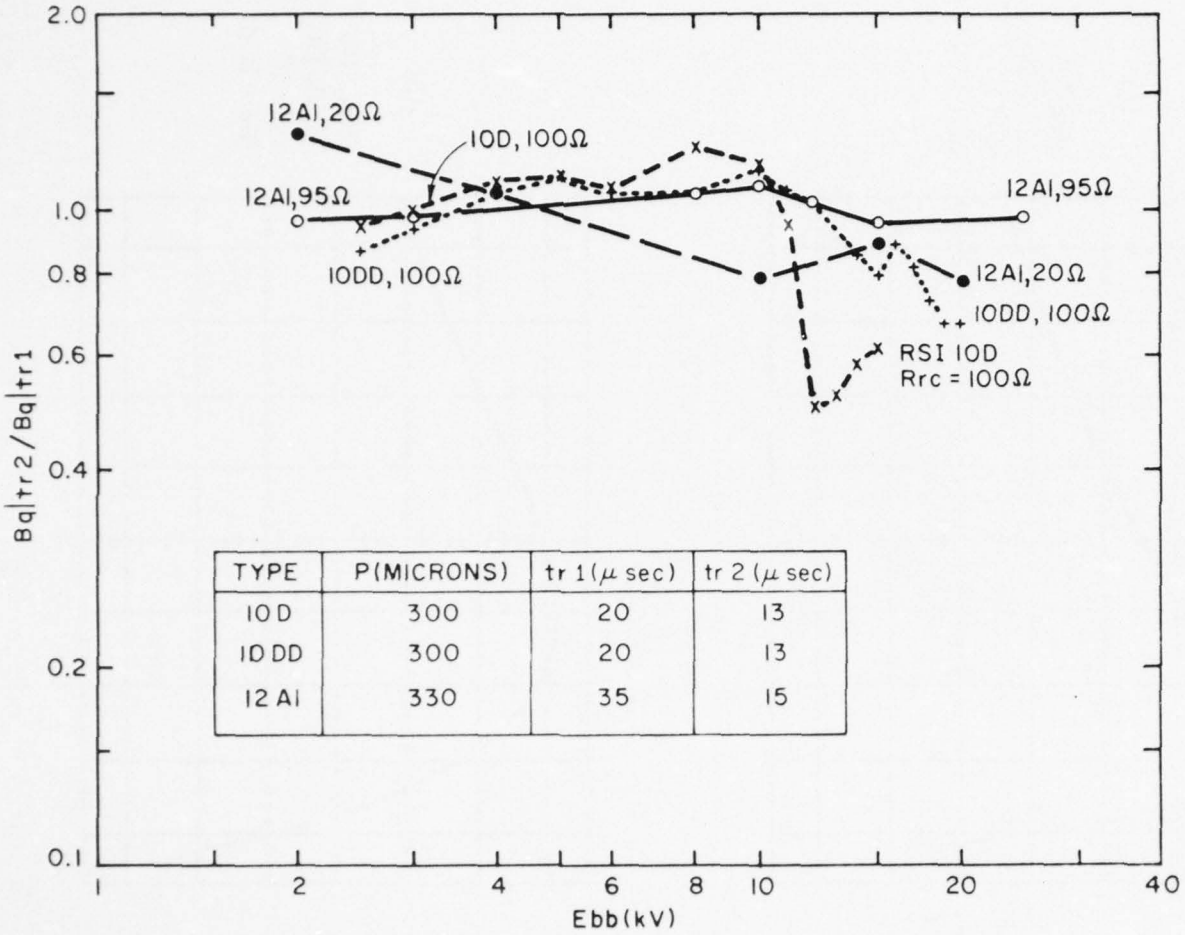

TYPE	P(MICRONS)	tr 1 (μ sec)	tr 2 (μ sec)
10 D	300	20	13
10 DD	300	20	13
12 AI	330	35	15

Figure 47. Relative Interruption Characteristics with Magnetic Field Rise Time as a Parameter. The effect of reduced tr is to lower Bq at high Ebb.

interruption period must not be so long that damage to the channel will ensue. Therefore, the effects of such transient heating on the sidewall material — 95% alumina — should be considered.

Alumina has a melting point slightly in excess of 2000°C and a fusion (softening) point of about 1800°C. Most manufacturers recommend a maximum working (loaded) temperature of about 1500°C.

For the purposes of this discussion, assume that the RSI is operating under conditions of average current, column drop, and ambient temperature such that the steady-state temperature at the inner surface of the interaction column is 400°C. Then estimate the maximum time allowable for the interruption of 1000 A at 50 kV (the design goal), assuming that the sidewall temperature is not to exceed 1400°C at the end of the interruption. Under this condition, no damage should occur to the device.

If the peak power dissipated in the walls is 1/2 Ebb x 1/2 ib, and the average power over the interruption period is assumed to be one-half the peak power, the average power is thus:

$$P_A = 1/2 \times 1/2 \times 5 \times 10^4 \times 1/2 \times 10^3$$
$$= 6.25 \times 10^6 \text{ watts.}$$

On the extremely pessimistic assumption that all of this power must be dissipated only at the end-surface of the inter-chute barrier nearest to the discharge, one computes for the RSI 12A with such a surface area of 8.89 cm^2 that the incident power density is

$$Fi = 6.25 \times 10^6/8.89 = 7.03 \times 10^5 \text{ watts/cm}^2.$$

On the overly optimistic assumption that the entire chute area (including the wall at the end of the chute) of 120.7 cm^2 were available for absorbing the incident power, the flux would be reduced proportionately. The actual effective area is not obvious, but for purposes of the calculation, take the effective area to be the geometric mean of the two extremes. Thus:

$$A_{eff} = \sqrt{A_{min}\, A_{max}} = \sqrt{8.89 \times 170.7} = 32.8 \text{ cm}^2$$

from which

$$Fi = P_A/A_{eff} = 62.5 \times 10^6/32.8 = 1.905 \times 10^5 \text{ watts/cm}^2$$

The temperature rise may be expressed by

$$\Delta T = \frac{2}{\pi} \sqrt{\frac{\Delta t}{\lambda \sigma}} Fi$$

where

ΔT = temperature rise (°C)
Δt = time of the incident flux (sec)
λ = thermal conductivity (joules/cm-sec-°C)
= 0.25 for alumina
σ = heat capacity (joules/cm^3-°C)
= 1.8 for alumina
Fi = incident flux density (watts/cm^2)

Setting $\Delta T = 1000$, $Fi = 7.03 \times 10^5$ (worst case) and solving for Δt,

$$\Delta t = 2.25 \text{ μsec}$$

For $Fi = 1.905 \times 10^5$,

$$\Delta t = 30.6 \text{ μsec.}$$

The conclusions are that for an interruption time of less than 2.2 μsec, no damage will occur to the channel; for interruption times greater than 30 μsec, the probability of damage increases materially (depending on the true effective area).

(4) Energy Deposited in a Series Load

Assuming that, on the average, one-half the fault current flowed to the load over the interruption period, the total charge transferred is simply

$$Q = i\Delta t/2.$$

When the fault current is limited to 1000 A and the interruption time is 2.8 μsec as above, the charge transferred is

$$0.5 \times 10^{3} \times 2.8 \times 10^{-6} = 1.4 \times 10^{-3} \text{ coulombs.}$$

If the load were arcing with a voltage of 50 V, the energy deposited therein would be

$$W = VQ = 50 \times 1.4 \times 10^{-3} = 70 \text{ millijoules.}$$

If the interruption time is allowed to increase to 10 μsec, the grid current is then less than 1 A, the temperature increase in the channel is 570°C, and the energy deposited in the load is still only 250 millijoules.

c. Conclusions

The discussion of this section has addressed the topic of self-interruption as it applies to RSI's, and also the various effects of the length of the interruption period on RSI design and performance. Based on theoretical considerations and experimental observations, certain conclusions can be reached:

1. The relatively long RSI interaction channel does not cause a material decrease in the threshold for self-quenching-induced current instabilities when compared with that commonly observed for standard hydrogen thyratrons.

2. The quench-limited, long-pulse, current-pressure characteristic has been established for a representative RSI.

AD-A069 840 EG AND G INC SALEM MASS ELECTRONIC COMPONENTS DIV F/G 9/5
REPETITIVE SERIES INTERRUPTER II.(U)
APR 79 R F CARISTI, D V TURNQUIST DAAB07-76-C-1301
UNCLASSIFIED DELET-TR-76-1301-F NL

2 OF 2
AD
A069840

END
DATE
FILMED
7-79
DDC

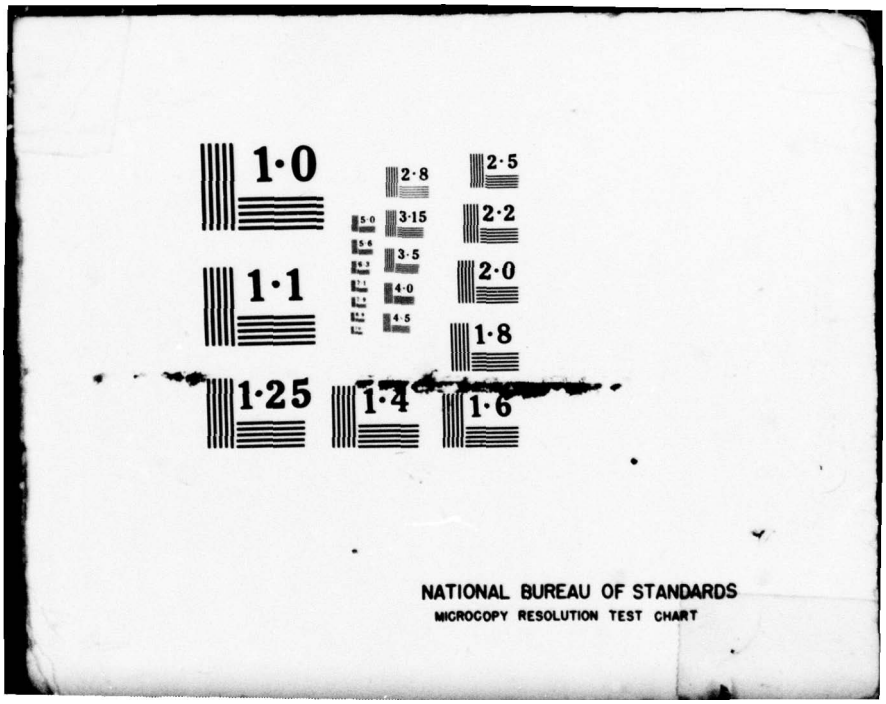
1·0
1·1
1·25
2·8
3·15
3·5
4·0
4·5
2·5
2·2
2·0
1·8
1·4
1·6
NATIONAL BUREAU OF STANDARDS
MICROCOPY RESOLUTION TEST CHART

(3) Interruption Time and Grid Capacitance

It is not readily apparent how one would proceed to calculate the effective capacitance, Cg, present at the gird during interruption. However, Cg can be estimated by inferring a value for the effective grid capacitance after interruption and deionization. From typical grid waveforms, one thus infers that Cg $\approx$ 500 pF for the RSI 10DD, and values for Cg of this order are typical for the 10 Series RSI's.

Upon interruption, Cg must charge from its steady-state potential of ecd, the column drop, to Ebb, the supply voltage. The average current required to charge Cg is thus

$$iCg = Cg\ (Ebb-ecd)/\Delta t$$

where Δt is the interruption time as before.

For a typical 10 Series tube such as the 10DD, assume

Ebb = 10 kV
ecd = 800 V
Cg = 500 pF
Δt = 2 μsec

from which

$$iCg = 2.3\ A.$$

Currents of exactly this value have been observed under the stated conditions. When the magnetic field is applied, the cathode current drops to zero but anode current continues to flow until Cg is charged.

To limit iCg to 2.5 A, an interruption time of about 2.8 μsec is required. This period is well within the maximum time limitation from the point of view of ceramic damage from a single pulse (30 μsec) as discussed above, and such a rise time capability has already been demonstrated.

(4) Energy Deposited in a Series Load

Assuming that, on the average, one-half the fault current flowed to the load over the interruption period, the total charge transferred is simply

$$Q = i\Delta t/2.$$

When the fault current is limited to 1000 A and the interruption time is 2.8 μsec as above, the charge transferred is

$$0.5 \times 10^{3} \times 2.8 \times 10^{-6} = 1.4 \times 10^{-3} \text{ coulombs.}$$

If the load were arcing with a voltage of 50 V, the energy deposited therein would be

$$W = VQ = 50 \times 1.4 \times 10^{-3} = 70 \text{ millijoules.}$$

If the interruption time is allowed to increase to 10 μsec, the grid current is then less than 1 A, the temperature increase in the channel is 570°C, and the energy deposited in the load is still only 250 millijoules.

c. Conclusions

The discussion of this section has addressed the topic of self-interruption as it applies to RSI's, and also the various effects of the length of the interruption period on RSI design and performance. Based on theoretical considerations and experimental observations, certain conclusions can be reached:

1. The relatively long RSI interaction channel does not cause a material decrease in the threshold for self-quenching-induced current instabilities when compared with that commonly observed for standard hydrogen thyratrons.

2. The quench-limited, long-pulse, current-pressure characteristic has been established for a representative RSI.

3. The self-interruption process does not hinder RSI operation, and in fact serves to lower Bq.

4. The effect of decreasing the rise time of the magnetic field is to reduce Bq at high Ebb. The rise time dependence of Bq is complex, and it assumes increased importance as Ebb is increased.

5. The principal advantage to be gained from minimizing the interruption time is to decrease the heating of the interaction channel during the interruption period.

6. At the 50 kV, 1000 A level, interruption times as long as 30 μsec are not likely to cause damage to the RSI. Interruptions of 2 μsec are absolutely safe and this interruption time has been achieved experimentally.

7. It is desirable to decrease the stray capacitance at the grid, and it is possible to do so by increasing the length of the air gap without increasing the input energy requirement of the magnetic field circuitry.

8. It is desirable to limit the grid capacitance charging current in the holdoff section to a few amperes since this value is known from experimentation to cause no particular difficulties, whereas higher currents cause arcing within the tube.

9. At the 50 kV level, the grid capacitance should be reducible to 120 pF and the charging current will be 2.5 A if the interruption time is 2.8 μsec.

10. Over a 2.8 μsec interruption period, the energy deposited in the load is only 70 millijoules and the interaction channel will not be damaged by the energy deposited therein ($\Delta T = 302°C$).

11. If the interruption time is allowed to be as long as 10 μsec, ΔT is only 570°C, and the energy deposited in the load is only 250 millijoules.

5.0 TUBE DROP

The subject of tube drop is best discussed by treating each of its aspects separately. A final design can then be established which represents the best compromise among the various pertinent considerations. The principal factors of interest are:

1. Total Steady-State Drop — Total tube drop etd is the sum of the column drop, the holdoff section drop, and the cathode-to-column drop. The holdoff section drop is of the order of 100 V and the cathode-to-column drop is 50 V or less. The column drop may be 400 to 1000 V or more for an efficient, high voltage interrupter. Thus etd is dominated by the column drop.

2. Column Drop vs Field Energy Required for Interruption — Earlier work with smooth-bore interaction channels dealt extensively with the inverse relationship between column length (and hence column drop) and the magnetic field energy required to interrupt a given current at a given voltage. Although this relationship still exists, in a gross sense, the development of the highly efficient chuted channel geometry has materially reduced its significance. Field energies of at most a few tens of joules delivered to a chuted column are sufficient to interrupt discharges of several tens of megawatts, so field energy requirements are no longer the dominant consideration.

3. Column Drop vs Voltage Level of the Interruption — During interruption, the entire voltage Ebb appears across the interaction channel. This condition prevails until the holdoff section recovers, and holdoff is thus transferred to the grid-anode space. The voltage gradient along the interaction channel must be uniformly low if arcing is to be avoided therein. Furthermore, interruption is a rapid process, as it must be if the energy deposited in the channel is to be kept within reasonable bounds. It follows that voltage Ebb must uniformly develop across the channel on a time scale consistent with that of the interruption.

4. Channel Heating Due to Average Forward Current — For the relatively low average current set forth in the technical guidelines for the RSI II Program, channel heating due to average current is not a significant concern. However, if the RSI is to keep pace with the general level of high voltage technology, operation at much higher average currents must be anticipated, and the ability to remove heat from the interaction channel becomes an important consideration.

5. Current and Time Dependence of Total Tube Drop — In some applications, variations in the steady-state tube drop are of little or no concern, provided that such variations are within reasonably broad limits. In other applications, such variations are of serious consequence.

The more important aspects of tube drop are discussed below.

a. Total Tube Drop — First Order Estimate for a Typical Device

Accurate measurements of the total tube drop for the RSI 11's (30 kV test holdoff sections for the RSI 10DD) and also for the RSI 13's (50 kV test holdoff sections for the RSI 12 Series) revealed that the total drop of these devices, i.e., the anode-to-ground drop during conduction, was typically of the order of 110 to 130 V. When such structures were appended to an RSI interaction channel, a somewhat different situation obtained in that the anode-grid structure (which comprises the actual holdoff structure) was appended to the "top" of the channel, while the cathode and body cylinder of a standard EG&G Type 7322 thyratron was appended to the "bottom."

Measurements of the voltage at the lower flange of the RSI channel consistently showed about 40 to 50 V at this point. The difference in voltage between the upper flange and the anode was typically 70 to 100 V. These measurements were thus consistent with the total drops recorded for the test vehicles.

A typical column drop for a single section (15 kV) channel was of the order of 300 to 400 V, depending on gas pressure, diameter, and forward current. The total drop for multiple sections is the sum of the individual section drops; therefore, a 50 kV device requiring a triple section channel will operate with a column drop of 900 to 1200 V.

Relatively little is to be gained from attempting to reduce the drop of the holdoff section; first, because it constitutes but a fraction of the total RSI drop, and second because changes likely to reduce its drop are also likely to degrade its holdoff capabilities.

Some freedom exists to reduce the column drop by shortening the channel and by increasing the bore diameter, but such changes will also serve to increase the field necessary to achieve interruption and also increase the likelihood of column arcing during interruption.

Using an average figure for column drop of 350 V per section, and a total holdoff and cathode section drop of 130 V, it may be concluded that a typical, triple-section 50 kV device will operate with a total forward drop of approximately 1200 V.

b. Column Drop vs Voltage Level of the Interruption

With the development of the highly efficient chuted-channel geometry, the need for long columns to maintain the interrupting magnetic field at a reasonable level became much less important as a design consideration. Column length is now principally dictated by the maximum field which the column will tolerate during interruption before the onset of internal arcing. When an arc forms, the discharge becomes extremely difficult to interrupt — sufficiently so that the RSI may no longer perform its intended function.

The RSI 12 Series of tubes was designed to operate with a field of 50 kV over 21 inches of column length (937 V/cm) during interruption. This was slightly higher than the corresponding value of 908 V/cm for the 10 Series of tubes. Of the 10 Series, only the 10E showed any signs of arcing, and the evidence was less than conclusive. Our experimentally gained experience nonetheless suggests that higher electric fields during interruption should be avoided, and that for a reasonable factor of safety, even lower fields might be in order for a production device.

Since the minimum column length is thus determined by the maximum electric field before arcing (900 V/cm), and the maximum channel diameter for reasonable interrupting fields at such a column length is 0.150 inch, and such

columns are known to operate with a forward drop of, for instance, 350 V per section (20 V/cm), a "rule-of-thumb" relation exists between Ebb and the column drop such that

$$l = \frac{Ebb\ (V)}{900\ (V/cm)}$$

where l is the total length of the interaction column
and

$$ecd = l\ (cm) \times 20\ (V/cm)$$

where ecd is the column drop.
Thus

$$ecd = \frac{20}{900} \times Ebb$$

or, roughly, ecd ≈ etd ≈ Ebb x 2% if the drop of the holdoff section is neglected.

Clearly, design freedom exists to alter these numbers to some extent whenever appropriate, but tube drops of 1% or 3% are not likely to occur in practice.

It is important that voltage Ebb be distributed with reasonable uniformity over the full length of the interaction channel during the actual interruption. If a local field of high intensity develops over some significant length of the column, the probability of arc formation in the channel is greatly increased. If an arc forms, the discharge becomes extremely difficult to interrupt. Furthermore, local heating of the channel may be severe, and if tracking occurs, the probability for subsequent erratic behavior is thereby enhanced. It follows that a uniform field distribution during interruption is probably the principal criterion for a successful RSI design.

The RSI 12A1 was equipped with a tungsten probe located at a point approximately one-third "up" the column; i.e., just before the first fold, so that the gradient along the column could be observed to at least some extent. Figure 48 shows representative data for the 12A1 when operated with Ebb = 20 kV, P = 250 microns, and the magnetic field intentionally set so as to provide a long interruption time. In Figure 48(a), the waveforms shown are (in descending order) the tube current, the upper flange, the probe, and the lower flange. (The probe and flange waveforms were taken on successive shots so that the same high voltage probe could be used for each measurement. As a result, minor details of the waveforms may differ.) Figure 48(b) shows the upper flange and probe waveforms only, and at a faster sweep speed.

In Figure 48(a), the drop of the column may be discerned during conduction, but this is not pertinent to the present discussion. During interruption, the upper flange rises to Ebb (20 kV) as it should, while the lower flange rises to a little less than 8 kV (40 percent of Ebb). The lower flange waveform, as anticipated, is of no consequence. Also from Figure 48(a), the long decay of the column potential may be observed. It is presently believed that this decay is the column deionization time, and not the effect of any stray capacitance.

From Figure 48(b), and despite the noise on the waveforms during interruption, it is concluded that at no time during the interruption does the ratio of the probe voltage to the flange voltage differ materially from that which applies at the end of the interruption.

Data of the nature of that of Figure 48 were taken for the RSI 12A1 as a function of Ebb and appear in Figure 49, which shows the ratio of the probe potential to the flange potential over a range of Ebb from 5 to 25 kV. Operation at higher Ebb was erratic because of a holdoff problem with the tube. Two cases are shown in Figure 49. In the first case, the column and probe were resistively graded to determine if capacitance voltage division might be taking place. In the second case, the column was ungraded, and the pressure was decreased to increase tube holdoff capability. Various impedance

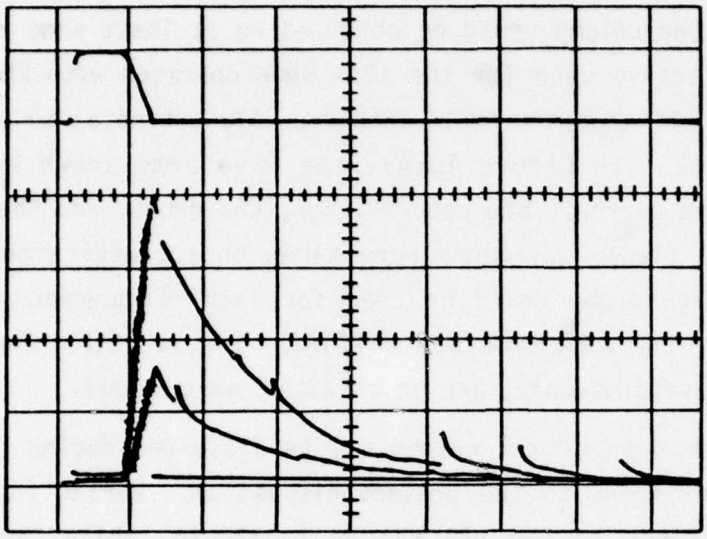

(a)

ib, 200A/DIV
VOLTAGE WAVEFORMS:
TOP FLANGE,
PROBE, BOTTOM
FLANGE, 5kV/DIV
t, 20μS/DIV
Ebb = 20kV
P = 250 MICRONS
RSI 12A

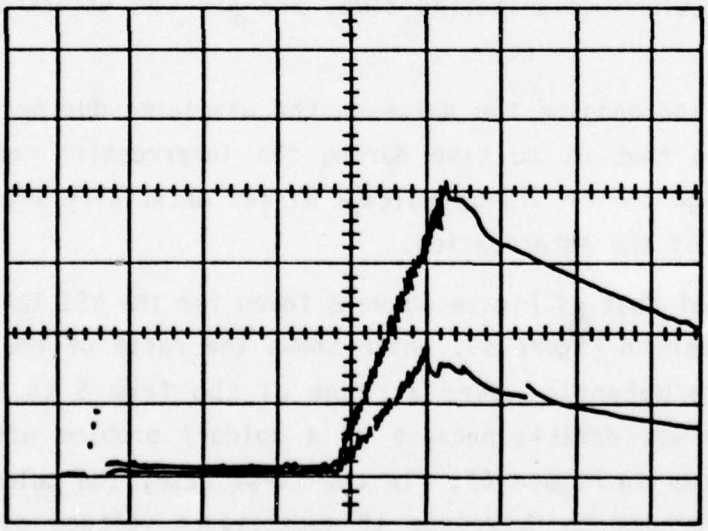

(b)

TOP FLANGE AND
PROBE WAVEFORMS
AT 5kV/DIV AND
5 μS/DIV

Figure 48. Waveforms During Interruption – RSI 12A1. Both the probe and upper flange waveforms show a substantially linear increase, but the probe voltage was somewhat higher than anticipated, as described in the text.

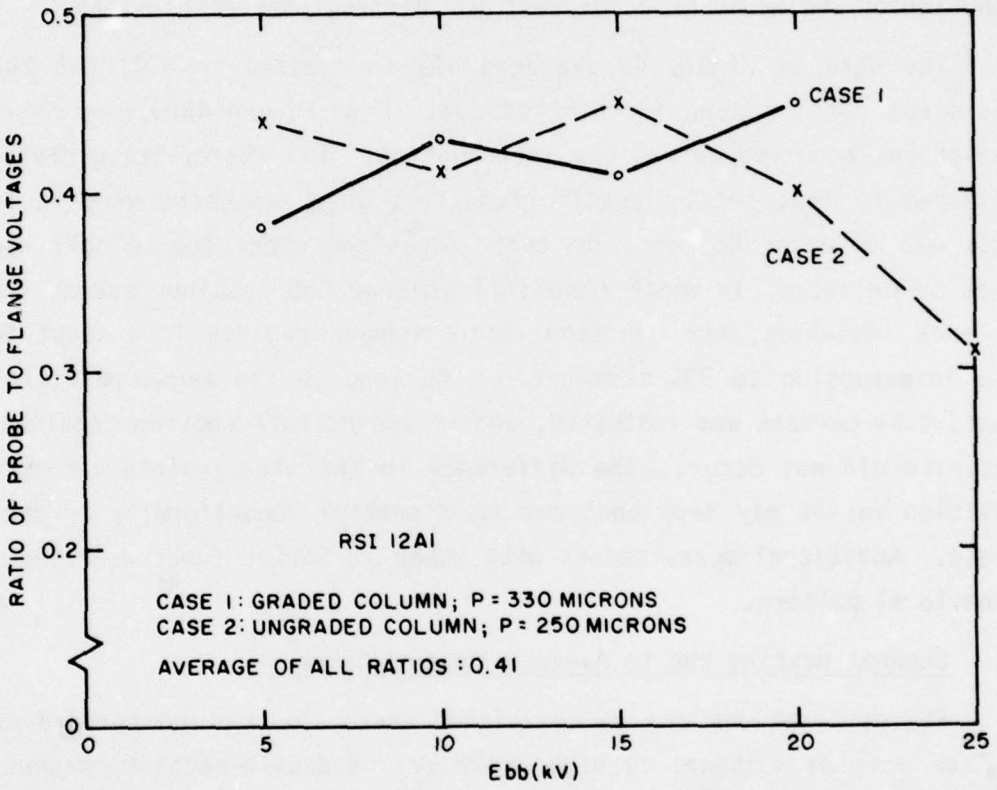

Figure 49. Ratio of Probe Voltage to Upper Flange Voltage During Interruption – RSI 12A1. No clear trend is in evidence for either the graded or ungraded case over the range of Ebb investigated.

levels were investigated for the graded case, and it was found that neither the voltage ratios nor the time constant of the column decay were materially affected thereby, from which it is concluded that capacitance effects are not at play in these data.

Figure 49 also shows that no clear trend is in evidence for the voltage ratio (whether graded or ungraded) over the range of Ebb investigated. This is highly desirable since gross variations in field along the column as a function of Ebb would be a forecast for difficulties at high Ebb.

The data of Figure 49 averaged 41% as opposed to 33%, but the voltage ratio was not a strong function of Ebb. From Figure 48(b), no extraordinary variations occurred during the interruption. The steady-state division ratio adjusted to that set by grading resistors when resistors were in fact used. This was observed to occur on those occasions where the holdoff section was slow to deionize, in which case full voltage Ebb remained across the column. In such instances, the division ratio changed rapidly from about 40% during the interruption to 33% thereafter. As long as the magnetic field was present, tube current was inhibited, and if the holdoff section regained control, restrike did not occur. The difference in the steady-state and interruption division ratios may have been due to a spatial nonuniformity in the magnetic field. Additional measurements with other 12 Series tubes revealed a similar behavioral pattern.

c. Channel Heating Due to Average Forward Current

RSI applications can be envisioned where the average forward current is 5 A or more at voltages as high as 30 kV. A double-section channel would be required, and assuming a worst-case column drop of 400 V per section, the power dissipated in the column would be 2 x 400 x 5 = 4 kW, a nontrivial heat load for a structure having the mass, dimensions, and internal structure of an RSI interaction channel. Water cooling of the channel is in order for such operating conditions. Temperature profiles and coolant flow rates specific to such operation for various channel geometries and purities of alumina were calculated, assuming a maximum safe working temperature of 600°C. The vendor was requested to investigate the feasibility of fabricating channels with the appropriate cooling passages built into the channel. The overall conclusions

were that RSI operation at these power levels was feasible and that suitable channels could be fabricated. It would, however, be operated with maximum thermal safety factor, accomplished in practice by reducing the column drop to a reasonable minimum consistent with the available field energy and operating voltage, thus reducing the input power to the column. Channels would be fabricated from high density alumina to take advantage of the higher thermal conductivity of higher density alumina at elevated temperatures, ensuring against the formation of localized "hot spots" that might lead to channel fracture at maximum heat loads.

Under conditions of high dissipation in the interaction channel during conduction, uniformity of the voltage gradient along the channel becomes important. Experimental observations of gradient uniformity using the probe-equipped RSI 12A1 have shown that the gradient is sufficiently uniform so that local heating will not be a problem in a properly designed device.

d. Current and Time Dependence of Total Tube Drop

It is common practice to consider the voltage drop of gas discharge devices as being substantially independent of the discharge current. This is true only in the sense that gas-filled devices operate with a relatively constant drop when compared with vacuum tubes. In general, and depending on pressure and current density, a gas-filled tube such as a hydrogen thyratron operates with a very definite V-I characteristic, with some minimum voltage drop corresponding to some particular level of tube current. It is therefore reasonable to assume that an RSI, with its relatively long discharge column, will exhibit a well defined V-I characteristic.

The essence of the current dependence characteristic is revealed by an examination of Figure 50, which shows the grid-to-ground drop (essentially the column drop) for the RSI 10DD when subjected to capacitor discharges of differing initial currents at a tube pressure of 610 microns. From the oscillograms of Figure 50, the minimum drop occurred in both cases at a tube current of 25 to 30 A, and the general dependence of the tube drop on the tube current is readily apparent.

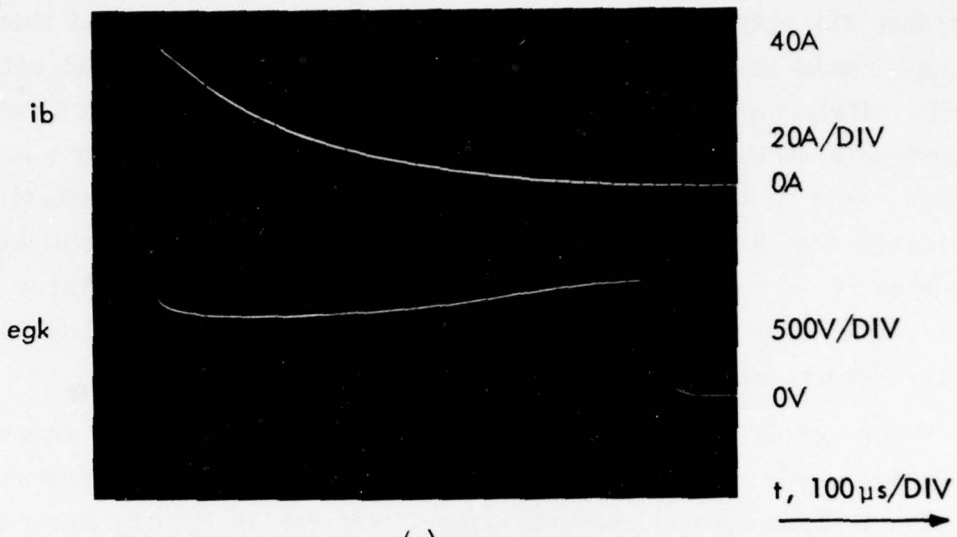

(a)

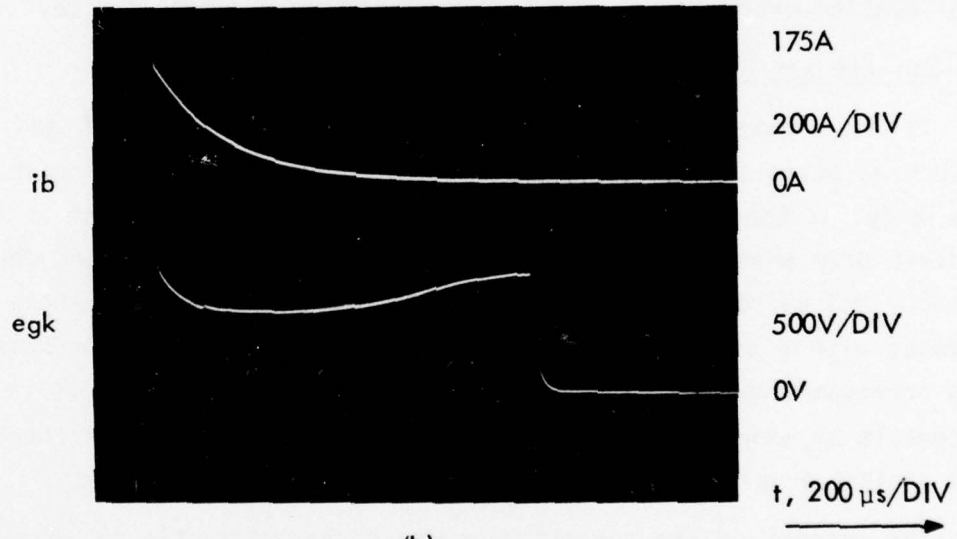

(b)

DATA SHOWS 1 PULSE AT 1 Hz.
RSI 10DD, P = 600 MICRONS

Figure 50. Dependence of Instantaneous Tube Drop on Instantaneous Anode Current – RSI 10DD.

The time dependence of the tube drop is not so readily determined, and has not been investigated experimentally during the RSI Program. Time-exposed oscillograms showing multiple waveforms of etd generally appear as a single trace, but this is the strongest statement one can make without having actively pursued an investigation aimed at generating the appropriate data. Long-term changes in etd due to heating and pressure changes would also require consideration.

In summary, RSI's exhibit a well defined and clearly understood V-I characteristic, but the time dependence of the total tube drop has not been subjected to scrutiny. Whether such current and time dependencies are of significance depends on each application.

e. Conclusions

The steady-state tube drop to be expected of an RSI depends on several compromises that enter into the design of any given tube. The principal component of the total tube drop is the column drop, and the column drop is proportional to the length of the interaction channel. The dominant consideration in choosing channel length for an efficient, chuted interrupter is not the magnetic field energy necessary to achieve the interruption, but rather the voltage level of the interruption (because arcing within the channel must be avoided). It is also important that the electric field be fairly uniform along the length of the channel during the interruption. For chuted interrupters of the 10 and 12 Series variety, i.e., designed to interrupt discharges of 300 to 1000 A at voltages of 15 to 50 kV with a magnetic field energy of (at most) a few tens of joules, a total tube drop of about 2 percent of Ebb for each design when optimized is expected. Such drops are observed in practice.

When operation at high average currents is required, active cooling of the channel is necessary, and uniformity in the voltage gradient along the column during conduction becomes important. Water-cooled channels capable of dissipating several kilowatts of average power can be fabricated, and a uniform gradient can be established.

The current dependency of the total tube drop is clearly defined and understood. The time dependency has not been investigated. Whether or not such dependencies are important depends on each application.

6.0 RESTRIKE AVOIDANCE

For an opening switch to be useful, it must not restrike; i.e., current interruption, once achieved, must be permanent. Earlier work with the RSI had been plagued with a variety of restrike problems, and the elimination of restrike was therefore assigned a high priority.

a. The Nature of Restrike

There is no fundamental reason why the RSI should restrike, given that the magnetic field is applied for a sufficiently long period of time. Holdoff section recovery times of 20 μsec and less, and column voltage decay times of the order of 100 μsec were observed. For the applicable gas pressure, relative dimensions, and capacitances of these regions in the tube, these times were reasonable. It was obvious that the duration of the magnetic field must exceed the holdoff section recovery time. It was less obvious (but had been experimentally determined) that the duration of the field should exceed the column deionization time or the time required for the stray capacitance at the grid to discharge, whichever time was greater. The point of this discussion is that for field times greater than a few hundred microseconds at most, the RSI should be absolutely free of restrike.

Previous work indicated that such was not the case; but based on the discussion above, an important conclusion could be reached. The apparent restriking with long magnetic fields must not be true restriking, but rather retriggering. The plan of attack was thus obvious; namely, identify and eliminate all mechanisms capable of contributing to the generation of false triggering signals. The most obvious such mechanism was ground loops in the experimental apparatus. Another was the capacity coupling of false triggers into the RSI grid due to the proximity of the grid to the magnet core. Still another was the coupling of false triggers via the AC line and heater circuits. Each of these mechanisms was investigated and found to be a contributing source of false triggers to the RSI. Finally, conditions were established such that:

1. The RSI would never trigger the magnet circuit.

2. The magnet circuit would never trigger the RSI.

3. The time between the triggering of the RSI and the onset of the field current was solely a function of the purposely introduced and electronically delayed magnet circuit trigger pulse.

4. The observed waveforms were sufficiently "clean" to permit detailed waveshape analyses.

When these conditions prevailed, "restrike" no longer occurred.

The oscillogram of Figure 51(b) is typical of the performance which was finally attained and is representative of the essence of RSI operation. The oscillogram is a time exposure showing about ten pulses at 2 Hz to provide an indication of the voltage and timing stability that was finally achieved. From Figure 51(b) notice that the discharge is permanently interrupted. The details of the waveforms of Figure 51(b) are discussed below.

At t = 0, the RSI is triggered and the magnet circuit delay begins. Tube current ib rapidly rises to the value (Ebb-etd)/Rrc as anode voltage eb drops to etd, the steady state tube drop. Just prior to the interruption, the electronic delay ends, the magnet circuit is triggered, and field current im begins its rise. At the time of interruption, ib drops to zero and eb returns to the voltage of the capacitor bank, which is then somewhat less than Ebb due to the charge removed by ib. The grid trigger is too narrow to be visible in the waveform of grid voltage eg, but the grid-to-cathode voltage drop (which includes the column drop) may be clearly seen during the RSI conducting period. Upon interruption, the grid must rise with the anode to the capacitor voltage as shown, at which potential it remains until the holdoff section deionizes (about 12 μsec in Figure 51(b)). Thereafter the grid decays exponentially to ground with a time constant determined by the effective grid capacitance, the grid circuit resistance, and in some complex fashion, the deionization properties of the interaction column. In Figure 51(b), the grid decayed to ground potential well in advance of the termination of the field pulse, and restriking of the discharge did not occur. The effects of varying the grid circuit resistance (and hence the grid decay time) need not be discussed in detail here, but in general, if the grid resistance is too low, the grid potential attempts to decay too quickly and the holdoff section does

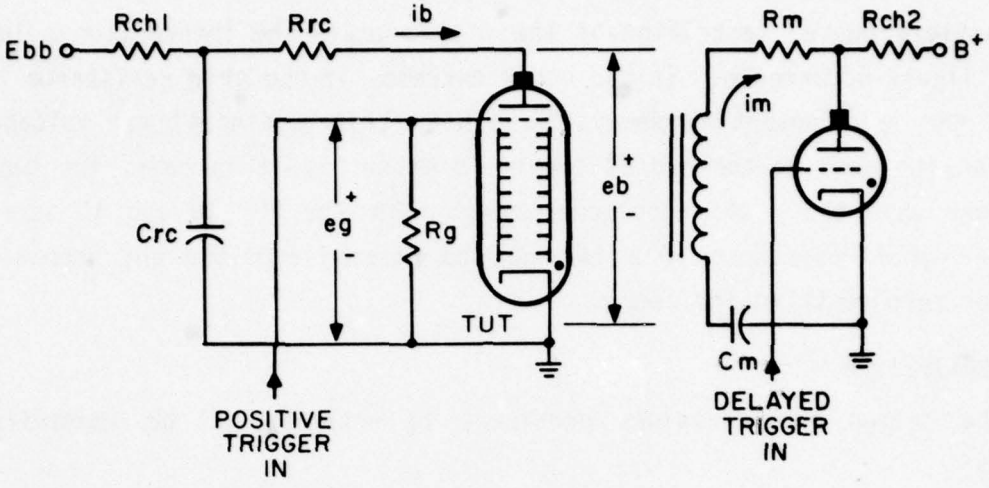

(a)

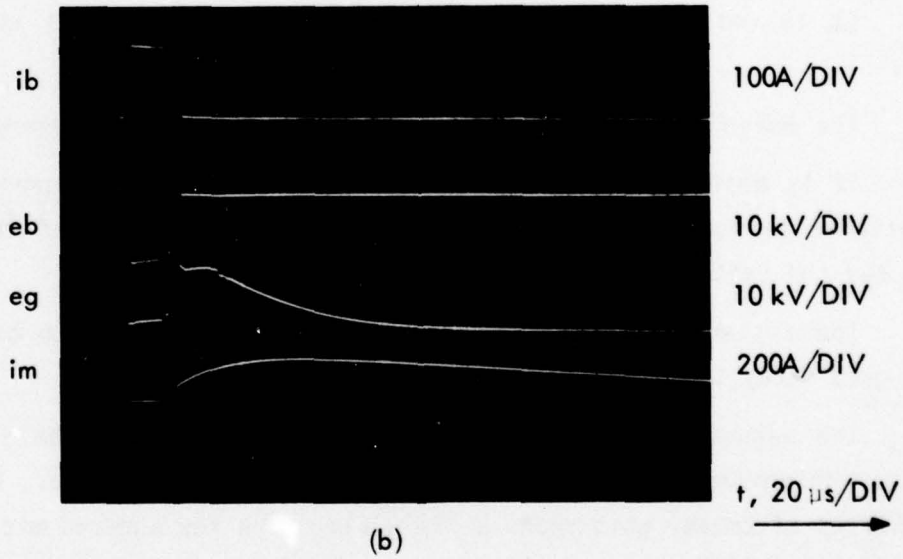

(b)

Figure 51. RSI Test Circuit and Typical Waveforms During Interruption. Grid decay following holdoff section de-ionization is evident.

not recover or may even conduct through the grid circuit. As long as the magnetic field is present, cathode current is inhibited, but upon termination of the field pulse, restriking of the discharge in the interaction column is then a likely occurrence. In the other extreme, if the grid resistance is too large, the grid potential decays so slowly that a significant voltage may exist on the grid at the end of the field pulse. In this case, the tube may retrigger when the field approaches zero. For the RSI 10 and 12 Series of tubes, a grid resistance of a few hundred kilohms provided the proper decay time for zero restrike incidence.

b. Conclusions

The design considerations pertinent to restrike may be summarized as follows:

1. The installation must be free of ground loops.

2. Because of the high capacitive coupling between the RSI grid and the magnet core, the core must be constrained to operate at the instantaneous potential of the RSI cathode.

3. It is desirable to minimize the stray capacitance at the grid of the RSI.

4. The holdoff section is best designed with quick recovery in mind.

5. It is best to operate the RSI at the lowest gas pressure consistent with reliable triggering. This minimizes the recovery time of the holdoff section and the deionization time of the interaction column.

6. The resistance present at the grid must be chosen to provide the optimum grid decay time.

7. The magnetic field should remain on the RSI until the interaction region has deionized and the grid potential has decayed to zero. For the 10 and 12 Series of tubes, this means a field time of a few hundred microseconds, and permits a repetition rate well in excess of 1 kilohertz.

7.0 TRIGGERING, REPETITION RATE, AND LIFE

a. Triggering Characteristics

(1) Zero Keep-Alive

For all of the RSI's studied under Phase II of the Program, the interaction section was located in the grid-cathode region of the tube. A significant advantage in triggering stability is gained with this type of design as opposed to a post anode type of device.(6) Nonetheless, the location of the interaction channel in the grid-cathode space necessitates the use of a large triggering pulse, and unless additional steps are taken as described in this section, the anode delay time (tad) and time jitter (tj) characteristics of such an RSI are relatively poor when compared with those of a standard thyratron. This is illustrated by Figure 52, which shows tad and tj of about 500 nsec and 100 nsec, respectively, for the RSI 10D with epy = 10 kV, even at the relatively high tube pressure of 600 microns. The trigger was a 10 kV, 1 μsec pulse rising in about 100 nsec, at an impedance level of less than 1000 ohms. The conclusion drawn from Figure 52 was that material improvements in tad and tj would be feasible.

Toward that end, a high voltage, fast rising, low impedance trigger generator was built, and measurements of egy (min), tad, and tj versus epy and P were taken for a typical tube (RSI 10D) to establish base-line data from which progress could be determined. The output of the trigger generator is shown in the oscillogram of Figure 53, which shows a 10 kV pulse, 2 μsec wide, and reaching 10 kV in about 10 nsec. The output impedance of the generator was 500 ohms, and with a load of 500 ohms, the amplitude of the output pulse was thus reduced by a factor of two, but no other distortion of the pulse shape occurred. The open circuit voltage was continuously adjustable over the range from zero to 15 kV.

The triggering characteristics of the RSI 10D, when operated without keep-alive and when driven by the trigger generator described above, are as shown in Table 6. There are minor inconsistencies in the data of Table 6, but in general, the expected trends were observed with both tad and egy (min) decreasing with increasing epy and tube pressure. Time jitter tj was relatively constant at 100 to 200 nsec over the range of epy and P investigated.

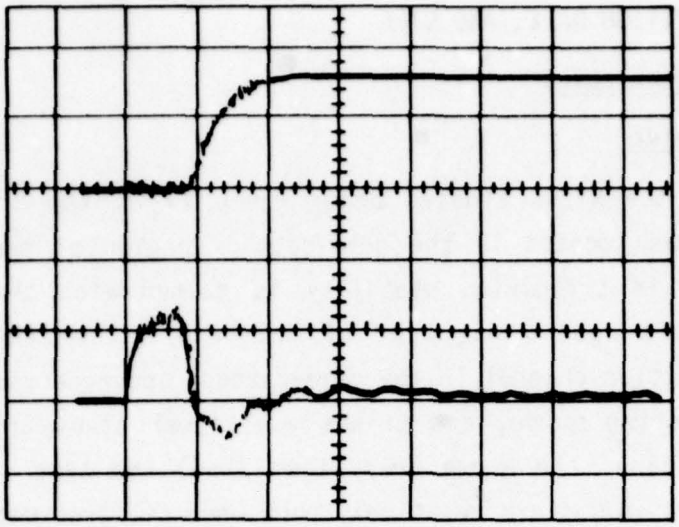

Figure 52. Anode Delay Time and Delay Time Jitter Without Keep-Alive — RSI 10D.

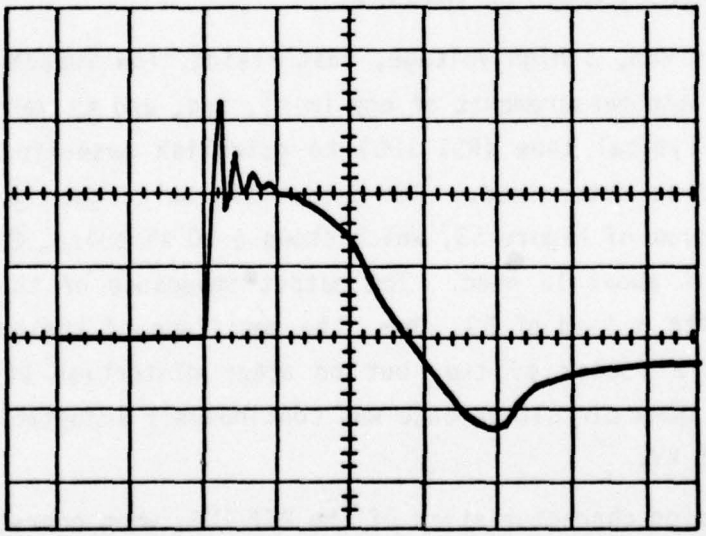

Figure 53. Output Voltage Waveform of High Voltage, Low Impedance Trigger Generator Built to Investigate Triggering Characteristics of RSI's.

Table 6. Triggering Characteristics Without Keep-Alive — RSI 10D (2 μsec Trigger, tr = 10 nsec, Zg = 500 ohms).

	epy (kV)	egy (min)	tad (μsec)	tj (nsec)
P = 235 microns	6	5.0	4.6	200
	8	5.0	3.8	100
	10	5.0	3.2	100
	12	5.5	2.7	100
P = 330 microns	4	3.5	6.5	200
	6	4.0	3.8	200
	8	4.0	3.2	200
	10	4.0	2.8	200
	12	4.0	2.8	200
P = 470 microns	4	2.8	5.1	200
	6	3.5	2.8	200
	8	4.0	2.5	150
	10	4.0	2.5	150
	12	3.5	2.5	200
P = 600 microns	4	2.5	3.5	150
	6	3.5	2.3	150
	8	2.8	2.4	200

(2) Effects of Keep-Alive

There are three convenient locations available for the introduction of a keep-alive current to the RSI – the lower flange of the interaction channel, the upper channel flange, and the control grid. Keep-alive currents applied to each of these elements produce different effects depending on which element (or elements) is chosen, as discussed below.

As might be expected, a keep-alive applied to the upper channel flange results in the most profound change in the tube triggering characteristics. This is illustrated by the oscillograms of Figure 54. Figure 54(a) shows the anode fall and the grid voltage waveform of the RSI 10D when operated at epy = 10 kV at a pressure of 400 microns and driven with a 10 kV trigger. A keep-alive current of only 20 μA was applied to the upper channel flange, and this keep-alive reduced tad from about 1 μsec to 600 nsec as shown. Figure 54(b) shows the collapse of the grid potential as the tube commutates, and about 3000 pulses are shown in the time exposure. From Figure 54(b), tj is at most about 10 nsec with an average value of even less. This is to be compared with a typical value for tj of about 150 nsec in the absence of keep-alive.

Various keep-alive currents were simultaneously applied to both the upper and lower flanges of the interaction channel. The results with epy and egy held constant are shown in Table 7. From Table 7, several points should be noted:

1. For each value of upper flange current, there is an optimum value of lower flange current.
2. The optimum lower flange current is about four times the upper flange current.
3. Little advantage is gained beyond I2 = 500 μA and I1 = 2 mA.
4. In general, the values shown for tad and tj are comparable to those of a standard thyratron.

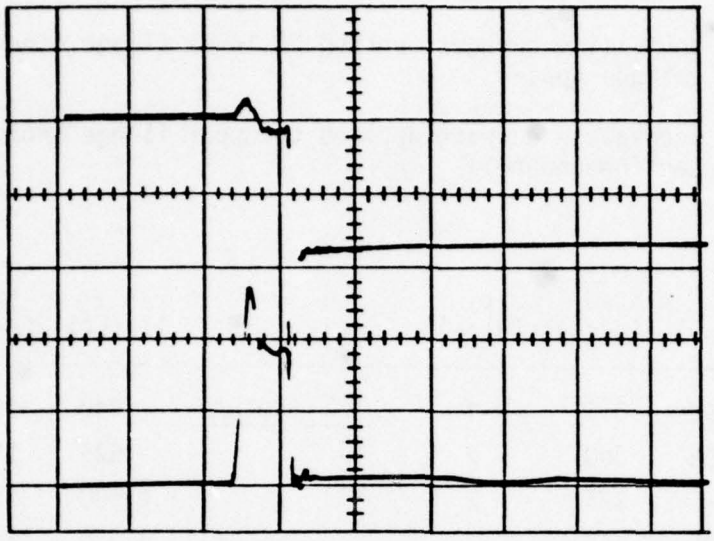

(a)

eb, 5kV/DIV

t, 1 μS/DIV

eg, 5kV/DIV
P = 400 MICRONS
epy = 10kV
RSI 10D

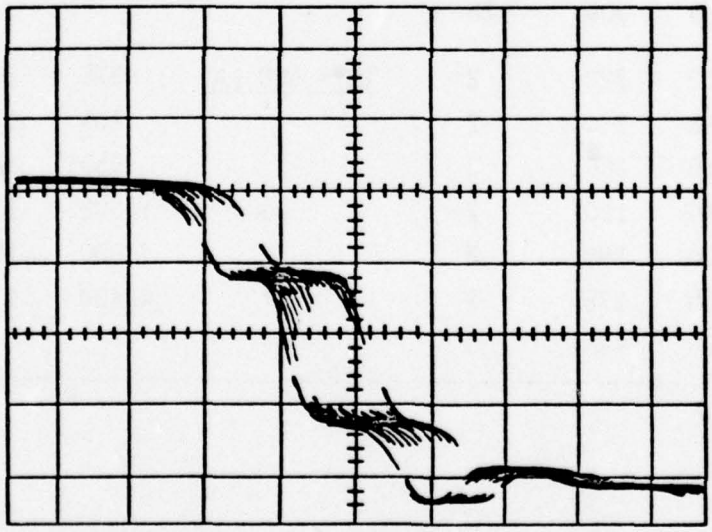

(b)

eg, 2kV/DIV
t, 10nS/DIV
P = 400 MICRONS
epy = 10kV
RSI 10D

Figure 54. Anode Delay Time and Delay Time Jitter of RSI 10D with Keep-Alive. A keep-alive current of only 20 microamperes applied to the upper flange of the interaction channel reduced the time jitter by over an order of magnitude.

Table 7. Effects of Keep-Alive Currents Applied to Channel Flanges (Data for RSI 10D with P = 400 microns and epy = 10kV).

I1 = keep-alive current applied to lower flange (channel-cathode space)

I2 = keep-alive current applied to upper flange (holdoff section-channel)

	I1 (μA)	tad (nsec)	tj (nsec)		I1 (μA)	tad (nsec)	tj (nsec)
I2 = 100 μA	90	315	2	I2 = 500 μA	440	200	2
	195	300	2		625	180	2
	365	275	2		1,100	170	2
	505	265	3		2,250	160	2
	890	255	7		3,650	160	2
	1,950	280	10		7,200	170	2
	3,200	300	12		19,000	160	10
	6,200	300	20				
I2 = 200 μA	200	220	2	I2 = 800 μA	375	200	2
	360	210	2		705	170	2
	510	200	2		950	170	3
	940	180	2		1,600	150	10
	1,900	180	2		3,600	150	3
	3,200	175	2		4,400	175	5
	6,400	185	3				

It has been observed that tad is most sensitive to a keep-alive applied to the lower flange. This is consistent with the improvement observed for tad in a standard thyratron when an auxiliary, or priming grid, is employed. A small (20 μA) keep-alive applied to the upper flange immediately reduces tj by an order of magnitude (100 nsec to 10 nsec) with even further reductions being possible by increasing the upper and lower flange currents. No change was observed in the forward holdoff capability of the tube when keep-alives were used.

There was, of course, no value of keep-alive which, when applied to the lower flange only, would cause the tube to remain in conduction after being triggered. There was, however, such a current for the top flange as described below.

The tube was operated in the circuit of Figure 55. A direct current of 1 mA was applied to the lower flange to ensure acceptable tad, with virtually any current applied to the upper flange being adequate to provide acceptable tj. Keep-alives were applied first to the upper flange and then to the control grid with the following results.

With the keep-alive applied to the upper flange, voltage E2 was gradually increased until the column "struck." Voltage E2 was then 1600 VDC, and current I2 was 6.5 mA. Voltage E2 could then be reduced until the channel current decreased to 3.4 mA, at which point the discharge would extinguish. If voltage E2 was set at some level higher than 1550 V but less than 1600 V, and the tube was then triggered, the tube would remain in conduction. For E2 less than 1550 V, the tube would recover holdoff after triggering.

Different but anticipated results were obtained when the keep-alive was applied to the control grid. Voltage E2 could be raised to 1800 V, at which point both the grid space and the channel would break down, followed, of course, by commutation of the tube. Reducing E2 well below the striking voltage would not cause the discharge to extinguish, i.e., the RSI was functioning as a closed switch.

The threshold current for stable conduction was about 6 mA. Voltage E2 could be set at arbitrary levels less than the breakdown voltage of 1800 V, and if a trigger were applied, the tube would commutate and remain in conduction.

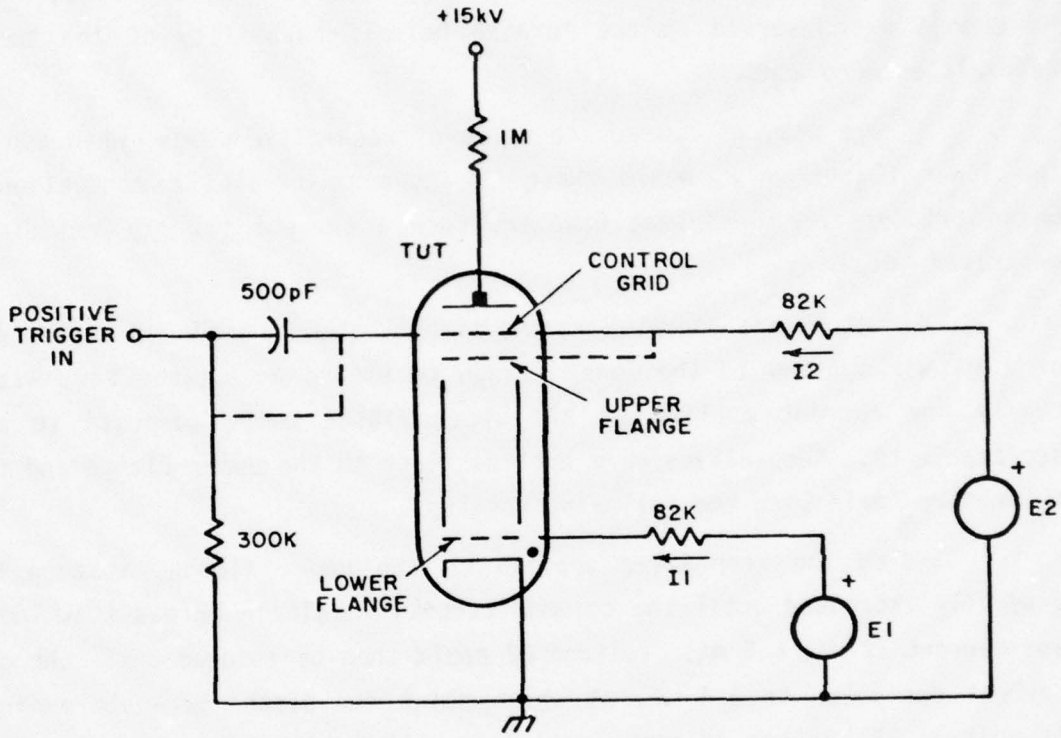

NOTES:

1. 300K GRID RESISTOR LOCATED AT CONTROL GRID WHEN KEEP-ALIVE APPLIED TO UPPER FLANGE.
2. TUT IS RSI 10D WITH P = 400 MICRONS
3. Ef = 6.3V

Figure 55. Circuit Used to Investigate the Effects of Keep-Alive.

Lower flange current I1 was varied over the range of 1 to 5 mA. As expected, the grid voltage and current thresholds remained substantially constant at 1800 V and 6 mA, respectively.

b. Pulse Repetition Rate

The technical guidelines for the RSI Program called for a maximum pulse repetition rate of 1000 Hz under normal pulse conditions. This requirement is obviously well below the limits of the device. The average tube current and the dissipation at the anode and in the interaction channel are well within the capabilities of standard tube designs, and no extended experimental work has been deemed necessary to verify RSI performance at a 1000 Hz pulse rate.

Other than the limitations imposed by maximum cathode current density and the dissipation at the anode and in the interaction channel, four factors having the potential to limit the RSI pulse repetition rate are: 1) transient heating of the interaction channel; 2) the grid decay time; 3) the channel deionization time; and 4) the holdoff section deionization and recovery time. The first two considerations apply more to interruption rate than the normal pulse repetition rate, while the latter two apply in both cases.

The integrated heat load imposed on the interaction channel during a series of rapidly repeated interruptions undoubtedly places a limit on the maximum interruption rate as opposed to the maximum repetition rate under normal pulse conditions. It would appear, however, that for an RSI being used as a protective device, the existence of such a situation would be indicative of a problem at the load serious enough to warrant system shutdown. For example, from the discussion of channel heating as a function of interruption time given in Section 6.0 of this report, it follows that for an RSI operating with a 3 μsec interruption time, even ten interruptions in rapid succession are not likely to damage the RSI, whereas a command for five interruptions would be indicative of severe arcing at the load.

The oscillogram of Figure 56 shows the grid decay time of the RSI 10DD when interrupting 200 A at 20 kV. At the time the oscillogram was made, restrike investigations were underway, and the field pulse had been lengthened to the shape shown to ensure against any restrike. Note that the grid

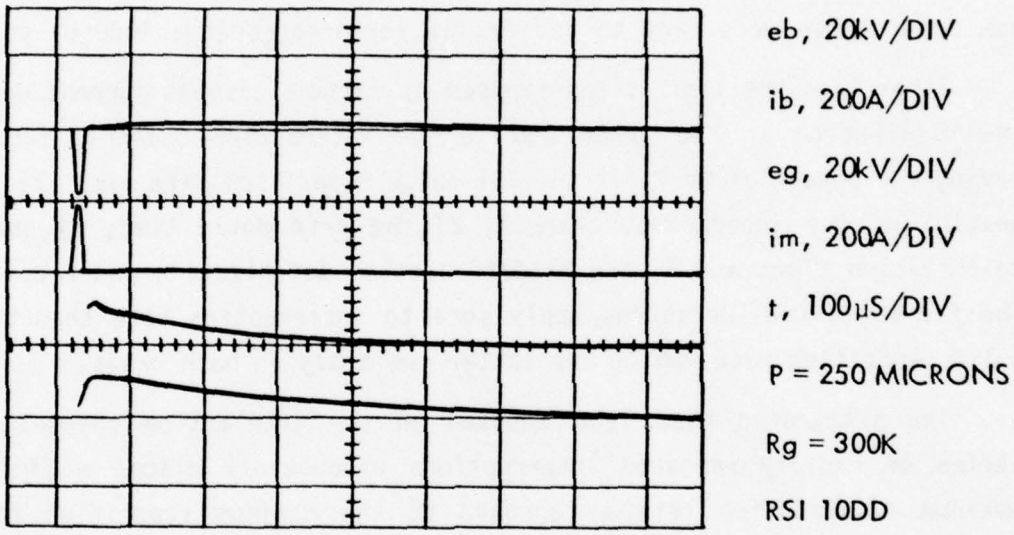

Figure 56. Typical Waveforms for the RSI 10DD when Interrupting 200 A at 20 kV. The grid potential decays to zero in about 450 microseconds, but much shorter decay times have been achieved.

potential has decayed to zero in about 450 μsec, implying an interruption capability of at least 2 kHz. By reducing the grid resistance, much shorter grid decay times have been observed. In a circuit free of ground loops and other false triggering mechanisms, the length of the field pulse can be reduced accordingly.

The oscillogram of Figure 51 shows a case where the total of the grid decay time and the holdoff section deionization time is of the order of 80 μsec. The oscillogram of Figure 48(a) shows a total channel decay time of about 100 μsec.

The oscillograms of Figure 57 show the results of a test contrived to determine if the holdoff section of the RSI 10DD would perform like that of a standard thyratron at elevated pulse repetition rates, and also to determine if any residual ionization that might remain in the interaction channel would affect tube performance. The pulse rate was limited by the capabilities of the driver circuit. All oscillograms were time exposed for several seconds. As expected, the current and voltage waveforms are substantially identical over the two decades investigated, 5 to 500 Hz.

A similar test was performed with the RSI 13A, the gradient grid holdoff section used with the 12 Series of RSI's. Figure 58 shows the current and voltage waveforms with epy = 25 kV and the tube pressure intentionally set high at 550 microns. The pulse rate was limited to 1430 Hz by the current capability of the DC power supply. The anode voltage waveforms of Figure 58(b) show that the tube is successfully holding off 25 kV after 250 μsec.

The overall conclusion is that RSI operation at 1 kHz is highly unlikely due to present problems, with 10 kHz operation being a realistic design goal.

c. Life

The factors which limit the life of hydrogen thyratrons in general are well understood and well documented and are not discussed here. The RSI differs from a standard thyratron principally because it contains an interaction channel. During interruption, the channel is subjected to significant transient heating. In principle, if the channel is capable of withstanding

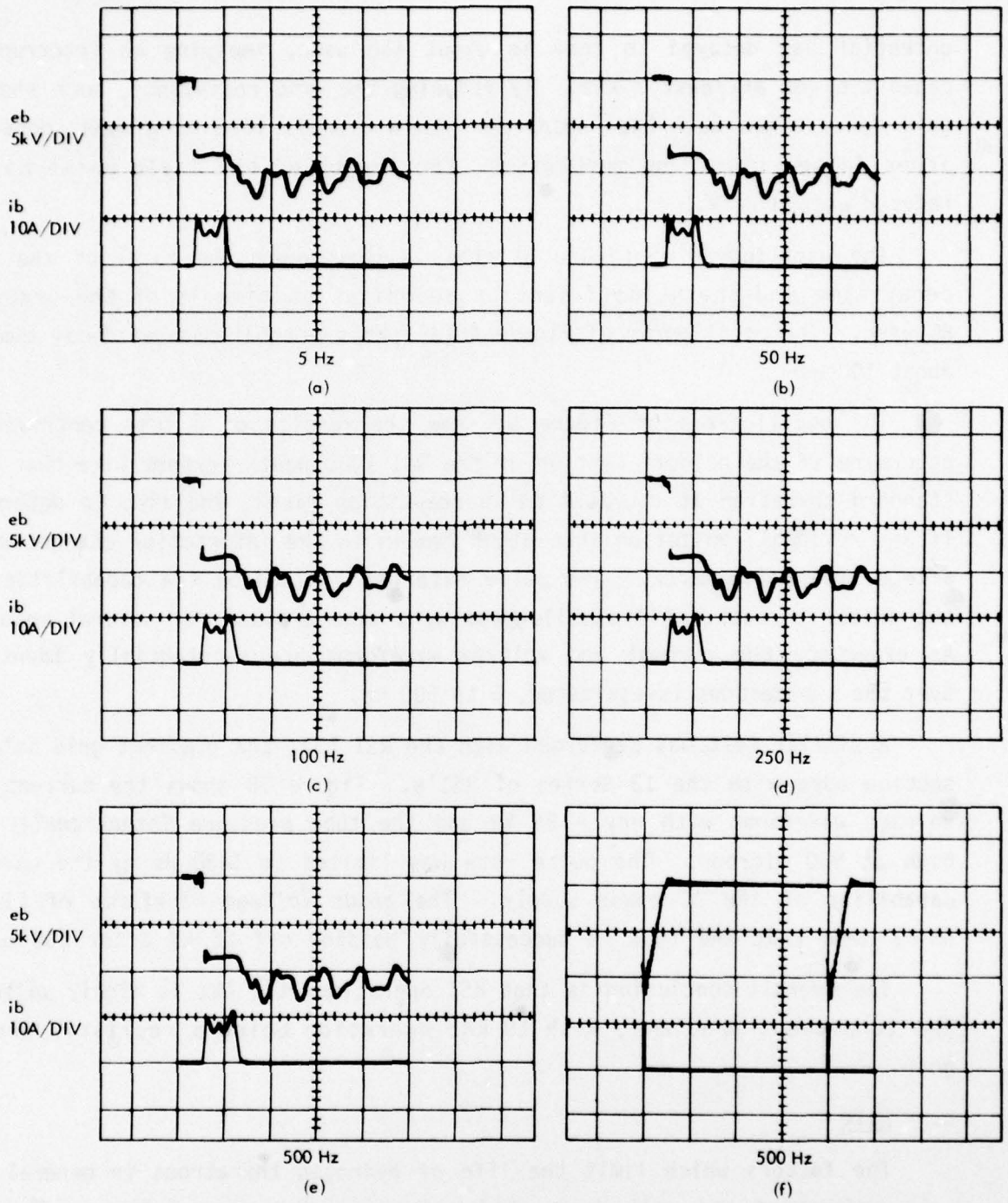

Figure 57. Anode Voltage and Anode Current Waveforms for the RSI 10DD When Operating in the Normal Mode. The waveforms are substantially identical for the two decades of pulse rate shown.

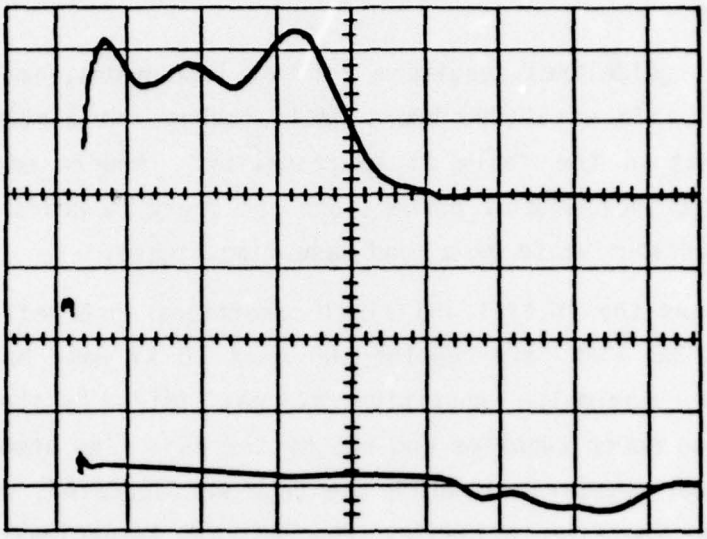

ib, 10A/DIV

eb, 25kV/DIV
t, 2 μS/DIV
P = 550 MICRONS
prr = 1430 HERTZ
RSI 13A

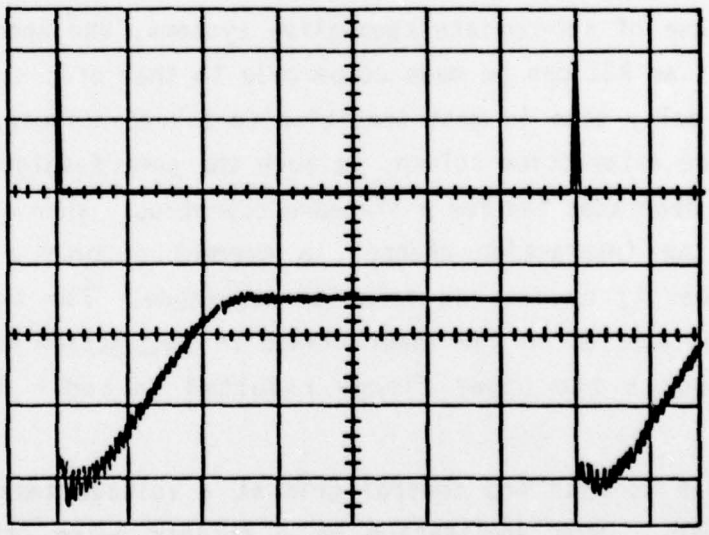

ib, 10A/DIV

eb, 25kV/DIV
t, 100 μS/DIV
P = 550 MICRONS
prr = 1430 HERTZ
RSI 13A

Figure 58. Current and Voltage Waveforms for the RSI 13A When Operating in the Normal Mode. Note that the tube successfully held off 25 kV after 250 microseconds.

the rigors of the interruption without arcing or ablation of its inner surface, it follows that the life of the RSI should be comparable to that of a standard thyratron.

The technical guidelines require a life of 1000 hours, including 20,000 interruptions. A life of 10,000 hours would perhaps be a more appropriate figure, and is within the realm of practicality. Modern microwave tubes operate with an arc incidence of perhaps one arc every 10 hours of operation. Thus, 1000 interruptions would be a good base-line figure.

Figure 59 shows the initial and final conditions observed during a life test of the RSI 10DD when interrupting 100 A at 10 kV with an interruption frequency of 10 Hz. The pulse repetition rate was limited by the capabilities of the high voltage power supplies and not by the RSI. The anode voltage was limited by the high pressure at which the tube was operated, which pressure was chosen to favor restrike incidence. The test was intentionally terminated after 100,000 interruptions without restrike and with no apparent damage to the tube or change in its characteristics.

d. Conclusions

Through the use of appropriate keep-alive systems, the anode delay time and time jitter of an RSI can be made comparable to that of a standard thyratron. The anode delay time is most sensitive to a keep-alive applied to the lower flange of the interaction column, in much the same fashion that driving an auxiliary grid decreases tad for a standard thyratron. When applied to the upper flange of the interaction channel, a current of only a few tens of microamperes reduces tj by over an order of magnitude. For the RSI 10D, a keep-alive of 2 mA applied to the lower flange in conjunction with a current of 500 μA applied to the upper flange resulted in tad = 160 nsec and tj = 2 nsec.

It is possible to bias the control grid at a voltage less than the DC breakdown potential. Upon application of a trigger pulse, the tube will commutate and remain in conduction, i.e., it will function as a closed switch. For the RSI 10D, the breakdown voltage is 1800 V, and the grid current for stable conduction is 6 mA. It is thus clear that the keep-alive requirements of these tubes are minimal.

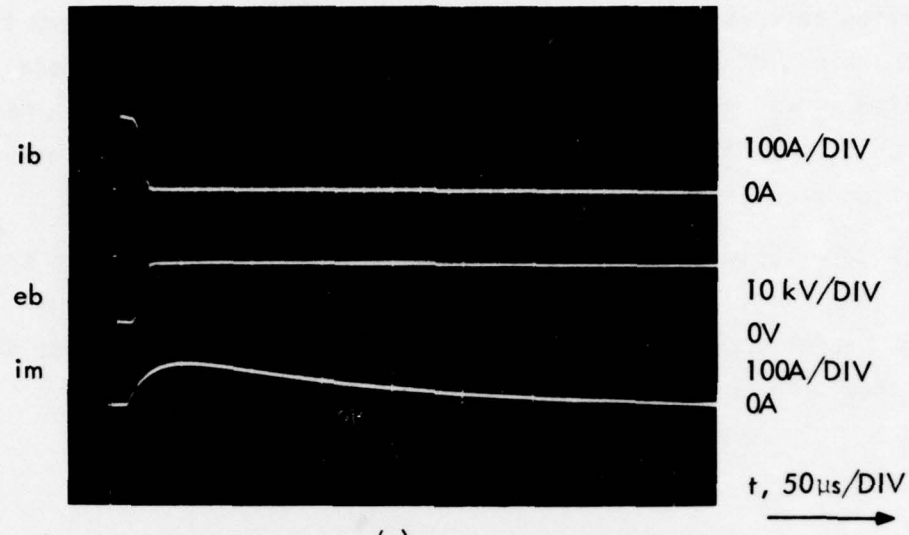

(a)

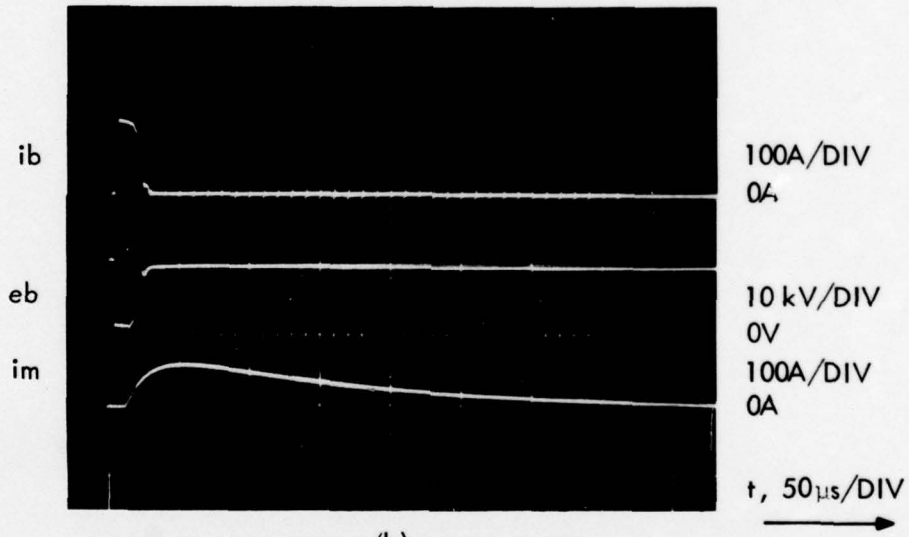

(b)

Figure 59. Initial Waveforms and Waveforms After 100,000 Interruptions — RSI 10DD. In principle, the life of an RSI should be comparable to that of a standard thyratron.

As with any gas discharge device, the fundamental limitation on pulse repetition rate is set by the pertinent deionization and recovery times of the device, i.e., the time required to re-establish the gas conditions that prevailed prior to the initiation of the previous discharge. For a typical RSI, this time is of the order of 100 μsec, implying a maximum pulse repetition rate of the order of 10 kHz.

In principle, the life of an RSI should be comparable to that of a conventional thyratron. Provided that no arcing or ablation of the interaction channel occurs, a life of thousands of hours and thousands of interruptions should be achievable.

8.0 PROGRAM SUMMARY

a. Experimental Results

The 10 and 12 Series of chuted interrupters were built and characterized for both interruption capability and total tube drop. From the 10 Series testing, it was confirmed that tubes of a relatively narrow bore were preferred over wider bore tubes because of their superior interruption efficiency, despite their somewhat higher voltage drop. It was also determined that "plasma reservoirs" should be avoided, i.e., the better channel geometries were found to be those wherein the channels contained both an unchuted and a chuted surface, against which latter surface the discharge was driven. It was also found that the channel should contain a large number of relatively short and closely spaced chutes, that the tube should be operated at the lowest pressure consistent with reliable triggering characteristics, and that multiple, folded interaction channels were both efficient and capable of working at high Ebb.

Typical column drops were of the order of 350 volts per section (20 volts/cm) for the 10 Series tubes. The most efficient of the series, the folded-channel RSI 10DD, operated at 25 kV, 18.5 A with a total drop of 830 volts, or 3.3% of epy. This tube successfully interrupted 600 A at 20 kV with a magnetic field energy of less than 8 joules being required to achieve the interruption.

From testing the 12 Series tubes, it was further determined that the optimum tube should have a bore diameter not materially less than 0.150 inch, contain a maximum number of short, narrow chutes, and also that the chutes should be set at an angle to accommodate the trajectory of the electrons.

Typical total tube drops for the triple-section 12 Series tubes were of the order of 1000 volts (2% of epy) under non-fault current conditions (18.5 A). The column drop was typically 870 volts (16.3 volts/cm) during conduction. During a 50 kV interruption, the electric field in the gas was 937 volts/cm.

The RSI 12C successfully interrupted 100 A at 50 kV, 180 A at 44 kV, 305 A at 26 kV, 700 A at 18 kV, and 1000 A at 15 kV. Operation at these levels was reliable and free of restrike. The magnetic field energy necessary to achieve these interruptions varied from a high of 32.8 joules in the high voltage case, to a low of 1.2 joules in the high current case. This indicates a strong dependence of Bq on Ebb, consistent with our earlier work on unchuted interrupters. Currents well in excess of 1000 A were routinely interrupted at low Ebb with several of the 12 Series tubes. At high Ebb, the interruption capabilities of the 12 Series tubes appeared to depend strongly on dB/dt; these tubes are capable of interrupting even higher currents at high Ebb given a suitably designed magnetic field generator.

It was also demonstrated experimentally that low pressure operation is desirable both to minimize the magnetic field required for interruption and also to promote the rapid recovery of the holdoff section. Rapid recovery in conjunction with appropriate circuit techniques were shown to reduce restrike incidence to near zero.

The total tube drop was consistently measured to be of the order of 2% of epy at normal RSI currents for tubes capable of operating with epy = 50 kV. The forward drop of the discharge column was observed to be uniform along the column length, and the drop across the column during the interruption, while not uniformly distributed, did not differ seriously therefrom. Interruption times as short as 2 μsec were observed.

Through the use of appropriate keep-alive discharges, the triggering characteristics of RSI's can be made comparable to those of standard thyratrons, and operation of the device as a closed switch was experimentally demonstrated.

b. Conclusions

The RSI has been shown to be a practical means for the repetitive interruption of high current at high voltage. Probably the most meaningful advances made during the RSI Program were the development of the chuted channel geometry during Phase I, and the elimination of restrike during Phase II. The chuted channel geometry allowed efficient RSI operation; the elimination of restrike made the RSI a useful device. This is not to say

that still lower Bq would not be advantageous, nor that an occasional restrike does not occur under certain operating conditions. The important point is that sufficient knowledge now exists so that a reasonably efficient and reliable interrupter, operating under conditions approaching (and in some instances exceeding) those of the technical guidelines, can be designed and built.

Interruption of 1000 A was achieved, as was interruption at 50 kV, although not simultaneously. It is believed nonetheless that the experimental RSI's built under Phase II of the Program are capable of interrupting higher powers than those experimentally demonstrated, owing to the limitations of experimental apparatus.

Various other aspects of RSI operation that have been investigated during Phase II are outlined below.

(1) Self-Interruption and the Effects of Interruption Time

The phenomenon of the self-interruption of a gas discharge at high current densities has been investigated to the extent that it applies to RSI design and operation. It has been established that self-interruption does not hinder RSI operation, and in fact serves to lower the magnetic field required to achieve interruption Bq. The relatively long RSI interaction channel does not cause a material decrease in the threshold current density for self-interruption when compared with that commonly observed for conventional hydrogen thyratrons.

The effect of decreasing the rise time of the magnetic field is to reduce Bq at high Ebb. The dependence of Bq on tr is complex, and assumes increasing importance as Ebb is increased.

Minimizing the interruption time serves to decrease the heating of the interaction channel during the interruption period. At the 50 kV, 1000 A level, interruption times as long as 30 μsec are not likely to cause damage to the RSI. Two-microsecond interruptions are absolutely safe, and this interruption time has been achieved in practice.

(2) Tube Drop

The steady-state tube drop to be expected of an RSI depends on several compromises that enter into the design of any given tube. The principal component of the total tube drop is the column drop, and the column drop is proportional to the length of the interaction channel. The dominant consideration in choosing channel length for an efficient, chuted interrupter is not the magnetic field energy necessary to achieve the interruption, but rather the voltage level of the interruption (because arcing within the channel must be avoided). It is also important that the electric field be uniform along the length of the channel during the interruption. For chuted interrupters of the 10 and 12 Series variety, i.e., those designed to interrupt discharges of 300 to 1000 A at voltages of 15 to 50 kV with a magnetic field energy of (at most) a few tens of joules, a total tube drop of about 2% of Ebb for each design when optimized is expected. Such drops are observed in practice.

When operation at high average currents is required, active cooling of the channel is necessary, and uniformity in the voltage gradient along the column during conduction becomes important. Water-cooled channels capable of dissipating several kilowatts of average power can be fabricated, and a uniform gradient can be established.

The current dependency of the total tube drop is clearly defined and understood. The time dependency has not been investigated. Whether or not such dependencies are important depends on the requirements of each application.

(3) Restrike Avoidance

There is no fundamental reason why an RSI should restrike, given that the magnetic field is applied for a sufficiently long period of time. For RSI's based on hydrogen thyratron technology and operated with interrupting magnetic fields lasting a few hundred microseconds, restrike simply should not occur. As experimentally demonstrated, for a properly designed and constructed RSI and its associated circuitry, restrike can in fact be avoided.

The design considerations pertinent to RSI operation without restrike may be summarized as follows:

1. The installation must be free of ground loops.
2. Because of the high capacitive coupling between the RSI grid and the magnet core, the core must be constrained to operate at the instantaneous potential of the RSI cathode.
3. It is desirable to minimize the stray capacitance at the grid of the RSI.
4. The holdoff section is best designed with quick recovery in mind.
5. It is best to operate the RSI at the lowest gas pressure consistent with reliable triggering. This minimizes the recovery time of the holdoff section and the deionization time of the interaction column.
6. The resistance present at the grid must be chosen to provide the optimum grid decay time.
7. The magnetic field should remain on the RSI until the interaction region has deionized and the grid potential has decayed to zero. For the 10 and 12 Series of tubes, this means a field time of no more than a few hundred microseconds, and permits a repetition rate well in excess of 1 kilohertz.

When these conditions were established for the experimental apparatus, restrike incidence was reduced to substantially zero.

(4) Triggering Characteristics, Repetition Rate, and Life

Through the use of appropriate keep-alive systems, the anode delay time (tad) and delay time jitter (tj) of an RSI can be made comparable to those of a standard thyratron, although relatively large triggers (several kilovolts) are required. For the RSI 10D, tad and tj of 160 nsec and 2 nsec respectively have been observed with a total keep-alive power requirement of less than 10 watts.

It is possible to bias the control grid at a voltage less than the DC breakdown potential of the total grid-to-cathode space. Upon the application of a trigger pulse, the tube will commutate and remain in conduction. For the RSI 10D, the grid breakdown voltage is 1800 V, and the grid current for stable conduction is 6 mA.

As with any gas discharge device, the fundamental limitation on pulse repetition rate is the time required to reestablish the gas conditions that prevailed prior to initiation of the previous discharge. For a typical RSI, this time is of the order of 100 μsec, implying a maximum pulse repetition rate of 10 kHz.

In principle, the life of an RSI should be comparable to that of a conventional thyratron. Provided that no arcing or ablation of the interaction channel occurs, a life of thousands of hours including thousands of interruptions should be achievable.

9.0 REFERENCES

1. Simon, R., and Turnquist, D.V., "Repetitive Series Interrupter II," Research and Development Technical Report ECOM-76-1301-6, April 1978, p. 5.

2. Simon, R., and Turnquist, D.V., "Repetitive Series Interrupter II," Research and Development Technical Report ECOM-76-1301-6, April 1978, p. 145.

3. Simon, R., and Turnquist, D.V., "Repetitive Series Interrupter II," Research and Development Technical Report ECOM-76-1301-6, April 1978, p. 58.

4. Goldberg, S., and Riley, D.F., Research Study on Hydrogen Thyratrons, Volume III, EG&G Inc., Boston, 1957.

5. Thomas, J., Vandenbrink, H., and Turnquist, D., "New Switching Concepts," Technical Report ECOM-00123-F, 1967.

6. Simon, R., and Turnquist, D.V., "Repetitive Series Interrupter II," Research and Development Technical Report ECOM-76-1301-6, April 1978, p. 4.

DISTRIBUTION LIST

12 Defense Documentation Center
ATTN: DDC-TCA
Cameron Station (Bldg 5)
Alexandria, VA 22314

1 Code R123, Tech Library
DCA Defense Comm Engrg Ctr
1860 Wiehle Ave
Reston, VA 22090

1 Defense Communications Agency
Technical Library Center
Code 205 (P.A. TOLOVI)
Washington, DC 20305

1 Office of Naval Research
Code 427
Arlington, VA 22217

1 Director
Naval Research Laboratory
ATTN: Code 2627aboratory
Washington, DC 20375

1 Commander
Naval Electronics Laboratory Center
ATTN: Library
San Diego, CA 92152

1 CDR, Naval Surface Weapons Center
White Oak Laboratory
ATTN: Library, Code WX-21
Silver Spring, MD 20910

1 Rome Air Development Center
ATTN: Documents Library (TILD)
Griffiss AFB, NY 13441

1 Hq, Air Force Systems Command
ATTN: DLCA
Andrews AFB
Washington, DC 20331

2 CDR, US Army Missile Command
Redstone Scientific Info Center
ATTN: Chief, Document Section
Redstone Arsenal, AL 35809

1 Commander
US Army Missile Command
ATTN: DRSMI-RE (Mr. Pittman)
Redstone Arsenal, AL 35809

3 Commandant
US Army Aviation Center
ATTN: ATZQ-D-MA
Fort Rucker, AL 36362

1 Director, Ballistic Missile Defense
Advanced Technology Center
ATTN: ATC-R, PO BOX 1500
Huntsville, AL 35807

1 Commander
HQ Fort Huachuca
ATTN: Technical Reference Div
Fort Huachuca, AZ 85613

2 Commander
US Army Electronic Proving Ground
ATTN: STEEP-MT
Fort Huachuca, AZ 85613

1 Commander
USASA Test & Evaluation Center
ATTN: IAO-CDR-T
Fort Huachuca, AZ 85613

1 Deputy for Science & Technology
Office, Assist Sec Army (R&D)
Washington, DC 20310

1 CDR, Harry Diamond Laboratories
ATTN: Library
2800 Powder Mill Road
Adelphi, MD 20783

1 Director
US Army Ballistic Research Labs
ATTN: DRXBR-LB
Aberdeen Proving Ground, MD 21005

1 Harry Diamond Laboratories, Dept of Army
ATTN: DELHD-RCB (Dr. J. Nemarich)
2800 Powder Mill Road
Adelphi, MD 20783

1 Commander
US Army Tank-Automotive Command
ATTN: DRDTA-RH
Warren, MI 48090

1 CDR, US Army Aviation Systems Command
ATTN: DRSAV-G
PO Box 209
St. Louis, MO 63166

1 TRI-TAC Office
ATTN: CSS
Fort Monmouth, NJ 07703

1 CDR, US Army Research Office
ATTN: DRXRO-IP
PO Box 12211
Research Triangle Park, NC 27709

1 CDR, US Army Research Office
ATTN: DRXRO-PH (Dr. R.J. Lontz)
PO Box 12211
Research Triangle Park, NC 27709

1 Commandant
US Army Air Defense School
ATTN: ATSA-CD-MC
Fort Bliss, TX 79916

1 Commander, DARCOM
ATTN: DRCDE
5001 Eisenhower Ave
Alexandria, VA 22333

1 Naval Surface Weapons Center
Dahlgren Laboratory
ATTN: Dr. M. Rose, Code DF-102
Dahlgren, VA 22448

1 Ballistic Missile Defense Advanced
Technology Center
ATTN: Dr. L. Havard, ATC-T
P.O. Box 1500
Huntsville, AL 35807

1 Mr. J. Stover
Hughes Aircraft Company
Post Office Box 3310
Fullerton, CA 92634

1 Mr. J. Weil
Raytheon Company
Boston Post Road
Wayland, MA 01778

1 Chief
Ofc of Missile Electronic Warfare
Electronic Warfare Lab, ECOM
White Sands Missile Range, NM 88002

Commander
US Army Electronics R&D Command
Fort Monmouth, NJ 07703
1 DELSD-L
1 DELEW-D
3 DELCS-D
1 DELET-D
3 DELET-BG
1 DELET-BG (Ofc of Record)
2 DELSD-L-S
1 DELET-D
25 Originating Office

2 MIT – Lincoln Laboratory
ATTN: Library (RM A-082)
PO Box 73
Lexington, MA 02173

1 NASA Scientific & Tech Infor Facility
Baltimore/Washington Intl Airport
PO Box 8757, MD 21240

2 Advisory Group on Electron Devices
201 Varick Street, 9th Floor
New York, NY 10014

1 ITT Electron Tube Division
3100 Charlotte Avenue
Easton, PA 18042

1 Air Force Aero Propulsion Laboratory
ATTN: Mr. R. Verga, AFAPL/POD-1
Wright Patterson Air Force Base
Ohio 45433

1 Mr. C.J. Eichenauer, Jr.
General Electric Company, HMED
Court Street
Syracuse, NY 13201

1 Mr. R.A. Gardenghi
Westinghouse Electric Corporation
Friendship International Airport
Box 1897, MS-636
Baltimore, MD 21203